PROJECTE FINAL DE CARRERA

Beamforming coordination techniques in OFDM Multi-hop Cellular Networks

Enginyeria de Telecomunicació
Autor: Marc Torrellas Socastro
Director: Adrián Agustín de Dios
Ponent: Josep Vidal Manzano

Barcelona, July 2011

CONTENTS

NOTATION AND ACRONYMS

Notation for matrices, vectors and scalars:

- Vectors are written with bold font and lower case. (**x**)
- Matrices are written with bold font and upper case. (**X**)
- $\max(a,b)$ and $\min(a,b)$ denote the maximum and the minimum between *a* and *b* respectively.
- $(a)^+$ operator denotes $\max(a,0)$.
- $\lfloor a \rfloor$ is the floor function, that is, the largest integer lower than a.
- $\mathbf{I}$ is the identity matrix
- $(.)^T$ means the transpose operator.
- $(.)^H$ means the conjugate transpose operator.
- $(\mathbf{A})_{ij}$ is the element of matrix $\mathbf{A}$ located in the ith row and the jth column.
- $|.|$ operator can be applied to scalars and matrices. When it is applied to scalars, it means the modulus of that number, while when the operator is applied to a matrix it means the determinant of that matrix.
- $\mathbf{A} \otimes \mathbf{B}$ is the Kronecker product of matrices $\mathbf{A}$ and $\mathbf{B}$.
- $gsvd(\mathbf{A},\mathbf{B})$ is the generalized singular value decomposition of $\mathbf{A}$ and $\mathbf{B}$.
- $eig(\mathbf{A},\mathbf{B})$ are the generalized eigenvectors of $\mathbf{A}$ and $\mathbf{B}$.
- $\mathbf{A}(a:b,c:d)$ is a sub-matrix obtained by selecting those elements located from the the ath row to the bth row and from the cth column to the dth column,

following the Matlab notation. $\mathbf{A}(b,:)$ is the row b of the matrix $\mathbf{A}$ and $\mathbf{A}(:,b)$ is the column b of the matrix $\mathbf{A}$.

- $diag(.)$ is an operator that can be applied to vectors or matrices with a different meaning. When it is applied to vectors, it returns a square diagonal matrix containing the values of the vector in its diagonal(**A**=diag(**b**)). Otherwise, when $diag(.)$ is applied to a matrix, it returns the main diagonal of that matrix (**a**=diag(**B**)).
- $\mathbf{A}^{-1}$ is the inverse matrix of the square matrix $\mathbf{A}$, such that $\mathbf{A}^{-1}\mathbf{A} = \mathbf{A}\mathbf{A}^{-1} = \mathbf{I}$.
- $\mathbf{A}^{\#}$ is the Moore Penrose pseudo-inverse of the matrix $\mathbf{A}$.
- $\mathbf{A}^{\perp}$ is the matrix whose spanned subspace is orthogonal to the subspace spanned by the columns of $\mathbf{A}$, see $span(\mathbf{A})$ definition.

Notation for sets and subspaces

- $span(\mathbf{A})$ is the subspace defined by all the linear combinations of the columns of $\mathbf{A}$.
- $null(\mathbf{A})$ is the subspace defined by vectors $\mathbf{v}$ such that $\mathbf{A}\mathbf{v} = \mathbf{0}$.
- $span(\mathbf{A}) \subset span(\mathbf{B})$ means that $span(\mathbf{A})$ is contained in $span(\mathbf{B})$. Consequently, for a vector $\mathbf{v}$ such that $\mathbf{v} \in span(\mathbf{A})$, we can say $\mathbf{v} \in span(\mathbf{B})$ but the converse does not hold.
- $span(\mathbf{A}) \cap span(\mathbf{B})$ is the subspace defined by vectors $\mathbf{v}$ such that $\mathbf{v} \in span(\mathbf{A})$ and $\mathbf{v} \in span(\mathbf{B})$.
- $span(\mathbf{A}) \cup span(\mathbf{B})$ is the subspace defined by vectors $\mathbf{v}$ such that $\mathbf{v} \in span(\mathbf{A})$ or $\mathbf{v} \in span(\mathbf{B})$. Note that $\left(span(\mathbf{A}) \cap span(\mathbf{B})\right) \subset \left(span(\mathbf{A}) \cup span(\mathbf{B})\right)$.

- $rank(\mathbf{A})$ is denoted as the minimum among the column rank and the row rank of the matrix $\mathbf{A}$. If nothing is stated, we assume $rank(\mathbf{A})$ as the column rank of the matrix $\mathbf{A}$.
- $\dim(S)$ is the cardinality of the set S.

Acronyms

AWGN	Additive White Gaussian Noise
BC	Broadcast Channel
BS	Base Station
CJ	Cadambe and Jafar
CSIT	Channel State Information at Transmitter side
DFT	Discrete Fourier Transform
DOA	Direction of Arrival
DoF	Degrees of Freedom
FDM	Frequency Division Multiplexing
GJ	Gou and Jafar
GM	Geometric Mean
GSVD	Generalized Singular Value Decomposition
i.i.d	independent and identically distributed
IA	Interference Alignment
IC	Interference Channel
ISI	Inter-symbol interference
LOS	Line of Sight
MAC	Multiple Access Channel
MIMO	Multiple Input Multiple Output
MinR	Min-Rate
MS	Mobile Station
NLOS	Non Line of Sight
OFDM	Orthogonal Frequency Division Multiplexing

pZF	Partial Zero Forcing
RACN	Relay-assisted cellular network
RLL	Razaviyayn, Lyubeznik and Luo
RS	Relay Station
SISO	Single Input Single Output
SNR	Signal to Noise Ratio
SR	Sum-rate
SVD	Singular Value Decomposition
TDM	Time Division Multiplexing
TDMA	Time Division Multiple Access
WSR	Weighted sum-rate
ZF	Zero Forcing
ZF-BD	Zero-Forcing Block Diagonalization

Agraïments

Després d' aquestes últimes setmanes ja ho puc dir: el PFC està aquí. Aquest treball ha estat fruït d' un gran esforç durant gairebé 2 anys. Tot va començar amb una beca després de fer l' assignatura de Processament de Senyal amb el meu professor Josep Vidal i finalment ha acabat esdevenint PFC. I la veritat és que n' estic molt content d' haver-ho fet perquè m' ha servit per aprendre moltíssimes coses que a la carrera no s' aprenen.

Hi ha bastantes persones a les que cal agrair que aquest projecte, com a fi de tota la carrera, hagi sortit endavant. En primer lloc, en Josep Vidal i l' Adrià Agustín, que amb el seu esforç, però sobretot paciència, m' han ajudat a endinsar-me en una àrea del coneixement tan complexa com aquesta. També he d' agrair els consells i comentaris d' altres persones, com l' Adriano Pastore i l' Olga Muñoz.

Vull donar les gràcies també a la meva família: els meus pares Consol i Toni i el meu germà Sergi. També a en Pol Moreno, perquè m' ha ajudat molt durant la carrera i l' ha fet molt més suportable, sobretot en les assignatures que ell i jo sabem.

Però segur que no m' haguessin anat tant bé les coses si no fos per la meva nòvia Anna Maria Carné, que m' ha ajudat a comprendre moltes coses de la vida, m' ha alegrat cada dia amb el seu somriure, o com a mi m'agrada dir-te amb la teva "llum". Gràcies per confiar en mi sempre, per aguantar els meus rollos, les meves històries diàries plenes de detalls.. Gràcies per obrir-me al teu grup d' amics, per enganxar-te a veure el futbol amb mi, perquè al novembre ens n' anem a viure junts (!!!), per mil i una coses que en aquesta pàgina no m'hi caben, però sobretot per omplir-me amb aquell "gusanillo" que si passa més d' un dia sense veure'ns fa que em falti alguna cosa.

Porque cuando se juntan dos ríos, se hace fuerte la corriente.

Marc Torrellas

Juliol 2011

Resum

El sistemes de comunicacions mòbils han experimentat grans avenços en els últims anys. D'ençà que els primers sistemes cel·lulars de telefonia mòbil van aparèixer, la demanda per part dels usuaris s' ha incrementat a un ritme molt elevat que, juntament amb el fet que l' ample de banda radioelèctric és limitat i s'ha de compartir, ha provocat que els sistemes de comunicació actuals hagin arribat al seu límit. Per aquest motiu és necessària la investigació de nous sistemes de transmissió sense fils més eficients per a poder cobrir aquesta demanda. La investigació i implementació d' aquests sistemes abarca diverses àrees de coneixement: des de l' electrònica utilitzada en les antenes dels terminals fins als protocols de transmissió de dades, dels quals se' n deriven els estàndards.

Aquest treball tracta sobre les transmissions multi-antena i l' ús de repetidors en xarxes cel·lulars. Un dels factors que limita la transmissió en aquestes xarxes és la interferència, que pot ser intra-cel·la quan és entre terminals de la mateixa cel·la i inter-cel·la, quan és entre terminals de cel·les diferents. Per aquest motiu s' estudiarà el canal interferent de 3 parells transmissor-receptor, que és un model de canal que no està caracteritzat totalment. Donada la seva dificultat, des de fa uns anys la majoria de treballs en la matèria han optat per estudiar el seu comportament a molt alta relació senyal soroll (SNR). En aquest context, una de les estratègies que ha pres més força és l' anomenada *interference alignment* (alineació d' interferència). En aquest treball es dissenyaran precodificadors lineals en funció del nombre d' antenes als terminals seguint aquesta estratègia i d' altres. L' objectiu és clar: abordar la gestió de la interferència i millorar la recepció dels senyals desitjats. Per fer-ho, es caracteritzaran algunes propietats del canal interferent (*graus de llibertat*) per a certes configuracions d' antenes arribant a resultats que fins ara només s' havien mostrat com a cotes superiors.

Tot seguit, es considerarà un xarxa cel·lular multisalt on cada cel·la contingui una estació base (BS), diversos repetidors (RS) i una gran quantitat d' estacions mòbils (MS). Entenem per estació mòbil qualsevol terminal que sigui capaç de mantenir una comunicació sense fils amb l' ample de banda corresponent i amb la possibilitat que el terminal estigui en moviment, bé sigui un telèfon mòbil, un ordinador portàtil, etc. La transmissió es divideix en dos salts en els quals s' envien missatges primer des de l' estació base al repetidor i seguidament, del repetidor a l' estació mòbil. El sistema de comunicacions assumeix que durant el primer salt totes les BSs transmeten simultàniament i, per tant, podem modelar el primer salt com un canal interferent. En general ambdós terminals s' instal·len en llocs elevats i amb visió directa (LOS). En conseqüència, els enllaços BS-RS presenten una

elevada SNR, i per aquest motiu podrem aplicar els resultats obtinguts pel canal interferent. Finalment, la duració de cadascun d' aquests dos salts, així com la potència transmesa per cada estació base es dissenyaran a través de la planificació de recursos, tenint en compte l' eficiència espectral i criteris de justícia entre usuaris.

Resumen

Los sistemas de comunicaciones móviles han experimentado grandes avances en los últimos años. Desde que los primeros sistemas celulares de telefonía móvil aparecieron, la demanda por parte de los usuarios se ha incrementado a un ritmo muy elevado que, junto con el hecho de que el ancho de banda radioeléctrico es limitado y se ha de compartir, ha provocado que los sistemas de comunicación actuales hayan llegado a su límite. Por este motivo es necesaria la investigación de nuevos sistemas de transmisión inalámbrica más eficientes para poder cubrir esta demanda. La investigación e implementación de estos sistemas abarca varias áreas de conocimiento: desde la electrónica utilizada en las antenas de los terminales hasta los protocolos de transmisión de datos, de los cuales se derivan los estándares.

Este trabajo trata sobre las transmisiones multi-antena y el uso de repetidores en redes celulares. Uno de los factores que limita la transmisión en estas redes es la interferencia, que puede ser intra-celda cuando es entre terminales de la misma celda e inter-celda, cuando es entre terminales de celdas diferentes. Por este motivo se estudiará el canal interferente de 3 pares transmisor-receptor, que es un modelo de canal que no está caracterizado totalmente. Dada su dificultad, desde hace unos años la mayoría de trabajos en la materia han optado por estudiar su comportamiento a muy alta relación señal ruido (SNR). En este contexto, una de las estrategias que ha tomado más fuerza es la llamada *interference alignment* (alineación de interferencia). En este trabajo se diseñarán precodificadores lineales en función del número de antenas en los terminales siguiendo esta estrategia y otras. El objetivo es claro: abordar la gestión de la interferencia y mejorar la recepción de las señales deseados. Para ello, se caracterizarán algunas propiedades del canal interferente (*grados de libertad*) para ciertas configuraciones de antenas llegando a resultados que hasta ahora sólo se habían mostrado como cotas superiores.

A continuación, se considerará un red celular multi-salto donde cada celda contenga una estación base (BS), varios repetidores (RS) y una gran cantidad de estaciones móviles (MS). Entendemos por estación móvil cualquier terminal que sea capaz de mantener una comunicación inalámbrica con el ancho de banda correspondiente y con la posibilidad de que el terminal esté en movimiento, bien sea un teléfono móvil, un ordenador portátil, etc. La transmisión se divide en dos saltos en los que se envían mensajes primero desde la estación base al repetidor y seguidamente, del repetidor en la estación móvil. El sistema de comunicaciones asume que durante el primer salto todas las BS transmiten simultáneamente, y por lo tanto podemos modelar el primer salto como un canal

interferente. En general ambos terminales se instalan en lugares elevados y con visión directa (LOS). Así pues, los enlaces BS-RS presentan una elevada SNR, por lo que podremos aplicar los resultados obtenidos para el canal interferente. Finalmente, la duración de cada uno de estos dos saltos, así como la potencia transmitida por cada estación base se diseñarán a través de la planificación de recursos teniendo en cuenta la eficiencia espectral y criterios de justicia entre usuarios.

Abstract

Mobile communication systems have experienced great advances in recent years. Since the first mobile cellular systems appeared, the demand from users has increased at a very high rate and, together with the fact that the bandwidth is limited and must be shared, it has caused that existing communication systems have reached their limit. As a consequence, it is necessary to search for new more efficient systems to meet this demand. The research and implementation of these systems includes several knowledge areas: from electronics used in the terminals to the data transmission protocols, which are derived in standards.

This work deals with multi-antenna transmissions and the use of relays in cellular networks. One of the factors limiting the transmission in these networks is interference, which can be intra-cell when it is between terminals of the same cell and inter-cell, when it is between terminals of different cells. For this reason we study the interference channel of 3 pairs transmitter-receiver, a channel model that is not fully characterized. Given the difficulty, since recent years most works in the field have chosen to study their behavior at very high signal to noise ratio (SNR). In this context, one strategy that has become more relevant is called *interference alignment*. In this work, linear precoders are designed based on the number of antennas at the terminals following this strategy and others. The goal is clear: address the management of interference and improve the reception of the desired signals. In this regard, we characterize some properties of the channel interference (*degrees of freedom*) for certain configurations of antennas reaching results so far only been shown as upper bounds.

Next, a multi-hop cellular network is considered where each cell contains a base station (BS), several relay stations (RS) and a large number of mobile stations (MS). We understand a mobile station as any terminal being able to maintain wireless communication with an appropriated bandwidth and the possibility to be in motion, either a cell phone, laptop, etc. The transmission is divided into two hops in which messages are sent first from the BS to the RS, and last from the RS to the MS. The communications system assumes that during the first hop all BSs transmit simultaneously, and therefore we can model the first hop as an interference channel. Likewise, in general both terminals are installed in high places with line of sight (LOS). Thus, the BS-RS links might have a high SNR, and hence we can apply the results obtained for the interference channel. Finally, the duration of each

of these two hops and the power transmitted by each BS is designed by means of the resource allocation, taking into account the spectral efficiency and fairness criteria between users.

1 INTRODUCTION

The wireless communications started with the first Morse code transmission by Guglielmo Marconi in 1895. However, until the mid-90, wireless communications were used only for broadcasting purposes such as radio and television distribution. Those networks allowed the users to receive information from a given source but not to use the reverse link. Last decades have witnessed a high proliferation of wireless services and devices such as mobile communications, WiFi or cordless phones, as a consequence of trying to satisfy the demand of *anywhere and anytime service*.

In contrast to wired communications, wireless communications present three important drawbacks: *radio spectrum scarcity*, *channel impairments* and *interference*.

On the one hand, the wireless radio spectrum is scarce. For example, the spectrum band envisioned for the mobile communications is 400 MHz – 3.5 GHz, but other services work in some parts of the spectrum, such as the Digital Terrestrial Television or WiFi, using 470-862 MHz and 2 GHz, respectively. The transmission coding strategy should be efficient in terms of bandwidth occupied.

On the other hand, the wireless channel presents several channel impairments, such as multipath fading, shadowing, pathloss or interference [1].

One way to combat the channel impairments is by means of diversity, improving the reliability of the wireless communication systems. The common attempts to get benefits from diversity are by means of time or frequency division multiplexing (TDM and FDM) so as to transmitting the same signal through different channels. Likewise, multiple antennas might be used for applying beamforming techniques based on the direction of arrival (DOA) of the transmitted signal, when there is Channel State Information at the Transmitter side (CSIT).

However, since mid-90s it is known that the use of multiple antennas at the source and the destination (multiple-input multiple-output, MIMO channel) allows increasing the transmitted rate compared with the single-antenna case. Such gain is known as *multiplexing gain*. Telatar showed in [2] that the capacity of the point-to-point MIMO channel increases linearly with the minimum number of transmitting and receiving antennas. Since then, researchers and scientists around the world have paid a lot of attention to adapt all the developed theory of the single-input single-output (SISO) channel to the MIMO case.

The multi-user communications are commonly grouped in different multi-user channels depending on the interaction and the role of the different terminals involved in the communication. Figure 1 depicts the principal multi-user channels: Broadcast channel (BC), Multiple Access channel (MAC) and Interference channel (IC),

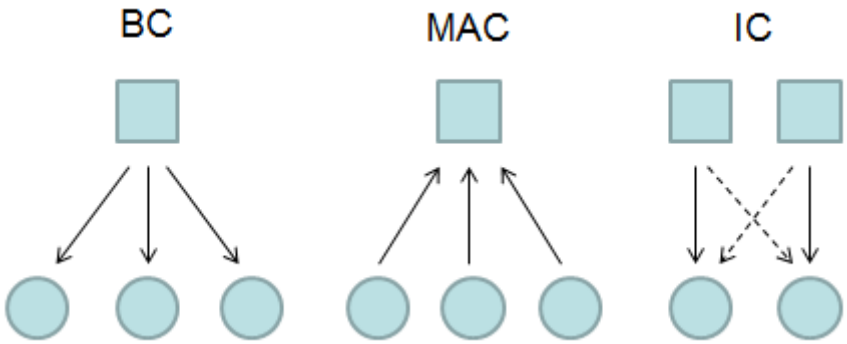

Figure 1: Channel classification. Broadcast Channel, Multiple Access Channel and *K*-user Interference Channel for $K = 2$. Solid lines represent intended transmissions while dashed lines represent unintended transmissions.

The BC models the downlink transmission in a cellular communication system, where one transmitter, which is commonly a BS, sends independent messages to multiple destinations or MSs. The MAC can address the uplink transmissions in a cellular system where multiple sources (MSs) send independent messages to a single destination (BS). These two channels have been widely characterized during the last three decades [3]. Finally, the IC, or more precisely the *K*-user IC, models the scenario where K source-destination pairs coexist in the same area, generating interference one to each other. In contrast to the BC and MAC, this channel is not completely characterized.

Finally, the *X*-channel, presented in Figure 2, models the situation where two sources communicate with two destinations. In contrast to the IC, here each source has independent messages intended to the two destinations. That channel subsumes the BC, MAC and IC.

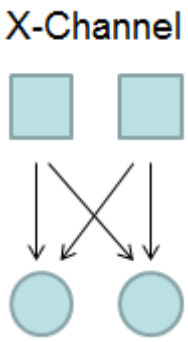

Figure 2: X channel

The capacity region of the IC is not known completely, but it is possible to analyze its *degrees of freedom* when the SNR is arbitrarily high [9][10]. The degrees of freedom (DoF) can be seen as the maximum number of messages transmitted in one channel use, and can be derived for all type of channels. Likewise, some strategies and precoding schemes which are DoF-optimal for the X-channel can be extended to the IC, such as interference alignment [16] and zero-forcing precoding [8].

The present work addresses the 3-user MIMO IC providing the following contributions:

- Improve the degrees of freedom upper bound
- Design linear MIMO precoders for any antenna configuration
- Show that the obtained DoF innerbound meets the DoF outerbound for many antenna configurations and hence, the DoF are established.

Cellular networks can be described with the channel models depicted in Figure 1 and Figure 2. These networks are composed of multiple cells, each one with one BS and MSs. Some results [3][4] showed that the introduction of a new terminal, named relay, could improve the performance of the system combating the channel impairments due to the shadowing and path-loss provided on the BS-MS links. However, the application of the relay-assisted transmission into practical systems was constrained by the current radio technology, which could not transmit and receive simultaneously in the same band. As a consequence, the RSs must operate in half-duplex mode, which impacts negatively on the theoretical improvements because of the use of relays and it discarded for a long time the use of relays. In this regard, recent results have been shown that although relays are not operating in full-duplex mode, they could also improve the

performance of cellular systems [5][6]. We consider the use of relays forwarding the message. In this regard, the transmission is divided in two hops. In the first hop, BSs transmit messages to the RS whereas in the second hop the RS transmit the same messages to the MS.

The contributions provided in this area are:

- Apply the linear transmit precoders derived for the IA scenario in the first-hop of a relay-assisted cellular network (RACN).
- Design the radio resource allocation considering the maximization of different criteria.

This work is organized as follows. Chapter 2 is a review of the MIMO channel, where some concepts that will be assumed next are explained. Chapter 3 addresses the analysis of the 3-user MIMO IC, providing upper bounds for the DoF of the channel and precoding schemes to approach them and, when it is possible, to achieve these upper bounds. Using the results of Chapter 3, an application of these precoding schemes for a RACN is presented in Chapter 4. Finally, conclusions and future work are stated in Chapter 5.

2 MIMO CHANNEL

This chapter reviews the MIMO channel. In this regard, section 2.1 presents the channel model, introducing the structure of the transmitted signal. Section 2.2 reviews the mutual information of that channel and how it can be approximated at high SNR. Section 2.3 introduces how the MIMO transmit precoder can be optimized in order to maximize the capacity in the low-medium SNR with maximum power constraint. This is done by the water-filling algorithm. Section 2.4 shows how to model the transmission through multiple channel uses, commonly known as time extension. Later, in section 2.5 we introduce the reciprocity property of the MIMO channels. Basically, it summarizes that we can guarantee the obtained MIMO capacity when terminal *A* is the source and terminal *B* is the destination, remains the same if terminal *B* and *A* become the source and the destination, respectively. We would like to emphasize that time extension and reciprocity will be two important concepts employed for dealing with the MIMO IC in chapter 3. Finally, section 2.6 addresses the transmission through multiple carriers using orthogonal frequency division multiplexing (OFDM).

2.1 CHANNEL MODEL

The point-to-point MIMO channel is obtained when source and destination are equipped with *M* and *N* antennas, respectively. Assuming a non-frequency selective channel, the signal received at the destination is characterized by:

$$\mathbf{y} = \mathbf{H}\mathbf{s} + \mathbf{n} \tag{1}$$

where $\mathbf{y} \in \mathbb{C}^{N\times 1}$ is the received signal vector, $\mathbf{H} \in \mathbb{C}^{N\times M}$ is the channel matrix where element $h_{ij}, i = 1...N, j = 1...M$ represents the channel gain between the jth antenna at the transmitter and the ith antenna at the receiver; $\mathbf{s} \in \mathbb{C}^{M\times 1}$ is the Gaussian transmitted signal and $\mathbf{n} \in \mathbb{C}^{N\times 1}$ is the additive white Gaussian noise (AWGN) vector at the receiver. We assume all noise terms are independent and identically distributed (i.i.d) zero mean complex Gaussian with power σ_n^2. Moreover, the channel coefficients are constant along the transmission time and perfect channel state information at the transmitter (CSIT) is assumed.

The transmitted signal is given by:

$$\mathbf{s} = \mathbf{V}\mathbf{x} \tag{2}$$

where $\mathbf{V} \in \mathbb{C}^{M \times d}$ denotes the transmit precoding matrix and $\mathbf{x} \in \mathbb{C}^{d \times 1}$ becomes the transmitted bitstream consisting of d Gaussian complex symbols.

2.2 MIMO MUTUAL INFORMATION

Channel capacity is defined as the maximum amount of information that can be reliably transmitted over a communications channel [3]. By the noisy-channel coding theorem, the channel capacity of a given channel is the limiting information rate (in units of information per unit time) that can be achieved with arbitrarily small error probability. For example, a channel capacity of $z\ bps/Hz$ implies that the maximum rate at which we can send information over the channel and recover the information at the output with a vanishingly low probability of error is $z\ bps/Hz$. Given the signal model depicted in (1), the general formula for the mutual information between transmitter and receiver of the MIMO channel in bps/Hz is [2][3]:

$$I(\mathbf{x};\mathbf{y}) = \log_2 \left| \mathbf{I} + \mathbf{H}\mathbf{R}_s\mathbf{H}^H\mathbf{R}_n^{-1} \right| \tag{3}$$

where $\mathbf{R}_s$ and $\mathbf{R}_n$ are the covariance transmit matrix and the covariance noise matrix respectively. The capacity is defined as the maximum value of the mutual information for a given channel:

$$C = \max_{\mathbf{s}} I(\mathbf{x};\mathbf{y}) = \max_{\mathbf{R}_s, tr(\mathbf{R}_s) < P_{x,\max}} \log_2 \left| \mathbf{I} + \mathbf{H}\mathbf{R}_s\mathbf{H}^H\mathbf{R}_n^{-1} \right| \tag{4}$$

where $P_{s,\max} = tr(\mathbf{R}_s)$ denotes the sum of the diagonal of $\mathbf{R}_s$ and is the total transmitted power. When there is not available CSIT, the best transmission strategy in terms of mutual information becomes equal power allocation per antenna [12], so the covariance transmit matrix becomes

$$\mathbf{R}_s = \frac{P_{s,\max}}{M}\mathbf{I} \tag{5}$$

On the other hand, section 2.3 addresses the proper transmission strategy when there is CSIT. For simplicity, we assume AWGN and hence the covariance noise matrix is given by:

$$\mathbf{R}_n = \sigma_n^2 \mathbf{I} \tag{6}$$

and the signal to noise ratio (SNR) is defined by,

$$\rho = \frac{P_{s,\max}}{\sigma_n^2} \tag{7}$$

Then, equation (3) becomes

$$I(\mathbf{x};\mathbf{y}) = \log_2 \left| \mathbf{I} + \frac{P_{s,\max}}{M\sigma_n^2} \mathbf{H}\mathbf{H}^H \right| = \log_2 \left| \mathbf{I} + \frac{\rho}{M} \mathbf{H}\mathbf{H}^H \right| \tag{8}$$

However, it is important to remark that all the mutual information and capacity analysis in this section could be done without the assumption of AWGN noise, considering an equivalent channel which is given by,

$$\mathbf{H}_{eq} = \mathbf{R}_n^{-1/2} \mathbf{H} \tag{9}$$

where $\mathbf{R}_n^{-1/2}$ is square root of the inverse of the noise correlation matrix. The square root of a matrix can be computed as setting its singular values equal to their square root. In such a case, we could derive an expression similar to (8).

In the following, we write the mutual information as a function of the singular values of the channel matrix. For this purpose, let us define the singular value decomposition (SVD) of matrix $\mathbf{H}$ as follows [13]:

$$\mathbf{H} = \mathbf{T}\Lambda\mathbf{S}^H \tag{10}$$

where $\mathbf{T} \in \mathbb{C}^{N\times N}$ and $\mathbf{S} \in \mathbb{C}^{M\times M}$ are unitary matrices commonly denoted by the left and the right singular vectors respectively and $\mathbf{\Lambda} \in \mathbb{C}^{N\times M}$ is a diagonal matrix containing the singular vectors $\lambda_i, i = 1...rank(\mathbf{H})$ of $\mathbf{H}$. From this result and using the identity $|\mathbf{I} + \mathbf{AB}| = |\mathbf{I} + \mathbf{BA}|$ it follows that (8) can be written as:

$$\lim_{\rho\to\infty} I(\mathbf{x};\mathbf{y}) = \lim_{\rho\to\infty} \sum_{i=1}^{rank(\mathbf{H})} \log_2\left(1+\frac{\rho}{M}\lambda_i^{\,2}\right) = rank(\mathbf{H}) \lim_{\rho\to\infty} \log_2(\rho) + \sum_{i=1}^{rank(\mathbf{H})} \log_2\left(\frac{\lambda_i^{\,2}}{M}\right) \quad (11)$$

The expression (11) for the mutual information can be interpreted as the sum of the mutual information in $rank(\mathbf{H})$ *spatial channels*, being λ_i^2 the channel gain of the ith spatial channel. At the high SNR regime the mutual information can be approximated by [1]:

$$\lim_{\rho\to\infty} I(\mathbf{x};\mathbf{y}) = \lim_{\rho\to\infty} \sum_{i=1}^{rank(\mathbf{H})} \log_2\left(1+\frac{\rho}{M}\lambda_i^{\,2}\right) \approx rank(\mathbf{H}) \lim_{\rho\to\infty} \log_2(\rho) + \sum_{i=1}^{rank(\mathbf{H})} \log_2\left(\frac{\lambda_i^{\,2}}{M}\right) \quad (12)$$

where the second term does not depends on the SNR. We define the *multiplexing gain* of the MIMO channel, which is generally referred to as the *spatial degrees of freedom* (DoF) as:

$$d = \lim_{\rho\to\infty} \frac{C(\rho)}{\log_2(\rho)} = rank(\mathbf{H}) \quad (13)$$

Notice that for a full-rank channel matrix the *DoF* are equal to $\min(M,N)$, that becomes the slope of the capacity curve when it is plotted versus $\log_2(\rho)$. Likewise, the number of *DoF* can be interpreted as the number of spatial channels between the transmitter and the receiver and thus, the number of symbols that can be transmitted without interference.

As a consequence, for $M < N$ one additional antenna at the transmitter increases by one the DoF and hence the slope of the curve, whereas if one additional antenna is placed on the receiver the DoF remain the same and the gain will be observed on the second term of (12), i.e the offset of the curve [1]. Figure 3 shows how the mutual information grows linearly with the $\min(M,N)$. For $(M,N)=(4,4)$ the slope of the curve at high SNR is the greatest, whereas for $(M,N)=(4,3)$ the offset of the curve is greater than the $(M,N)=(3,3)$ case.

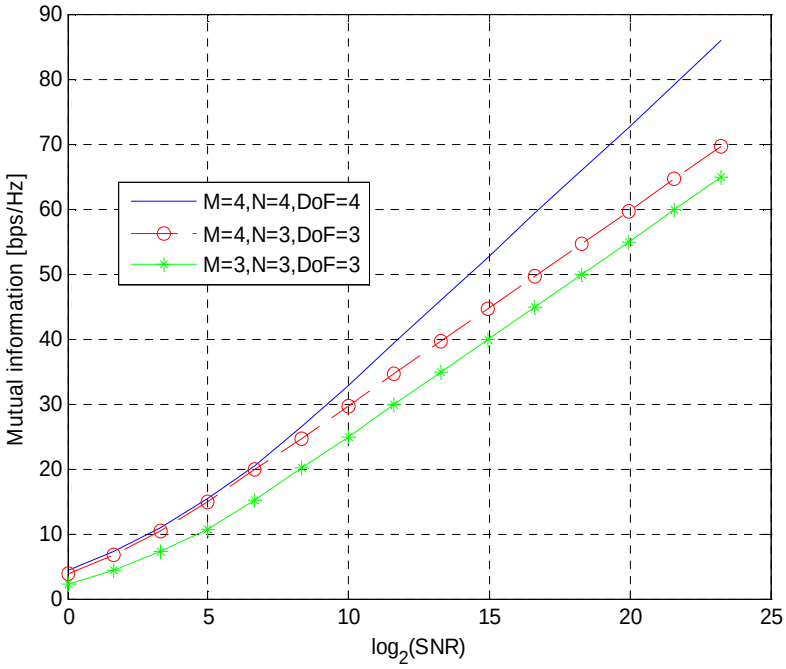

Figure 3: Mutual information in bps/Hz as a function of $\log_2$(SNR) for a MIMO channel for 3 different pairs (M, N)

2.3 MIMO CAPACITY: WATER-FILLING

The capacity of the MIMO Channel is obtained when assuming CSIT. In such a case, the precoding matrix is obtained as a result of the mutual information maximization (4):

$$C = \max_{\mathbf{s}} I(\mathbf{x};\mathbf{y}) = \max_{\mathbf{R}_s, tr(\mathbf{R}_s)<P_{x,\max}} \log_2 \left| \mathbf{I} + \mathbf{H}\mathbf{R}_s\mathbf{H}^H\mathbf{R}_n^{-1} \right|$$

where the transmit correlation matrix $\mathbf{R}_s$ is given by:

$$\mathbf{R}_s = \mathbf{V}\mathbf{R}_x\mathbf{V}^H \tag{14}$$

where $\mathbf{R}_x$ is the symbol correlation matrix. There are d bitstreams with uncorrelated and Gaussian symbols with variance equal to one, that is,

$$\mathbf{R}_x = E\left\{\mathbf{x}\mathbf{x}^H\right\} = \mathbf{I} \tag{15}$$

Let us assume the structure of matrix $\mathbf{V}$ is designed as the product of two matrices:

$$\mathbf{V} = \mathbf{U}P_{s,\max}\mathbf{\Sigma}^{1/2} = \mathbf{U}P_{s,\max}\begin{bmatrix} \sqrt{\phi_1} & 0 & \dots & 0 \\ 0 & \sqrt{\phi_2} & & \\ \vdots & & \ddots & \\ 0 & & & \sqrt{\phi_d} \end{bmatrix} \tag{16}$$

where $\mathbf{U} \in \mathbb{C}^{M\times d}$ is a unitary matrix and $\mathbf{\Sigma}^{1/2} \in \mathbb{C}^{d\times d}$ denotes a diagonal matrix whose elements ϕ_i stand for the fractional power allocation at the ith symbol, with the following constraint:

$$\sum_{i=1}^{d} \phi_i = 1 \tag{17}$$

In order to design matrix $\mathbf{V}$ let us decompose the channel matrix using the SVD,

$$\mathbf{H} = \mathbf{T}\boldsymbol{\Lambda}\mathbf{S}^H$$
$$\mathbf{S} = \begin{bmatrix} \mathbf{S}_1 & \mathbf{S}_2 \end{bmatrix} \qquad \boldsymbol{\Lambda} = \begin{bmatrix} \boldsymbol{\Lambda}_1 & \mathbf{0} \\ \mathbf{0} & \boldsymbol{\Lambda}_2 \\ \mathbf{0} & \mathbf{0} \end{bmatrix} \tag{18}$$

where $\mathbf{S}_1 \in \mathbb{C}^{M\times d}$ corresponds to the right singulars vectors associated to the highest d eigenvalues of $\mathbf{H}$, $\mathbf{S}_2 \in \mathbb{C}^{M\times M-d}$ are the remaining $M-d$ right singular vectors of $\mathbf{H}$, $\boldsymbol{\Lambda}_1 \in \mathbb{C}^{d\times d}$ is a diagonal matrix containing singular values associated to the right singular vectors in $\mathbf{S}_1$, while $\boldsymbol{\Lambda}_2 \in \mathbb{C}^{N-d\times N-d}$ contains the singular values associated to the right singular vectors in $\mathbf{S}_2$ Notice that here we assume $N>M$, but an alternating formulation could be expressed for the $M>N$ case.

Therefore, assuming AWGN noise, the mutual information may be upper bounded as follows:

$$I(\mathbf{x};\mathbf{y}) = \log_2\left|\mathbf{I} + \frac{1}{\sigma_n^2}\mathbf{H}\mathbf{R}_s\mathbf{H}^H\right| = \log_2\left|\mathbf{I} + \rho\mathbf{T}\boldsymbol{\Lambda}\mathbf{S}^H\mathbf{U}\boldsymbol{\Sigma}\mathbf{U}^H\mathbf{S}\boldsymbol{\Lambda}^H\mathbf{T}^H\right| =$$
$$= \log_2\left|\mathbf{I} + \rho\boldsymbol{\Lambda}\mathbf{S}^H\mathbf{U}\boldsymbol{\Sigma}\mathbf{U}^H\mathbf{S}\boldsymbol{\Lambda}^H\right| = \log_2\left|\mathbf{I} + \rho\boldsymbol{\Lambda}\tilde{\mathbf{R}}_s\boldsymbol{\Lambda}^H\right| \le \prod_{i=1}^{rank(\mathbf{H})}\log_2\left(1+\rho\lambda_i^2\left(\tilde{\mathbf{R}}_s\right)_{ii}\right) \tag{19}$$

where $(\ )_{ii}$ denotes the element on the ith row and the ith column. This inequality is satisfied with equality when $\tilde{\mathbf{R}}_s$ is a diagonal matrix. Therefore, by selecting the matrix $\mathbf{U}$ equal to

$$\mathbf{U} = \mathbf{S}_1 \tag{20}$$

the mutual information is maximized:

$$I(\mathbf{x};\mathbf{y}) = \log_2 \left| \mathbf{I} + \rho \mathbf{\Lambda} \mathbf{S}^H \mathbf{U} \mathbf{\Sigma} \mathbf{U}^H \mathbf{S} \mathbf{\Lambda}^H \right| = \log_2 \left| \mathbf{I} + \rho \mathbf{\Lambda} \begin{bmatrix} \mathbf{S}_1^H \\ \mathbf{S}_2^H \end{bmatrix} \mathbf{U} \mathbf{\Sigma} \mathbf{U}^H \left(\mathbf{\Lambda} \begin{bmatrix} \mathbf{S}_1^H \\ \mathbf{S}_2^H \end{bmatrix} \right)^H \right| =$$

$$= \log_2 \left| \mathbf{I} + \rho \begin{bmatrix} \mathbf{\Lambda}_1 \mathbf{S}_1^H \\ \mathbf{\Lambda}_2 \mathbf{S}_2^H \\ \mathbf{0} \end{bmatrix} \mathbf{S}_1 \mathbf{\Sigma} \mathbf{S}_1^H \begin{bmatrix} \mathbf{\Lambda}_1 \mathbf{S}_1^H \\ \mathbf{\Lambda}_2 \mathbf{S}_2^H \\ \mathbf{0} \end{bmatrix}^H \right| = \log_2 \left| \mathbf{I} + \rho \begin{bmatrix} \mathbf{\Lambda}_1 \\ \mathbf{0} \\ \mathbf{0} \end{bmatrix} \mathbf{\Sigma} \begin{bmatrix} \mathbf{\Lambda}_1 \\ \mathbf{0} \\ \mathbf{0} \end{bmatrix}^H \right| = \tag{21}$$

$$= \log_2 \left| \mathbf{I} + \rho \mathbf{\Lambda}_1^H \mathbf{\Lambda}_1 \mathbf{\Sigma} \right| = \sum_{i=1}^{d} \log_2 \left(1 + \rho \lambda_i^2 \phi_i \right)$$

where the maximum value of d is given by:

$$d = rank(\mathbf{H}) \tag{22}$$

Once defined matrix **U** (20), the power allocation over the different modes of the channel can be obtained as the solution of the following optimization problem shown in (23), which maximizes the mutual information, (21), subject to a power constraint, (17):

$$\begin{aligned} &\max_{\phi_i} \sum_{i=1}^{d} \log_2 \left(1 + \rho \phi_i \lambda_i^2 \right) \\ &\text{s.t} \quad \phi_i \geq 0 \\ &\sum_{i=1}^{d} \phi_i = 1 \end{aligned} \tag{23}$$

The optimum relative power allocated at each channel mode ϕ_i leads to the water-filling solution [1]:

$$\phi_i = \left(\mu - \frac{1}{\lambda_i^2 \rho} \right)^+ \tag{24}$$

where $(a)^+ = \max(a, 0)$ and μ is a Lagrange multiplier satisfying:

$$\sum_{i=1}^{d} \left(\mu - \frac{1}{\lambda_i^2 \rho} \right)^+ = 1 \tag{25}$$

The optimum solution is given by:

$$\phi_i = \left(\frac{1}{d} + \frac{1}{\rho d} \sum_{k=1}^{d} \frac{1}{\lambda_k^2} - \frac{1}{\lambda_i^2 \rho} \right)^+ , i = 1...d \tag{26}$$

Therefore, capacity can be rewritten as,

$$\begin{aligned} C &= \sum_{i=1}^{d} \log_2 \left(1 + \rho \lambda_i^2 \left(\frac{1}{d} + \frac{1}{\rho d} \sum_{k=1}^{d} \frac{1}{\lambda_k^2} - \frac{1}{\lambda_i^2 \rho} \right)^+ \right) \approx \sum_{i=1}^{d} \log_2 \left(\rho \lambda_i^2 \left(\frac{1}{d} + \frac{1}{\rho d} \sum_{k=1}^{d} \frac{1}{\lambda_k^2} - \frac{1}{\lambda_i^2 \rho} \right)^+ \right) = \\ &= d \log_2 (\rho) + \sum_{i=1}^{d} \log_2 \left(\lambda_i^2 \left(\frac{1}{d} + \frac{1}{\rho d} \sum_{k=1}^{d} \frac{1}{\lambda_k^2} - \frac{1}{\lambda_i^2 \rho} \right)^+ \right) \end{aligned} \tag{27}$$

where it can be observed that assuming CSIT does not increase the degrees of freedom achieved.

In the Figure 4 we simulate the same 3×4 channel matrix using water-filling and equal power allocation:

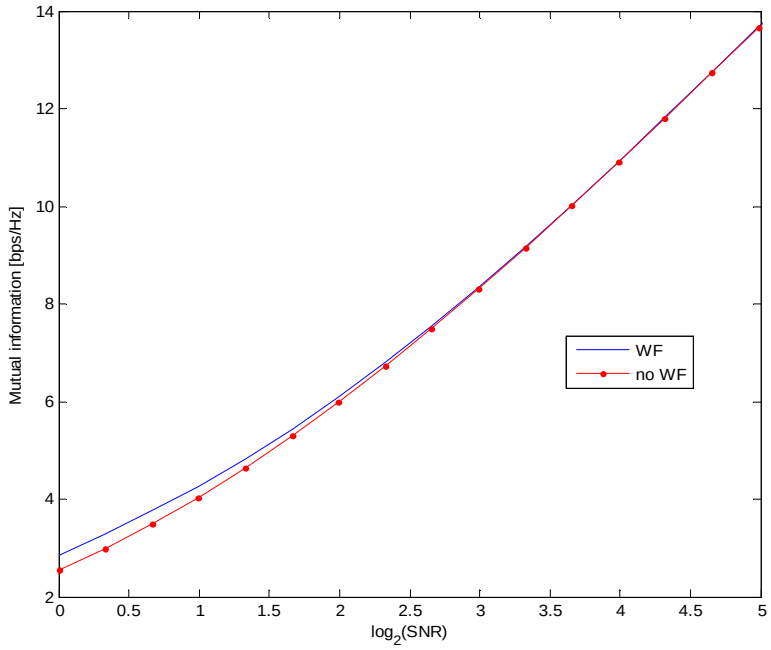

Figure 4: Mutual information in bps/Hz as a function of $\log_2$(SNR) with and wihout assuming CSIT for the same 3×4 channel matrix coefficients.

From the figure it can be seen that power allocation is useful when the SNR is low. When the SNR is sufficiently high, the mutual information achieved is the same. Table

1 and Table 2 show the relative power of each mode for each one of these two power allocation techniques for some values of the SNR:

SNR(dB)	0	5	10
Mode 1	0.78	0.538	0.39
Mode 2	0.21	0.356	0.34
Mode 3	0	0.10	0.26

Table 1: Relative power allocation using water-filling algorithm for SNR=0,5,10 dB

SNR(dB)	0	5	10
Mode 1	0.33	0.33	0.33
Mode 2	0.33	0.33	0.33
Mode 3	0.33	0.33	0.33

Table 2: Relative power allocation using equal power allocation for SNR= 0,5,10 dB

Hence, at medium and low SNR there might be some cases where capacity is achieved using a number of spatial modes lower than the total degrees of freedom d. In such a case, the power is distributed along the modes with the highest channel gain and the spatial modes with lowest channel gain are not used. For example, when SNR=0 we observe that no power has been allocated to mode 3. However, if the SNR is high, all the modes are used an almost equally powered. As a consequence, with power limitation mutual information is not always maximized if the degrees of freedom used are maximized.

.

2.4 TIME-EXTENSION

When our transmission is carried out through a time or frequency-selective channel, it could be profitable to transmit over different time slot or frequency bands in order to improve the diversity of the system. In such a case, the power allocation over

the different resources has to be optimized, getting the water-filling solution. Since it is equivalent to consider transmission by different frequency bands or time slots, for simplicity we consider only transmission along different time slots and we refer to that option as time extension. The received signal over T time slots since an arbitrary time instance t_0 is given by:

$$\begin{aligned} \mathbf{y}(t_0) &= \mathbf{H}(t_0)\mathbf{s}(t_0) + \mathbf{n}(t_0) \\ \mathbf{y}(t_0+1) &= \mathbf{H}(t_0+1)\mathbf{s}(t_0+1) + \mathbf{n}(t_0+1) \\ &\vdots \\ \mathbf{y}(t_0+T-1) &= \mathbf{H}(t_0+T-1)\mathbf{s}(t_0+T-1) + \mathbf{n}(t_0+T-1) \end{aligned} \tag{28}$$

which can be rewritten in a matrix form as follows:

$$\bar{\mathbf{y}}(t_0,T) = \bar{\mathbf{H}}(t_0,T)\bar{\mathbf{s}}(t_0,T) + \bar{\mathbf{n}}(t_0,T) \tag{29}$$

where $\bar{\mathbf{y}}(t_0,T)$, $\bar{\mathbf{s}}(t_0,T)$ and $\bar{\mathbf{n}}(t_0,T)$ are:

$$\bar{\mathbf{y}}(t_0,T) = \begin{bmatrix} \mathbf{y}(t_0) \\ \mathbf{y}(t_0+1) \\ \vdots \\ \mathbf{y}(t_0+T-1) \end{bmatrix} \quad \bar{\mathbf{s}}(t_0,T) = \begin{bmatrix} \mathbf{s}(t_0) \\ \mathbf{s}(t_0+1) \\ \vdots \\ \mathbf{s}(t_0+T-1) \end{bmatrix} \quad \bar{\mathbf{n}}(t_0,T) = \begin{bmatrix} \mathbf{n}(t_0) \\ \mathbf{n}(t_0+1) \\ \vdots \\ \mathbf{n}(t_0+T-1) \end{bmatrix} \tag{30}$$

and $\bar{\mathbf{H}}(t_0,T)$ is the time extension of the channel matrix $\mathbf{H}(t)$, which is expressed as:

$$\bar{\mathbf{H}}(t_0,T) = \begin{bmatrix} \mathbf{H}(t_0) & \mathbf{0} & \cdots & \mathbf{0} \\ \mathbf{0} & \mathbf{H}(t_0+1) & & \\ \vdots & & \ddots & \\ \mathbf{0} & & & \mathbf{H}(t_0+T-1) \end{bmatrix} \tag{31}$$

The extended channel model can be interpreted considering that each row block of $\bar{\mathbf{s}}(t_0,T)$ is transmitted in different time-slots (or subcarrier frequency) and having in general different channel matrices. For example, the signal at the (t_0+1)th time instant $\mathbf{s}(t_0+1)$ travels through the channel matrix $\mathbf{H}(t_0+1)$. If channel matrices are constant, the extended channel matrix is expressed by:

$$\mathbf{H}(t) = \mathbf{H} \quad ,\forall t$$

$$\bar{\mathbf{H}}(t_0, T) = \mathbf{I}_T \otimes \mathbf{H} = \begin{bmatrix} \mathbf{H} & \mathbf{0} & \dots & \mathbf{0} \\ \mathbf{0} & \mathbf{H} & & \\ \vdots & & \ddots & \\ \mathbf{0} & & & \mathbf{H} \end{bmatrix} \tag{32}$$

where $\otimes$ is the Kronecker product.

Notice that when we apply the time extension, (29), we get an equivalent MIMO channel matrix having *TN* receiving antennas and *TM* transmitting antennas. Therefore, the waterfilling algorithm presented in section 2.3 can be applied in order to get the power allocation over the different channel uses as well as over the spatial channel modes.

2.5 RECIPROCITY

Here we show that there is reciprocity of linear precoding such that if transmit and receive antennas are exchanged and equal conditions of interference and noise are assumed at each side, the mutual information is not hurt. Consider a single user transmission with M antennas at the transmitter and N antennas at the receiver as shown in Figure 5 .

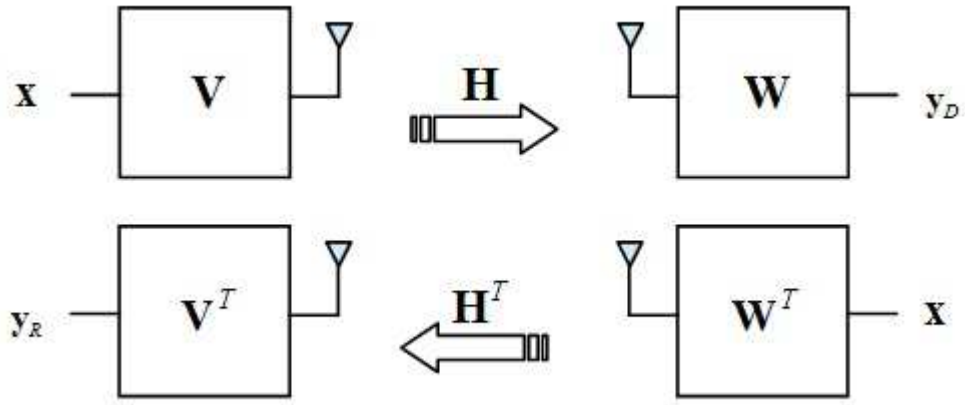

Figure 5: Direct Channel and Reciprocal Channel

Transmitter uses the $M \times d$ precoding matrix $\mathbf{V}$, while receiver uses the $d \times N$ receiver filter $\mathbf{W}$. The input-ouput relationship of the direct channel is:

$$\mathbf{y}_D = \mathbf{WHVx} + \mathbf{Wn}_T \tag{33}$$

where $\mathbf{H}$ is the $N \times M$ channel matrix, $\mathbf{x}$ is the $d \times 1$ AWGN transmitted bitstream, $\mathbf{n}_T$ is the $N \times 1$ AWGN noise term at the transmit side and the output of the direct channel is denoted by $\mathbf{y}_D$. Mutual information for the direct channel is equal to:

$$I(x; y_D) = \log_2 \left| \mathbf{I} + (\mathbf{WHV}) \mathbf{R}_x (\mathbf{WHV})^H \mathbf{R}_n^{-1} \right| \tag{34}$$

where the correlation matrix of the noise is given by:

$$\begin{aligned} \mathbf{R}_n &= E\left\{ (\mathbf{Wn})(\mathbf{Wn})^H \right\} = \mathbf{W} E\left\{ \mathbf{nn}^H \right\} \mathbf{W}^H = \mathbf{W} \mathbf{R}_{n_d} \mathbf{W}^H \\ \mathbf{R}_n^{-1} &= \left(\mathbf{W} \sigma_n^2 \mathbf{I} \mathbf{W}^H \right)^{-1} = \frac{1}{\sigma_n^2} \left(\mathbf{WW}^H \right)^{-1} \end{aligned} \tag{35}$$

Let us consider the SVD of matrix $\mathbf{W}$,

$$\begin{aligned} \mathbf{W} &= \mathbf{E\Pi F}^H \\ \mathbf{WW}^H &= \mathbf{E}\left(\mathbf{\Pi\Pi}^H \right) \mathbf{E}^H \\ \left(\mathbf{WW}^H \right)^{-1} &= \mathbf{E}^H \left(\mathbf{\Pi\Pi}^H \right)^{-1} \mathbf{E} \end{aligned} \tag{36}$$

where $\mathbf{E} \in \mathbb{C}^{d \times d}$, $\mathbf{\Pi} \in \mathbb{C}^{d \times N}$ and $\mathbf{F} \in \mathbb{C}^{N \times N}$. Remember that $\mathbf{W}$ is a $d \times N$ matrix with $d < N$ and hence, there would be some singular values equal to zero. (36) might be rewritten as follows:

$$\begin{aligned} \begin{bmatrix} & \mathbf{W} & \end{bmatrix} &= \mathbf{E} \begin{bmatrix} \mathbf{\Pi}_0 & \mathbf{0} \end{bmatrix} \mathbf{F}^H \\ \mathbf{WW}^H &= [\mathbf{E}] \begin{bmatrix} \mathbf{\Pi}_0 & \mathbf{0} \end{bmatrix} \begin{bmatrix} \mathbf{\Pi}_0^H \\ \mathbf{0} \end{bmatrix} [\mathbf{E}] = \mathbf{E\Pi}_0 \mathbf{\Pi}_0^H \mathbf{E}^H \\ \left(\mathbf{WW}^H \right)^{-1} &= \mathbf{E\Pi}_0^{-2} \mathbf{E}^H \end{aligned} \tag{37}$$

where $\mathbf{\Pi}_0 \in \mathbb{C}^{d \times d}$. Additionally, we consider an arbitrary correlation between the transmitted symbols. Since the correlation matrix is symmetric, the left and the right singular vectors are the same [13] and hence, the SVD can be written as

$$\mathbf{R}_x = \mathbf{U\Sigma U}^H \tag{38}$$

where $\mathbf{U},\mathbf{\Sigma}\in\mathbb{C}^{d\times d}$. As a consequence, (34) can be rewritten as follows:

$$\begin{aligned} I(\mathbf{x};\mathbf{y}_D) &= \log_2\left|\mathbf{I}+(\mathbf{WHV})\mathbf{U}\mathbf{\Sigma}\mathbf{U}^H(\mathbf{WHV})^H\frac{1}{\sigma_n^2}\left(\mathbf{WW}^H\right)^{-1}\right| = \\ &= \log_2\left|\mathbf{I}+(\mathbf{WHV})\mathbf{U}P_{T,\max}\tilde{\mathbf{\Sigma}}^{1/2}\tilde{\mathbf{\Sigma}}^{H/2}\mathbf{U}^H(\mathbf{WHV})^H\frac{1}{\sigma_n^2}\mathbf{E}\mathbf{\Pi}_0^{-2}\mathbf{E}^H\right| = \\ &= \log_2\left|\mathbf{I}+\rho(\mathbf{HV})\mathbf{U}\tilde{\mathbf{\Sigma}}^{1/2}\tilde{\mathbf{\Sigma}}^{H/2}\mathbf{U}^H(\mathbf{HV})^H\mathbf{W}^H\mathbf{E}\mathbf{\Pi}_0^{-2}\mathbf{E}^H\mathbf{W}\right| = \\ &= \log_2\left|\mathbf{I}+\rho(\mathbf{HV})\mathbf{U}\tilde{\mathbf{\Sigma}}^{1/2}\tilde{\mathbf{\Sigma}}^{H/2}\mathbf{U}^H(\mathbf{HV})^H\mathbf{F}\mathbf{\Pi}^H\mathbf{\Pi}_0^{-2}\mathbf{\Pi}\mathbf{F}^H\right| = \\ &= \log_2\left|\mathbf{I}+\rho\left(\mathbf{HVU}\tilde{\mathbf{\Sigma}}^{1/2}\right)\left(\mathbf{HVU}\tilde{\mathbf{\Sigma}}^{1/2}\right)^H\right| = \\ &= \log_2\left|\mathbf{I}+\rho\mathbf{A}\mathbf{A}^H\right| \end{aligned} \tag{39}$$

where $\mathbf{A}=(\mathbf{HV})\mathbf{U}\tilde{\mathbf{\Sigma}}^{1/2}$ and $\tilde{\mathbf{\Sigma}}$ is a normalized channel matrix such that $tr\left(\tilde{\mathbf{\Sigma}}\right)=1$.

For the reciprocal channel, the input-output relationship is:

$$\mathbf{y}_R = \mathbf{V}^T\mathbf{H}^T\mathbf{W}^T\mathbf{x}+\mathbf{V}^T\mathbf{n}_R{}^T \tag{40}$$

where $\mathbf{n}_R$ is the $N\times 1$ AWGN noise term at the receive side and it has the same statistical properties as $\mathbf{n}_T$. Thus, the mutual information of the reciprocal channel can be expressed as follows:

$$\begin{aligned} I(\mathbf{x};\mathbf{y}_R) &= \log_2\left|\mathbf{I}+\left(\mathbf{V}^T\mathbf{H}^T\mathbf{W}^T\right)\mathbf{R}_x\left(\mathbf{V}^T\mathbf{H}^T\mathbf{W}^T\right)^H\mathbf{R}_{n_R}^{-1}\right| \\ \mathbf{R}_{n_R} &= E\left\{\left(\mathbf{V}^T\mathbf{n}\right)\left(\mathbf{V}^T\mathbf{n}\right)^H\right\} = \mathbf{V}^T E\left\{\mathbf{n}\mathbf{n}^H\right\}\mathbf{V}^* = \mathbf{V}^T\mathbf{R}_{n_d}\mathbf{V}^* = \mathbf{V}^T\sigma_n^2\mathbf{V}^* \end{aligned} \tag{41}$$

Similarly to the direct channel, SVD can be applied to obtain:

$$\begin{aligned} I(\mathbf{x};\mathbf{y}_R) &= \log_2\left|\mathbf{I}+\rho\left((\mathbf{WHV})^T\right)\mathbf{U}\tilde{\mathbf{\Sigma}}^{1/2}\tilde{\mathbf{\Sigma}}^{H/2}\mathbf{U}^H\left((\mathbf{WHV})^*\right)\left(\mathbf{V}^T\mathbf{V}^*\right)^{-1}\right| = \\ &= \log_2\left|\mathbf{I}+\rho\mathbf{A}^T\mathbf{A}^*\right| \end{aligned} \tag{42}$$

Using $|\mathbf{B}|=|\mathbf{B}^*|$ for any matrix $\mathbf{B}$ and $|\mathbf{I}+\mathbf{AB}|=|\mathbf{I}+\mathbf{BA}|$ for any matrices $\mathbf{A},\mathbf{B}$ with suitable dimensions, the mutual information of the reciprocal channel results equal to the mutual information of the direct channel:

$$I(\mathbf{x};\mathbf{y}_R) = \log_2\left|\mathbf{I}+\rho\mathbf{A}^T\mathbf{A}^*\right| = \log_2\left|\left(\mathbf{I}+\rho\mathbf{A}^T\mathbf{A}^*\right)^*\right| = \\ = \log_2\left|\left(\mathbf{I}+\rho\mathbf{A}^H\mathbf{A}\right)\right| = \log_2\left|\left(\mathbf{I}+\rho\mathbf{A}\mathbf{A}^H\right)\right| = I(\mathbf{x};\mathbf{y}_D) \tag{43}$$

2.6 OFDM

This section reviews the orthogonal frequency division multiplexing (OFDM) scheme and extend this ideas to the MIMO case.

2.6.1 OFDM SISO

When the channel is time-varying or frequency selective we can multiplex the data over time or frequency slots, i.e. TDM and FDM, in order to avoid bad channel conditions. Hence, combating the channel variability and improving the system throughput. However, inter-symbol interference (ISI) comes up an additional drawback. In this regard, OFDM removes that drawback by using simpler transmitters and receivers than in the FDM or TDM cases.

OFDM is a frequency-division multiplexing scheme utilized as a digital multicarrier modulation method. A set of N_c independent orthogonal subcarriers are used to transmit data. A modulation with an alphabet of *M* symbols is encoded on each subcarrier, where $\log_2 M$ are the bits transmitted through each subcarrier. Let the transmitted signal at the *n*th time instant be:

$$s(n,k) = \frac{1}{\sqrt{N_c}}\sum_{i=0}^{N_c-1} x_i(n,k)e^{j\frac{2\pi}{N_c}i\cdot n}, \quad n = 0...N_c-1 \tag{44}$$

where x_i is a complex symbol of the modulation alphabet, k is the frame index and n is the time index. From (44), notice that the duration of each frame is N_c samples. Notice that (44) is the expression of a Discrete Fourier Transform (DFT). Conversely, the demodulation could be done by using inverse DFT (IDFT) at the receiver side. The OFDM system can be implemented as shown in Figure 6:

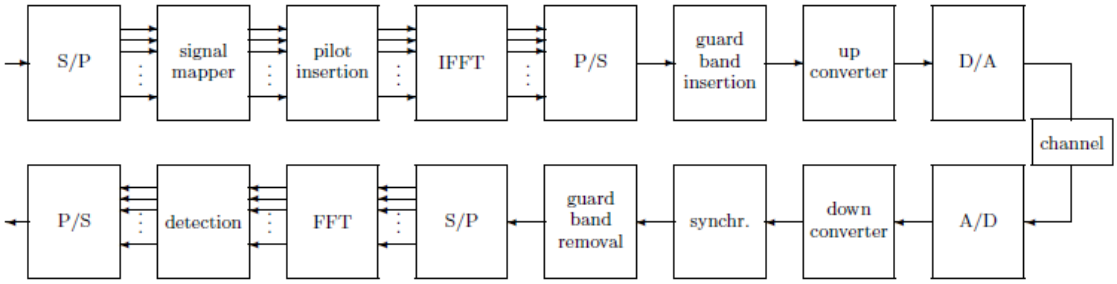

Figure 6: Block diagram of an OFDM system

Figure 7 shows the role of each index of the equation depicted in (44):

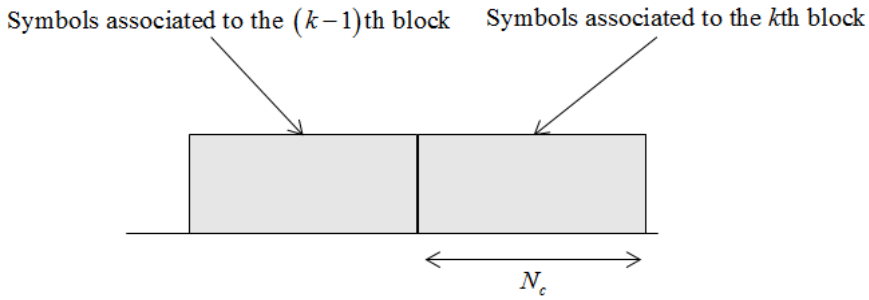

Figure 7: Two frames of the OFDM system without cyclic prefix

We assume that the channel remains the same during the transmission of each frame. Let the impulse response of the channel during the transmission of the kth frame be of duration P samples, i.e $h(n,k) \neq 0, n = 0...P-1$ with $0 \leq P \leq N_c$. The received signal is given by:

$$y(n,k) = h(n,k) * s(n,k) + w(n,k) = \sum_m h(n-m,k)\, s(m,k) + w(n,k) \qquad (45)$$

where $w(n)$ is the AWGN noise term and * is the convolution operator. The last expression can be rewritten in matrix form as:

$$\begin{bmatrix} y(0,k) \\ y(1,k) \\ \dots \\ y(N_c-1,k) \end{bmatrix} = \begin{bmatrix} h(0) & 0 & \dots & 0 & 0 & 0 & \dots & 0 \\ h(1) & & & & & 0 & \dots & 0 \\ \dots & & & & & & & \dots \\ h(P-2) & & & & & & & 0 \\ h(P-1) & & & & & & & 0 \\ 0 & & & & & & & \dots \\ \dots & & & & & & & \dots \\ 0 & \dots & & h(P-1) & h(P-2) & \dots & h(1) & h(0) \end{bmatrix} \begin{bmatrix} s(0,k) \\ s(1,k) \\ \dots \\ s(N_c-1,k) \end{bmatrix} +$$

$$+ \begin{bmatrix} 0 & 0 & \dots & 0 & h(P-1) & h(P-2) & \dots & h(1) \\ 0 & & & & & h(P-1) & \dots & h(2) \\ \dots & & & & & & & \dots \\ 0 & & & & & & & h(P-2) \\ 0 & & & & & & & h(P-1) \\ 0 & & & & & & & \dots \\ \dots & & & & & & & \dots \\ 0 & \dots & & 0 & 0 & \dots & 0 & 0 \end{bmatrix} \begin{bmatrix} s(0,k-1) \\ s(1,k-1) \\ \dots \\ s(N_c-1,k-1) \end{bmatrix} + \begin{bmatrix} w(0,k) \\ w(1,k) \\ \dots \\ w(N_c-1,k) \end{bmatrix} =$$

$$\mathbf{y}_k = \mathbf{H}_0\mathbf{s}_k + \mathbf{H}_1\mathbf{s}_{k-1} + \mathbf{w}_k \tag{46}$$

As a consequence, (46) shows that the received signal $\mathbf{y}_k$ can be written in terms of the desired received signal $\mathbf{H}_0\mathbf{s}_k$, the inter-symbol interference (ISI) $\mathbf{H}_1\mathbf{s}_{k-1}$ and the noise $\mathbf{w}_k$. In order to suppress the interference, OFDM uses a cyclic prefix strategy: the last G symbols of the $(k-1)$th frame are the same as the last symbols of the kth frame. The duration of the cyclic prefix must be greater than the channel impulse response:

$$G \geq P \tag{47}$$

The next figure shows how the cyclic prefix is introduced:

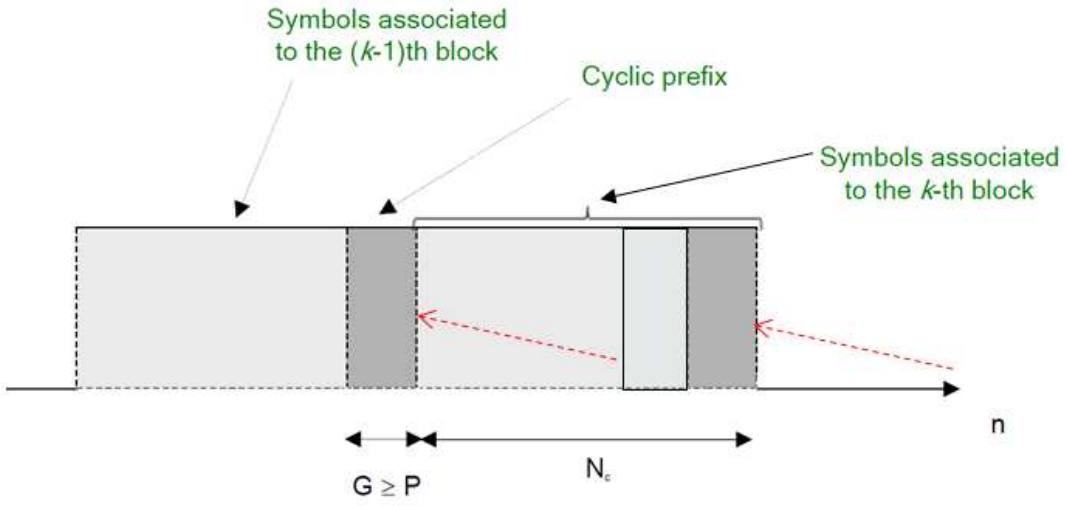

Figure 8: Two frames of the OFDM system with cyclic prefix

where it can be seen that the last symbols of the kth block are repeated at the last of the $(k-1)$th block. For simplicity, we assume $G = P$. As a consequence, (46) is simplified as follows:

$$\begin{bmatrix} y(0,k) \\ y(1,k) \\ \dots \\ y(N_c-1,k) \end{bmatrix} = \begin{bmatrix} h(0) & 0 & \dots & 0 & h(P-1) & h(P-2) & \dots & h(1) \\ h(1) & & & & & h(P-1) & \dots & h(2) \\ \dots & & & & & & & \dots \\ h(P-2) & & & & & & & h(P-2) \\ h(P-1) & & & & & & & h(P-1) \\ 0 & & & & & & & \dots \\ \dots & & & & & & & \dots \\ 0 & \dots & & h(P-1) & h(P-2) & \dots & h(1) & h(0) \end{bmatrix} \begin{bmatrix} s(0,k) \\ s(1,k) \\ \dots \\ s(N_c-1,k) \end{bmatrix} + \begin{bmatrix} w(0,k) \\ w(1,k) \\ \dots \\ w(N_c-1,k) \end{bmatrix}$$

$$\mathbf{y} = \mathbf{H}\mathbf{s} + \mathbf{w} \tag{48}$$

where, for simplicity, we suppress the frame index k.

From (48), it follows that $\mathbf{H}$ is a circulant matrix, i.e the rows are cyclic shifts of each other. It turns out for those type of matrices that the Fourier transform matrix becomes an eigenvector matrix of the channel. Hence the channel can be decomposed as,

$$\mathbf{H} = \mathbf{F}\boldsymbol{\Lambda}\mathbf{F}^H \tag{49}$$

where $\mathbf{F}$ is the Fourier transform matrix and $DFT_P(.)$ is the P samples DFT operator. Since $\mathbf{s}$ is the DFT of the symbols $\mathbf{x}$ (44), the channel can be diagonalized computing the IDFT of the received signal:

$$\begin{gathered}\mathbf{y}=\mathbf{Hs}+\mathbf{n}=\mathbf{HFx}+\mathbf{n}\\ \mathbf{r}=\mathbf{F}^H\mathbf{y}=\mathbf{F}^H\mathbf{HFx}+\mathbf{F}^H\mathbf{w}=\mathbf{F}^H\mathbf{F}\Lambda\mathbf{F}^H\mathbf{Fx}+\mathbf{F}^H\mathbf{n}=\Lambda\mathbf{x}+\mathbf{F}^H\mathbf{n}\end{gathered} \tag{50}$$

Thus, each data symbol is transmitted through an independent channel and all the ISI is removed.

2.6.2 Extension of OFDM for MIMO channels

When a transmission through multiple carriers is employed, the formulation of the received signal can be accommodated as a channel extension (see section 2.4). In such a case, the extended channel matrix can be written as

$$\mathbf{H}_{OFDM}=\begin{bmatrix}\mathbf{H}_1 & & & \\ & \mathbf{H}_2 & & \\ & & \ddots & \\ & & & \mathbf{H}_{N_c}\end{bmatrix} \tag{51}$$

where $\mathbf{H}_i$ is a matrix which represents the MIMO channel matrix for the ith subcarrier. In this regard, power allocation can be obtained by the water-filling algorithm considering that we have an equivalent MIMO channel of $NN_c \times MN_c$ antennas, where the channel matrix is block diagonal.

3 INTERFERENCE CHANNEL

This chapter addresses the analysis of the 3-user MIMO interference channel. In this regard, several concepts presented in Chapter 2 for the MIMO Channel will be used. First, section 3.1 reviews the characterization of the interference channel in the literature and introduces the strategies used for this channel. The channel model used throughout this chapter will be introduced in section 3.2. In Section 3.3, we review and improve the existing *outerbounds* on the DoF of the 3-user MIMO IC, while in section 3.4 we proposes some schemes (*innerbounds*). Finally, the results of the entire chapter are presented in section 3.5, where we will show that for most antenna configurations, our innerbounds achieve the outerbounds and hence, are DoF-optimal.

3.1 INTRODUCTION

Interference management is an important topic investigated by many scientists on the last decade. While traditional methods, such as orthogonal transmissions (either on time or frequency) have been implemented to avoid the interference, some recent results point that simultaneous transmission of messages with proper design of transceivers and receivers is a better transmission strategy. In this respect, *zero-forcing* (ZF) and *interference alignment* (IA) are the strategies to deal with interference when linear transmitters and receivers are envisioned. While the former designs the precoding matrices to suppress interference at unintended receivers [8], the later allows the existence of interference at the unintended receivers, at the cost of allocating the desired signals on a linearly independent spatial dimension. The key idea is that at each receiver all the generated interference by unintended sources overlap in a common subspace. Figure 9 illustrates an example of interference alignment for the 3-user IC where each user sends only one bitstream through one beamforming vector. Notice that for each user the received signal vector differs from the transmitted one due to rotations and magnitude scaling caused by the corresponding channel matrix. Figure 10 shows a zoom of the second receiver dimensional space.

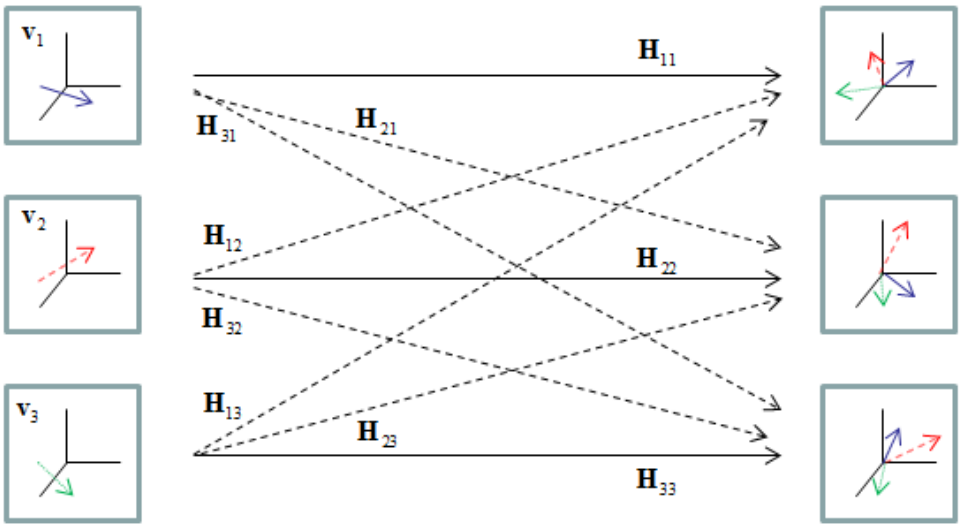

Figure 9: Interference alignment example for the 3-user IC with 3 antennas at each transmitter and each receiver and $d = 1$ for each user.

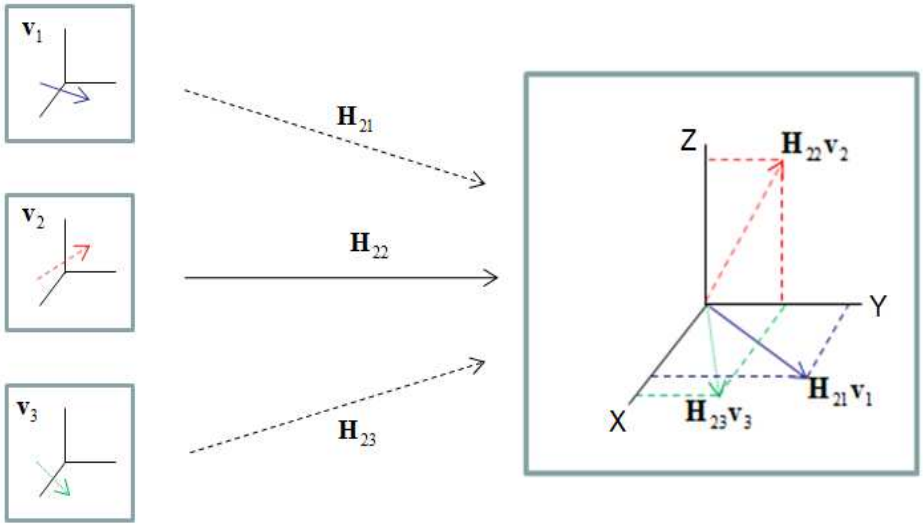

Figure 10: Details of the second receiver dimensional space for the example of Figure 9.

As it can be seen in Figure 10, the desired received vector is linearly independent of the other two interfering received vectors, which lie on the XY plane of the 3D receiver dimensional space. It is important to remark that interference alignment only requires that the desired received vector has at least one component orthogonal to the interference vectors, but it is not necessary that the desired received vector is orthogonal to the interfering received vectors.

Interference alignment concept was first introduced by Maddah-Ali et al. in [9] for the MIMO X channel [10][11]. As it has been mentioned in Chapter 1, the MIMO X channel subsumes the 2-user IC. A recent result in the MIMO X channel which is of our interest is [14], where the generalized singular value decomposition (GSVD) is introduced as a tool to meet the IA constraints.

The MIMO IC capacity characterization is complex and still remains an open-problem, but its performance at high SNR regime can be modelled by means of the degrees of freedom (DoF) of the channel. However, the actual DoF are not known in general, but can be upperbounded by an *outerbound* on the degrees of freedom of the channel.

One characterization of this outerbound was defined by Host-Madsen and Nosratinia in [15], where they derived that the DoF are upper bounded by *K/2* for the K-user IC with single antenna nodes and constant channel coefficients at each node. The authors also conjectured that the maximum DoF that could be achieved in a *K*-user SISO IC would be 1.

Based on the Maddah-Ali et al. scheme, Cadambe and Jafar extended interference alignment from the X channel to the *K*-user SISO IC with frequency-selective channels in [16], showing that *K/2* DoF can be obtained, i.e “everyone gets half the cake”. Hence, for frequency-selective channels the conjecture in [15] was rejected and the DoF became completely characterized. Likewise, for the 3-user MIMO IC with constant or time-varying channel coefficients and *M* antennas at each node, they provide one scheme able to get *3M/2* DoF. They also derived an outerbound on the DoF for the *K*-user MIMO IC equal to *KM/2* and hence, for *K=3* those achieved DoF becomes the actual DoF for those channel configurations. Cadambe and Jafar scheme for the 3-user MIMO IC with constant channel coefficients is reviewed in this chapter in section 3.4.3.1.

However, the characterization of the *K*-user SISO IC with constant channel coefficients remained uncharacterized and the conjecture in [15] was yet valid, leaving a gap between the 1 DoF that could be achieved and the *K/2* DoF which were the best upper bound on the DoF of the channel. The latest advance for this channel was presented in [17], where separating real and imaginary parts of the channel allows achieving 1.2 DoF. This work definitely removed the conjecture in [15] and contributed to narrow the gap between the outerbound and the innerbound for this channel.

Motahari et. al employed results from Diophantine approximation in Number theory to design the transmit precoders and meet the interference alignment conditions, [18]. There it was shown that interference can be aligned based on the properties of rationals and irrationals. They showed that for almost all *K*-user real Gaussian IC fading with constant channel coefficients, *K/2* DoF can be achieved. From this result, they extended their scheme to the *K*-user MIMO IC with M antennas at each node, showing that *KM/2* DoF could be achieved whether the channel has constant or time varying coefficients. As a consequence, the outerbound derived in [16] was achieved and the DoF for this channel with constant channel coefficients became completely characterized.

The MIMO IC with M antennas at each transmitter and N antennas at each receiver (MIMO $M \times N$ IC) was analyzed in [19], where outerbounds and innerbounds on the DoF are defined. Similarly, in [20] an outerbound is defined to address the *K*-user asymmetric IC, that is, different number of antennas at each transmitter-receiver pair. The outerbounds presented in [19][20] are reviewed in section 3.3 and will be used as a benchmark for our proposed strategies.

In this chapter, we analyze the 3-user IC with constant channel coefficients. First we present the system model in section 3.2. Section 3.3 reviews some outerbounds in the literature and formulates one outerbound improving them. Innerbounds are presented in section 3.4 and finally, comparison between our inner DoF and the outer DoF is done in section 3.5.

3.2 CHANNEL MODEL

We consider the 3-user MIMO interference channel (IC). Three source-destination pairs coexist in the system, where the pair (M_j, N_j) defines the number of antennas at the jth source and the jth destination, respectively. Each source only transmits messages to its associated destination. The received signal at the jth receiver is described by

$$\mathbf{y}_j = \mathbf{H}_{jj}\mathbf{V}_j\mathbf{x}_j + \sum_{\substack{i=1 \\ i\neq j}}^{3} \mathbf{H}_{ji}\mathbf{V}_i\mathbf{x}_i + \mathbf{n}_j \tag{52}$$

where $\mathbf{y}_j$ is the $N_j \times 1$ received signal vector at the jth receiver, $\mathbf{x}_j$ is the $d_j \times 1$ Gaussian signal transmitted by the jth transmitter with uncorrelated components, $\mathbf{V}_j$ is the $M_j \times d_j$ precoding matrix of the jth transmitter, $\mathbf{H}_{ji}$ is the $N_j \times M_i$ channel matrix from transmitter i to receiver j and $\mathbf{n}_j$ is the $N_j \times 1$ additive white Gaussian noise (AWGN) vector at the jth receiver. We assume all noise terms are i.i.d zero mean complex Gaussian with unit variance. Moreover, the channel coefficients are constant along the transmission time and CSIT is assumed. Unless otherwise stated, we assume a symmetric antenna configuration and transmitted bitstreams:

$$M_j = M, \quad N_j = N, \quad d_j = d \tag{53}$$

The signal model presented in (52) can be easily updated in order to accommodate those cases where signal is transmitted through different time instances or frequency carriers, as explained in section 2.4. In such a case, (52) can be rewritten as:

$$\begin{aligned}
\bar{\mathbf{y}}_j(t_0,T) &= \bar{\mathbf{H}}_{jj}(t_0,T)\bar{\mathbf{V}}_j\bar{\mathbf{x}}_j + \sum_{\substack{i=1 \\ i\neq j}}^{3} \bar{\mathbf{H}}_{ji}(t_0,T)\bar{\mathbf{V}}_i\bar{\mathbf{x}}_i + \bar{\mathbf{n}}_j(t_0,T) \\
\bar{\mathbf{H}}_{ji}(t_0,T) &= \mathbf{I}_T \otimes \mathbf{H}_{ji} \\
\bar{\mathbf{y}}_j(t_0,T) &= \left[\mathbf{y}_j^H(t_0) \quad \mathbf{y}_j^H(t_0+1) \quad \ldots \quad \mathbf{y}_j^H(t_0+T-1)\right]^H \\
\bar{\mathbf{n}}_j(t_0,T) &= \left[\mathbf{n}_j^H(t_0) \quad \mathbf{n}_j^H(t_0+1) \quad \ldots \quad \mathbf{n}_j^H(t_0+T-1)\right]^H
\end{aligned} \tag{54}$$

where $\bar{\mathbf{V}}_j$ is the $M_j T \times d_j T$ precoding matrix of the jth transmitter and $\bar{\mathbf{x}}_j$ is the $d_j T \times 1$ Gaussian signal transmitted by the jth transmitter with uncorrelated components. In the sequel, the time index will be suppressed in order to simplify notation.

At the jth receiver, the received signal $\bar{\mathbf{y}}_j$ is processed with a linear $dT \times N_j T$ receiver filter $\bar{\mathbf{D}}_j$ and decoding is done with $\bar{\mathbf{z}}_j$, defined as:

$$\bar{\mathbf{z}}_j = \bar{\mathbf{D}}_j \bar{\mathbf{y}}_j = \bar{\mathbf{D}}_j \left(\bar{\mathbf{H}}_{jj} \bar{\mathbf{V}}_j \bar{\mathbf{x}}_j + \sum_{\substack{i=1 \\ i \neq j}}^{3} \bar{\mathbf{H}}_{ji} \bar{\mathbf{V}}_i \bar{\mathbf{x}}_i + \bar{\mathbf{n}}_j \right) \tag{55}$$

Notice that if interference is completely suppressed, then we have an equivalent channel equal to $\bar{\mathbf{H}}_{eq} = \bar{\mathbf{D}}_j \bar{\mathbf{H}}_{jj} \bar{\mathbf{V}}_j$. In such a case, the DoF would be:

$$d_j = \frac{1}{T} rank\left(\bar{\mathbf{D}}_j \bar{\mathbf{H}}_{jj} \bar{\mathbf{V}}_j \right) \tag{56}$$

following the results of the MIMO channel described in chapter 2. Notice that since channel extension is employed, the DoF achieved by the extended system have to be divided by T .

The sum DoF of the system is:

$$d_\Sigma = d_1 + d_2 + d_3 \tag{57}$$

Finally, notice that (56) allows the achieved DoF to be equal to a rational number. This means that if we find any integer number T such that $d_j T$ is an integer, then d_j DoF can be achieved transmitting $d_j T$ bitstreams during T channel uses.

3.3 OUTERBOUNDS ON THE DOF

An *outerbound* or *upperbound* of a magnitude is a value which is greater than or equal to the maximum value that this magnitude can get. Throughout section 3.3, outerbounds on the DoF for the 3-user MIMO IC will be reviewed and improved, formulating the results in Theorem 3.3.2-1**.**

3.3.1 Introduction

From the above definition, it follows that an outerbound is better than other if it is the minimum between them. We say that an outerbound of a magnitude is tight when it is equal to the maximum value that this magnitude can get. As a consequence, an upper bound value for the rate cannot be accepted as the maximum rate of that channel if there is not one coding strategy achieving this value.

Although the capacity of the MIMO IC is still an open problem, we can describe the performance of that channel at the high SNR regime in terms of DoF (56). However, in contrast to other channels, such as point-to-point MIMO, MIMO BC, MIMO MAC where the DoF are known exactly, the DoF of the MIMO IC can only be upper bounded in general (outer DoF).

The MIMO IC with M antennas at each transmitter and N antennas at each receiver (MIMO $M \times N$ IC) was analyzed in [19], where outerbounds and innerbounds on the DoF were defined. Similarly, in [20] an outrebound was defined to address the *K*-user asymmetric IC, that is, different number of antennas at each transmitter-receiver pair. The outerbounds presented in [19], [20] are reviewed in this section 3.3 and will be used as a benchmark for our proposed strategies.

3.3.2 Outerbound improvement

In this section, we refine the outerbound on the DoF provided in [19] and [20] for the MIMO IC where sources are equipped with $\{M_1, M_2, M_3\} = M$ antennas and destinations with $\{N_1, N_2, N_3\} = N$. The outerbounds considered in this work characterize the sum DoF of a 3-user MIMO IC, assuming that the sum DoF is equally divided over the users. Let us introduce the following lemma:

Lemma 3.3.2-1: Consider the 3-user MIMO IC with (M,N) antennas at each transmitter-receiver pair. Now consider the same channel increasing the number of antennas in any of the two sides. The outer DoF in the second case cannot be lower than in the first case.

Proof: Since there are more antennas in the second case than in the first one, the outer degrees of freedom cannot decrease and they have to be at least equal for the two cases. Let us consider that we have d DoF in the first case. Now consider that those antennas in the second case which are not available in the first case are disconnected. Hence, we get the same antenna configuration than in the first case, and by definition d DoF can be achieved.

□

The outerbound is formalized in the following theorem:

Theorem 3.3.2-1: For the 3-user MIMO IC with (M,N) antennas at each transmitter-receiver pair, the total number of degrees of freedom per user is upper bounded by:

$$DoF = \begin{cases} \dfrac{M+N}{4} & 1 \le r < \dfrac{5}{3} \\ \dfrac{2\min(M,N)}{3} & \dfrac{5}{3} \le r < 2 \\ \dfrac{\max(M,N)}{3} & 2 \le r < 3 \\ \min(M,N) & r \ge 3 \end{cases} \tag{58}$$

where $r = \dfrac{\max(M,N)}{\min(M,N)}$.

Proof: The proof is presented in Appendix A.

□

Figure 11 compares the degrees of freedom per user achieved by the single-user MIMO channel and the outerbound on the DoF per user defined in this section for the 3-user MIMO IC . Likewise, the outerbound on the DoF sum for the 3-user MIMO IC is also sketched. The DoF are obtained assuming $N = 4$ antennas per destination as a function of the transmitting antennas, M . It can be observed that each user loses DoF

when he shares the channel with other users, but the sum DoF is better than the single-user MIMO. Consequently, it is much more efficient to consider the IC than to orthogonalize the users like in TDMA or FDMA traditional schemes.

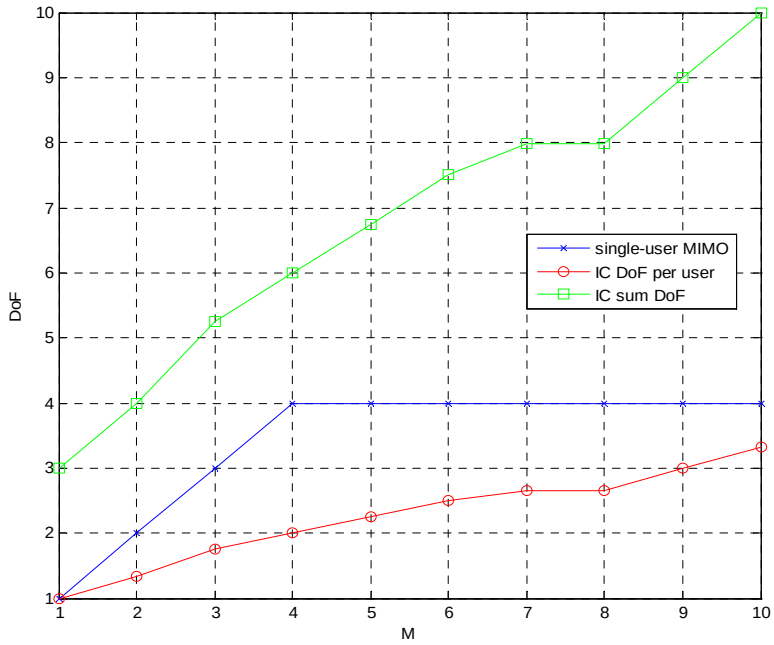

Figure 11: Comparison of the single user MIMO and the 3-user MIMO IC for $N = 4$. DoF per user and DoF sum as a function of the antennas at each transmitter M.

Finally, Figure 12 and Figure 13 compares the outerbound defined in Theorem 3.3.2-1 with the other outerbounds defined in [19] and [20]. Notice that the outerbound defined in Theorem 3.3.2-1 is lower than or equal to any other.

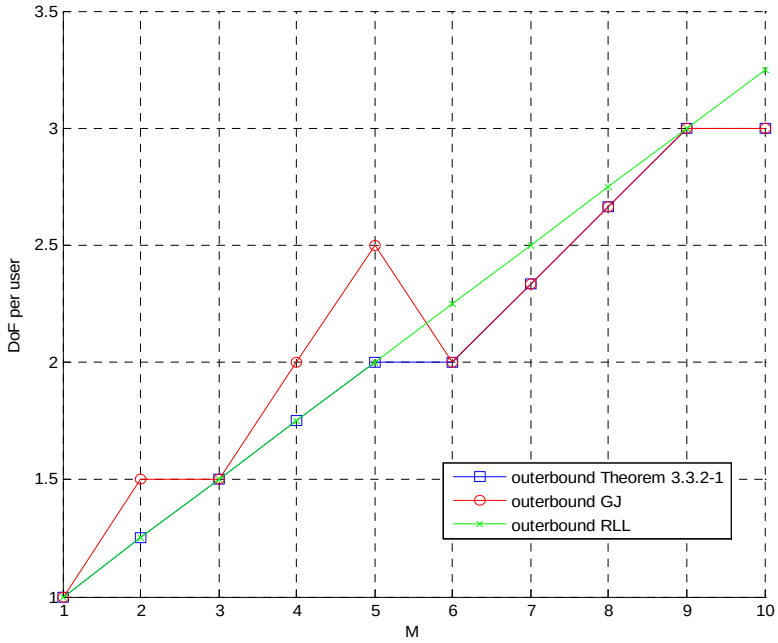

Figure 12 Outerbounds comparison for N=3. DoF per user as a function of the antennas at each transmitter M .

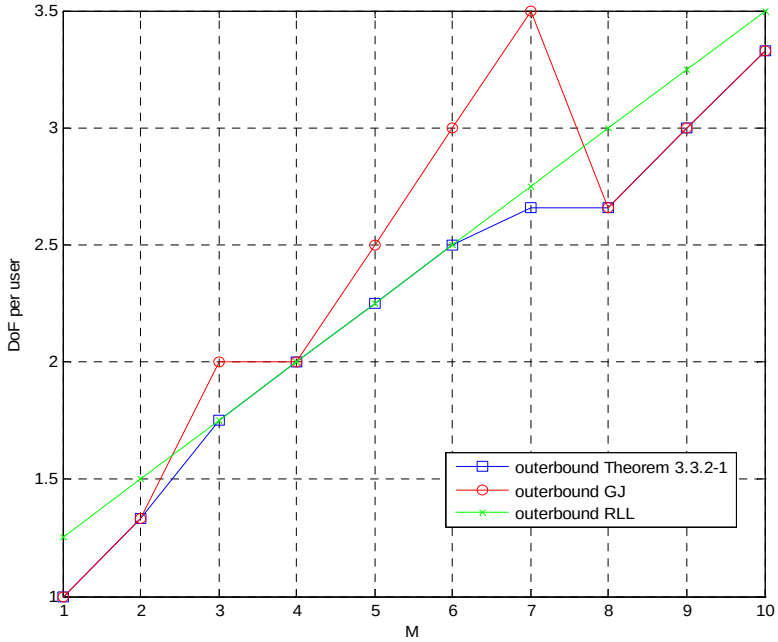

Figure 13: Outerbounds comparison for N=4. DoF per user as a function of the antennas at each transmitter M .

3.4 INNERBOUNDS ON THE DOF

This section presents the achievable degrees of freedom or innerbounds obtained under different techniques, some of them originally investigated in this work. It turns out that the derived innerbounds meet the outerbounds introduced in section 3.3 for almost all antenna configurations, showing the optimality of our proposed technique and thus providing the degrees of freedom of the MIMO interference channel, as the slope of the mutual information at high SNR.

The techniques presented in this section are based on linear precoding using the principles of linear algebra for both transmitters and receivers. Concepts from linear algebra such as null space or linear independence are used to design the transmitted signal so as to reduce interference not only in terms of signal power but also in terms of the dimension of spanned interference space. In this regard, we distinguish between two strategies: ZF and IA. The first one tries to transmit the desired signals such that it does not create interference to the unintended users, while the last one pursues to minimize the dimension of the space spanned by the interfering signals.

This section is organized as follows. Section 3.4.1 will state the precoders design problem for different transmission strategies. Next, in subsection 3.4.2 the ZF precoding strategy will be analyzed. IA strategy is treated in section 3.4.3. Subsection 3.4.3.1 is devoted to review the Cadambe and Jafar (CJ) precoding scheme based on interference alignment. This scheme works only for the same antenna deployment at the transmitter and the receiver ($M = N$). In this respect, a first attempt of interference alignment is done with the intersection space precoding in subsection 3.4.3.2. A combination of interference alignment and zero-forcing strategies is presented in subsection 3.4.4, although this strategy does not follow formally the same interference alignment principles considered in section 3.4.3. Using the same idea, subsection 3.4.5 introduces the GSVD precoding,that in addition to use simultaneously ZF and IA, it also performs partial ZF precoding, which is a combination of ZF and IA. Finally, section 3.4.6 discusses the DoF optimization when asymmetric antenna deployment or deficient rank channel matrices are considered. Hence, unless otherwise stated we assume full rank channel matrices and the deficient case will be analyzed in this section.

3.4.1 Problem statement

The schemes proposed on the sequel are designed in order to maximize the DoF of the MIMO IC. This section presents the problem formulation employed to design our precoders. Let us review the system model presented in section 3.2 for the processed signal $\bar{\mathbf{z}}_j$ at the jth receiver:

$$\bar{\mathbf{z}}_j = \bar{\mathbf{D}}_j \bar{\mathbf{y}}_j = \bar{\mathbf{D}}_j \left(\bar{\mathbf{H}}_{jj} \bar{\mathbf{V}}_j \bar{\mathbf{x}}_j + \sum_{\substack{i=1 \\ i \neq j}}^{3} \bar{\mathbf{H}}_{ji} \bar{\mathbf{V}}_i \bar{\mathbf{x}}_i + \bar{\mathbf{n}}_j \right)$$

Assuming we are able to suppress completely the received interference, the MIMO interference channel becomes three parallel point to point MIMO channels. In this regard, section 3.2 showed that the DoF for each one of these channels is defined by $d_j = \frac{1}{T} rank\left(\bar{\mathbf{D}}_j \bar{\mathbf{H}}_{jj} \bar{\mathbf{V}}_j \right)$. Let us assume we employ receive zero-forcing (ZF) filters to get rid of interference. In other words, we impose:

$$\bar{\mathbf{D}}_j = \mathbf{P}_j^{\perp} \tag{59}$$

where $\mathbf{P}_j^{\perp}$ is a $d_j T \times NT$ receive ZF filter of the jth user. This receive filter implements an orthogonal projection matrix projecting $\bar{\mathbf{y}}_j$ onto the orthogonal subspace spanned by interference at each receiver. It is given by,

$$\begin{aligned} &\mathbf{P}_j^{\perp} = \mathbf{I}_N - \mathbf{B}_j \left(\mathbf{B}_j^H \mathbf{B}_j \right)^{-1} \mathbf{B}_j^H \\ &\text{with} \quad \mathbf{B}_j = \left[\bar{\mathbf{H}}_{jk} \bar{\mathbf{V}}_k \quad \bar{\mathbf{H}}_{ji} \bar{\mathbf{V}}_i \right], \;\; i, j, k \in \{1,2,3\} \;\; , k \neq j, i \neq j \end{aligned} \tag{60}$$

where $\mathbf{B}_j$ models the interference space at the jth destination. After processing the received signal we get a signal free of interference,

$$\bar{\mathbf{z}}_j = \mathbf{P}_j^{\perp} \left(\bar{\mathbf{H}}_{jj} \bar{\mathbf{V}}_j \bar{\mathbf{x}}_j + \sum_{\substack{i=1 \\ i \neq j}}^{3} \bar{\mathbf{H}}_{ji} \bar{\mathbf{V}}_i \bar{\mathbf{x}}_i + \bar{\mathbf{n}}_j \right) = \mathbf{P}_j^{\perp} \bar{\mathbf{H}}_{jj} \bar{\mathbf{V}}_j \bar{\mathbf{x}}_j + \mathbf{P}_j^{\perp} \bar{\mathbf{n}}_j \tag{61}$$

The transmit precoders are designed in order to maximize the sum DoF, which can be formulated as a solution of the following optimization problem,

$$\max_{\mathbf{V}_1,\mathbf{V}_2,\mathbf{V}_3,T} \sum_{j=1}^{3} \frac{1}{T} rank\left(\mathbf{P}_j^{\perp} \bar{\mathbf{H}}_{jj} \bar{\mathbf{V}}_j\right)$$
$$\text{st } \mathbf{P}_j^{\perp} \bar{\mathbf{H}}_{jk} \bar{\mathbf{V}}_k = \mathbf{0}, \;\; j,k \in \{1,2,3\} \;\; , \;\; k \neq j \tag{62}$$

The problem in (62) has to be solved on *T* and the precoding matrices by an entity that collects all MIMO channels $\bar{\mathbf{H}}_{jk}$ involved However, we would not know if the achieved DoF are the optimum solution of the problem, that is, DoF-optimal.

Our strategy, which is based in the strategy followed by Guo and Jafar in [19], will be to assume that the outerbound is tight and then, design *T* such that this outerbound is equal to an integer number. Therefore, the problem simplifies to design only the precoding matrices, which will be designed following different strategies, presented throughout the rest of the section 3.4.

We assume ZF receiving filters without knowing if they are the optimum option for the receivers. This is because the degrees of freedom are obtained analytically when the interference is completely suppressed. With this limitation, we will assume the maximum degrees of freedom can be achieved.

We do not consider channel extension so as to simplify notation, unless needed. Moreover, in general we will assume that the number of transmit antennas is at least the number of receive antennas (with certain particularities for each scheme), while the opposite case is included by the reciprocity property seen in section 2.5.

.

3.4.2 Zero Forcing precoding

The ZF precoding strategy consists on designing the precoding matrices so as not to generate interference at the unintended receivers. A general framework is described for the MIMO BC in where the precoding matrix associated to each user steers nulls in the directions of other users. The same principle can be extended to the MIMO IC. In this regard, the transmit precoding matrices $\mathbf{V}_j$ must satisfy the following conditions,

$$\begin{bmatrix}\mathbf{H}_{21}\\ \mathbf{H}_{31}\end{bmatrix}\mathbf{V}_1 = \mathbf{0} \quad \begin{bmatrix}\mathbf{H}_{12}\\ \mathbf{H}_{32}\end{bmatrix}\mathbf{V}_2 = \mathbf{0} \quad \begin{bmatrix}\mathbf{H}_{13}\\ \mathbf{H}_{23}\end{bmatrix}\mathbf{V}_3 = \mathbf{0} \tag{63}$$

As a consequence, $\mathbf{V}_1$, $\mathbf{V}_2$ and $\mathbf{V}_3$ are chosen as:

$$\mathbf{V}_1 = null\left(\begin{bmatrix}\mathbf{H}_{21}\\ \mathbf{H}_{31}\end{bmatrix}\right) \quad \mathbf{V}_2 = null\left(\begin{bmatrix}\mathbf{H}_{12}\\ \mathbf{H}_{32}\end{bmatrix}\right) \quad \mathbf{V}_3 = null\left(\begin{bmatrix}\mathbf{H}_{13}\\ \mathbf{H}_{23}\end{bmatrix}\right) \tag{64}$$

where $null(\mathbf{A})$ is a basis that spans the null space of matrix $\mathbf{A}$.

Lemma 3.4.2-1 states the DoF achieved by ZF precoding:

Lemma 3.4.2-1: For the 3-user MIMO IC with constant channel coefficients, (M,N) antennas at each pair transmitter-receiver with $M > N$, the following DoF per user can be achieved by ZF precoding:

$$DoF_{ZF} = \min\left((M-2N)^+, N\right) \tag{65}$$

where $(a)^+ = \max(0,a)$

Proof: Since channels are $N \times M$ matrices whose elements are chosen from a continuous distribution, the $2N \times M$ block matrices defined in (63) are assumed to be full rank and they have null spaces of dimension $(M-2N)^+$.

Consequently, when $M > 2N$ each user can transmit $M - 2N$ messages without generating interference to unintended users. However, since a receiver with N antennas can at most decode N messages, the DoF achieved by ZF precoding can be expressed as in (65).

Finally, notice that this scheme can only be used for $M > 2N$.

□

Theorem 3.4.2-1: The 3-user MIMO IC with (*M*, *N*) antennas at each pair transmitter-receiver has N degrees of freedom if $M > 3N$.

Proof: The proof is obtained by verifying that the achievable DoF presented in Lemma 3.4.2-1 are equal to the outerbound shown in Theorem 3.3.2-1 for $M > 3N$.

□

Lemma 3.4.2-1 shows that ZF precoding can only be used when $M > 2N$ and it follows from Theorem 3.4.2-1 that it achieves the total degrees of freedom when $M > 3N$. In the next section we present the IA precoding, which is an alternate precoding strategy that tries to solve the problem in (62) achieving the maximum DoF for any pair (M, N).

3.4.3 Interference Alignment precoding

In contrast to the previous section where the interference is avoided, here the IA precoding is designed taking into account the coexistence of the interference and desired signals subject to certain conditions. The approach of interference alignment is to align the generated interference from unintended transmitters into a common space at the receiver side, being the dimension of this space as small as possible. This interference is then suppressed using the receive zero-forcing filter $\mathbf{P}_j^{\perp}$ (60).

Hence, the transmit precoder $\mathbf{V}_j$ is designed following two directions. In the first place, we want to minimize the dimension of the space spanned by the generated interference at each receiver. In this regard, it is reduced by half forcing this interference to lie on the same subspace. Conditions to meet the interference alignment are summarized by,

$$\begin{aligned} span\left(\mathbf{H}_{12}\mathbf{V}_2\right) &= span\left(\mathbf{H}_{13}\mathbf{V}_3\right) \\ span\left(\mathbf{H}_{21}\mathbf{V}_1\right) &= span\left(\mathbf{H}_{23}\mathbf{V}_3\right) \\ span\left(\mathbf{H}_{31}\mathbf{V}_1\right) &= span\left(\mathbf{H}_{32}\mathbf{V}_2\right) \end{aligned} \tag{66}$$

Remember that $\mathbf{H}_{ji}$ denotes the $N \times M$ channel matrix from the ith transmitter to the jth receiver.

On the other hand, the transmit precoder $\mathbf{V}_j$ has to satisfy:

$$rank\left(\mathbf{P}_j^{\perp}\mathbf{H}_{jj}\mathbf{V}_j\right) = rank\left(\mathbf{H}_{jj}\mathbf{V}_j\right) \tag{67}$$

which means that the receive filter cannot reduce the rank of the receive matrix $\mathbf{H}_{jj}\mathbf{V}_j$ associated to the desired signal. It can be proved that (67) is satisfied with probability 1 if the channel matrices do not have any special structure [22][23].

Lemma 3.4.3-1 shows the conditions for which IA can be used:

Lemma 3.4.3-1: Each IA condition shown in equation (66) can be ensured only if $N < 2M$.

Proof: We recall on the fact that $\mathbf{H}_{jk}\mathbf{V}_k$ is a linear combination of the columns of $\mathbf{H}_{jk}$. Hence, the precoding matrices have to generate linear combinations of channel matrices columns such that the resulting space lie on the intersection of the channel matrices involved on each equation.

To illustrate this idea, consider the following alignment problem:

$$span\left(\mathbf{H}_1\mathbf{A}\right) = span\left(\mathbf{H}_2\mathbf{B}\right) \tag{68}$$

This equation implies that a linear combination $\mathbf{A}$ of the columns of $\mathbf{H}_1$ has to span the same space spanned by a linear combination $\mathbf{B}$ of the columns of $\mathbf{H}_2$. Since:

$$\begin{aligned} span\left(\mathbf{H}_1\mathbf{A}\right) &\subseteq span\left(\mathbf{H}_1\right) \\ span\left(\mathbf{H}_2\mathbf{B}\right) &\subseteq span\left(\mathbf{H}_2\right) \end{aligned} \tag{69}$$

the space spanned by a linear combination $\mathbf{A}$ of the columns of $\mathbf{H}_1$ is still contained on the space spanned by the columns of $\mathbf{H}_1$.

As a consequence, the space spanned by a linear combination $\mathbf{A}$ of the columns of $\mathbf{H}_1$ and the space spanned by a linear combination $\mathbf{B}$ of the columns of $\mathbf{H}_2$ have to lie onto the space defined by the intersection of $span(\mathbf{H}_1)$ and $span(\mathbf{H}_2)$. Formally:

$$span(\mathbf{H}_1\mathbf{A}) = span(\mathbf{H}_2\mathbf{B}) \Rightarrow \begin{cases} span(\mathbf{H}_1\mathbf{A}) \subseteq span(\mathbf{H}_1) \cap span(\mathbf{H}_2) \\ span(\mathbf{H}_2\mathbf{B}) \subseteq span(\mathbf{H}_1) \cap span(\mathbf{H}_2) \end{cases} \quad (70)$$

A matrix $\mathbf{H}_3$ such that that $span(\mathbf{H}_3) = span(\mathbf{H}_1) \cap span(\mathbf{H}_2)$, that is, a basis for the intersection space, might be computed as $\mathbf{H}_3 = null\left(\left[null(\mathbf{H}_1) \quad null(\mathbf{H}_2)\right]\right)$.

However, the converse in (70)does not hold in general, that is, equations of the right-hand side of (70) are not equivalent to the alignment equation of the left-hand side of (70). This is because $span(\mathbf{H}_1) \cap span(\mathbf{H}_2)$ can be subspace of high dimension and hence, equations of the right-hand side of (70) can be ensured without satisfying the alignment equation of the left-hand side of (70). Figure 14 illustrates the concept with two examples. The left-hand side case satisfies the two sides of (70) whereas the picture depicted in the right-hand side obeys to a case where the alignment condition does not hold but the right-hand side equations of (70) do:

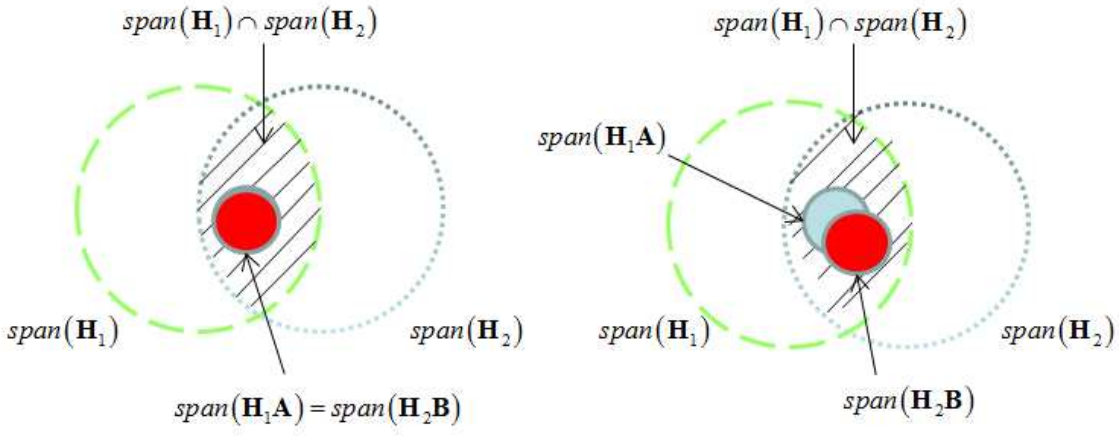

Figure 14: Intersection of two subspaces. Two cases explained in Lemma 3.4.3-1

From the Grassman formula (see section 5.9 of [24]), the dimension of that space is:

$$\begin{aligned}
&\dim\left(span\left(\mathbf{H}_1\right)\cap span\left(\mathbf{H}_2\right)\right)= \\
&\quad=\dim\left(span\left(\mathbf{H}_1\right)\right)+\dim\left(span\left(\mathbf{H}_2\right)\right)-\dim\left(span\left(\left[\mathbf{H}_1 \quad \mathbf{H}_2\right]\right)\right)= \\
&\quad=\min\left(M,N\right)+\min\left(M,N\right)-\min\left(N,2M\right)= \\
&\quad=2\min\left(M,N\right)-\min\left(N,2M\right)=\left\{\begin{matrix} N & N<M \\ 2M-N & M<N<2M \\ 0 & N>2M \end{matrix}\right\}=\left\{\begin{matrix} N & N<M \\ \left(2M-N\right)^{+} & N>M \end{matrix}\right\}
\end{aligned} \tag{71}$$

Consequently, we can write

$$\dim\left(span\left(\mathbf{H}_1\right)\cap span\left(\mathbf{H}_2\right)\right)>0 \quad \Leftrightarrow \quad 0<N<2M \tag{72}$$

which is necessary condition for the existence condition stated in this lemma.

□

The system of equations in (66) was first defined by Cadambe and Jafar at [16]. In that work, the authors present one scheme for the 3-user case with $M=N$ achieving the total degrees of freedom. In the next section the Cadambe and Jafar scheme is reviewed and section 3.4.3.2 addresses the case when *M* and *N* are not equal.

3.4.3.1 CJ precoders

In this section, we review the Cadambe & Jafar (CJ) scheme described in [16]. The interference alignment conditions shown in (66) are addressed as:

$$\begin{aligned}
span\left(\mathbf{H}_{12}\mathbf{V}_2\right)&=span\left(\mathbf{H}_{13}\mathbf{V}_3\right) \\
\mathbf{H}_{21}\mathbf{V}_1&=\mathbf{H}_{23}\mathbf{V}_3 \\
\mathbf{H}_{31}\mathbf{V}_1&=\mathbf{H}_{32}\mathbf{V}_2
\end{aligned} \tag{73}$$

Notice that (66) is more general than (73). Since (66) forces $\mathbf{H}_{21}\mathbf{V}_1$ and $\mathbf{H}_{23}\mathbf{V}_3$, as well as $\mathbf{H}_{31}\mathbf{V}_1$ and $\mathbf{H}_{32}\mathbf{V}_2$, to merely lie on the same subspace, here $\mathbf{H}_{21}\mathbf{V}_1$ and $\mathbf{H}_{23}\mathbf{V}_3$,as well as $\mathbf{H}_{31}\mathbf{V}_1$ and $\mathbf{H}_{32}\mathbf{V}_2$, are designed to be the same matrix. The results shown in [16] can be formulated by following theorem:

Theorem 3.4.3-1: For the 3-user MIMO IC with constant channel coefficients and M antennas at each pair transmitter-receiver, the total number of degrees of freedom is $M/2$.

Proof: The proof is presented in Appendix B. Basically it can be shown that the innerbound matches the outerbound defined in Theorem 3.3.2-1.

□

One limitation of this technique is that it only works for the case $M = N$, because inversion of channel matrices is needed. We try to overcome this drawback in the following sections.

3.4.3.2 Intersection space precoding

In this section we present a first attempt of interference alignment for the $M \neq N$ case based on the principles explained on the proof of Lemma 3.4.3-1. Achievable DoF and transmit conditions are also derived.

The proposed method is developed for $M < N$ but, as mentioned in section 2.5, there is no loss of generality because of reciprocity.

From the key idea of the proof of Lemma 3.4.3-1, it follows that the system of equations defining IA

$$\begin{aligned} span(\mathbf{H}_{12}\mathbf{V}_2) &= span(\mathbf{H}_{13}\mathbf{V}_3) \\ span(\mathbf{H}_{21}\mathbf{V}_1) &= span(\mathbf{H}_{23}\mathbf{V}_3) \\ span(\mathbf{H}_{31}\mathbf{V}_1) &= span(\mathbf{H}_{32}\mathbf{V}_2) \end{aligned}$$

can be rewritten as follows:

$$\begin{aligned} span(\mathbf{H}_{12}\mathbf{V}_2) = span(\mathbf{H}_{13}\mathbf{V}_3) &\Rightarrow \begin{cases} span(\mathbf{H}_{12}\mathbf{V}_2) \subseteq span(\mathbf{A}_1) \\ span(\mathbf{H}_{13}\mathbf{V}_3) \subseteq span(\mathbf{A}_1) \end{cases} \\ span(\mathbf{H}_{21}\mathbf{V}_1) = span(\mathbf{H}_{23}\mathbf{V}_3) &\Rightarrow \begin{cases} span(\mathbf{H}_{21}\mathbf{V}_1) \subseteq span(\mathbf{A}_2) \\ span(\mathbf{H}_{23}\mathbf{V}_3) \subseteq span(\mathbf{A}_2) \end{cases} \\ span(\mathbf{H}_{31}\mathbf{V}_1) = span(\mathbf{H}_{32}\mathbf{V}_2) &\Rightarrow \begin{cases} span(\mathbf{H}_{31}\mathbf{V}_1) \subseteq span(\mathbf{A}_3) \\ span(\mathbf{H}_{32}\mathbf{V}_2) \subseteq span(\mathbf{A}_3) \end{cases} \end{aligned} \quad (74)$$

$$\begin{aligned} span(\mathbf{A}_1) &= span(\mathbf{H}_{12}) \cap span(\mathbf{H}_{13}) \\ span(\mathbf{A}_2) &= span(\mathbf{H}_{21}) \cap span(\mathbf{H}_{23}) \\ span(\mathbf{A}_3) &= span(\mathbf{H}_{31}) \cap span(\mathbf{H}_{32}) \end{aligned}$$

where $span(\mathbf{A}_i), i=1,2,3$ is the space defined by the intersection of interfering channel matrices at each receiver.

Notice that equations in (74) are less restrictive than (66). While (66) forces interference to lie on the same subspace of *span*($\mathbf{A}_i$), equation in (74) only forces interference to lie on a subspace of *span*($\mathbf{A}_i$).

It is the weakness of this method: we know the space where we want to design interference to lie, but by separating each equality in (66) into two isolated equations we do not exploit all *DoF* that could be achieved.

The next figure illustrates this problem for the antenna pair $(M,N)=(5,6)$, where the receive antennas are represented for one receiver, e.g receiver 1. Interference at receiver 1 lies on $span(\mathbf{H}_{12}\mathbf{V}_2)$ and $span(\mathbf{H}_{13}\mathbf{V}_3)$, which are contained in $span(\mathbf{H}_{12})$ and $span(\mathbf{H}_{13})$, respectively. Antennas with horizontal and red lines represent $span(\mathbf{H}_{12})$ and antennas with vertical and blue lines representing $span(\mathbf{H}_{13})$. Since channel matrices are drawn from a continuous distribution, they cannot span exactly the same subspace but there could exist an intersection between these two spaces, which is depicted with the two colours.

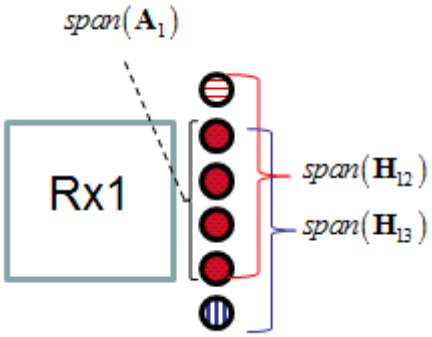

Figure 15: Representation of the dimensional space of receiver 1.

Using the Grassman formula we know that $span(\mathbf{H}_{12}) \cap span(\mathbf{H}_{13})$ has dimension 4:

$$\begin{aligned} &\dim\left(span(\mathbf{H}_{12}) \cap span(\mathbf{H}_{13})\right) = \\ &= \dim\left(span(\mathbf{H}_{12})\right) + \dim\left(span(\mathbf{H}_{13})\right) - rank\left(\begin{bmatrix}\mathbf{H}_{12} & \mathbf{H}_{13}\end{bmatrix}\right) \\ &= 2M - N = 4 \end{aligned} \tag{75}$$

Back to the IA problem defined in (66), we are forcing $span(\mathbf{H}_{12}\mathbf{V}_2)$ and $span(\mathbf{H}_{13}\mathbf{V}_3)$ to lie on the same subspace of $span(\mathbf{A}_1)$. Since there are 6 dimensions at each receiver, we can design the precoding matrices for user 2 and 3 in order to lie on 3 dimensions of the interference, and hence let 3 dimensions of the receiver space free for desired signals.

Figure 16 shows two examples of intersection space precoding. At the right-hand side, interference is aligned in a 3D dimensional subspace of $span(\mathbf{A}_1)$ and hence there are 3 dimensions free to be occupied by desired signals. At the left-hand side, each term of interference lies on a different dimensional space of $span(\mathbf{A}_1)$ and thus, there are only 2 dimensions free to be occupied by desired signals.

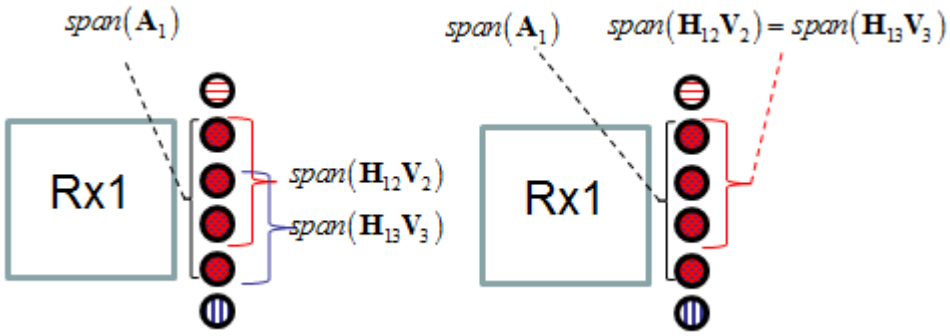

Figure 16: Two examples of intersection space precoding for $(M, N) = (5, 6)$

Intersection space precoding does not force $span(\mathbf{H}_{12}\mathbf{V}_2)$ and $span(\mathbf{H}_{13}\mathbf{V}_3)$ to lie on the same subspace of $span(\mathbf{A}_1)$. They only have to lie on a subspace of $span(\mathbf{A}_1)$ and hence, it obeys to the left-hand side of Figure 16. As a consequence, this scheme cannnot be DoF-optimal.

3.4.3.2.1 Design of the precoders

For the proper design of precoding matrices, the generalized singular value decomposition (GSVD) [13] is needed. This mathematic tool allows us to decompose channel matrices in (74) connecting them by a common full rank matrix:

Definition 1: Take any two matrices $\mathbf{A} \in \mathbb{C}^{m \times p}$ and $\mathbf{B} \in \mathbb{C}^{n \times p}$. Then the GSVD defines unitary matrices $\mathbf{U}_1 \in \mathbb{C}^{m \times m}$ and $\mathbf{U}_2 \in \mathbb{C}^{n \times n}$, a non-singular matrix $\mathbf{W} \in \mathbb{C}^{p \times p}$ and diagonal matrices $\mathbf{S}_1 \in \mathbb{C}^{m \times p}$ and $\mathbf{S}_2 \in \mathbb{C}^{n \times p}$ such that,

$$\begin{aligned} &[\mathbf{U}_1, \mathbf{U}_2, \mathbf{S}_1, \mathbf{S}_2, \mathbf{W}] = gsvd(\mathbf{A}, \mathbf{B}) \\ &\begin{cases} \mathbf{A} = \mathbf{U}_1 \mathbf{S}_1 \mathbf{W}^H \\ \mathbf{B} = \mathbf{U}_2 \mathbf{S}_2 \mathbf{W}^H \end{cases}, \quad \mathbf{S}_1^H \mathbf{S}_1 + \mathbf{S}_2^H \mathbf{S}_2 = \mathbf{I} \end{aligned} \tag{76}$$

GSVD can also be defined with the common full-rank matrix by the left for matrices with the same number of rows:

$$\begin{cases} \mathbf{A} = \mathbf{W} \mathbf{S}_1 \mathbf{U}_1{}^H \\ \mathbf{B} = \mathbf{W} \mathbf{S}_2 \mathbf{U}_2{}^H \end{cases}, \quad \mathbf{S}_1^H \mathbf{S}_1 + \mathbf{S}_2^H \mathbf{S}_2 = \mathbf{I} \tag{77}$$

This alternate definition will be used by GSVD precoding in section 3.4.5.

Consider now the equations involving precoding matrix for the 3rd user:

$$\begin{aligned} span(\mathbf{H}_{13} \mathbf{V}_3) &\subseteq span(\mathbf{A}_1) \\ span(\mathbf{H}_{23} \mathbf{V}_3) &\subseteq span(\mathbf{A}_2) \end{aligned} \tag{78}$$

and let us apply the GSVD (76) to the channel matrix of each equation. Therefore, the channel matrices can be decomposed as follows:

$$\begin{aligned} \mathbf{H}_{13} &= \mathbf{U}_{13} \mathbf{S}_{13} \mathbf{W}_{13}{}^H \\ \mathbf{H}_{23} &= \mathbf{U}_{23} \mathbf{S}_{23} \mathbf{W}_{13}{}^H \end{aligned} \tag{79}$$

where $\mathbf{U}_{23}$ and $\mathbf{U}_{13}$ are $N \times N$ unitary matrices, $\mathbf{S}_{23}$ and $\mathbf{S}_{13}$ are $N \times M$ diagonal matrices and $\mathbf{W}_{23}$ is a common right full rank $M \times M$ matrix. Applying this result:

$$\begin{aligned} span(\mathbf{H}_{13} \mathbf{V}_3) = span\left(\mathbf{U}_{13} \mathbf{S}_{13} \mathbf{W}_{13}{}^H \mathbf{V}_3\right) &\subseteq span(\mathbf{A}_1) \\ span\left(\mathbf{S}_{13} \mathbf{W}_{13}{}^H \mathbf{V}_3\right) &\subseteq span\left(\mathbf{U}_{13}^H \mathbf{A}_1\right) \\ span\left(\mathbf{S}_{13} \bar{\mathbf{V}}_3\right) &\subseteq span\left(\mathbf{U}_{13}^H \mathbf{A}_1\right) \end{aligned} \tag{80}$$

where we note $\bar{\mathbf{V}}_3 = \mathbf{W}_{13}{}^H \mathbf{V}_3$. Similarly, we can write:

$$span\left(\mathbf{S}_{23}\mathbf{W}_{23}{}^{H}\mathbf{V}_{3}\right)\subseteq span\left(\mathbf{U}_{23}^{H}\mathbf{A}_{2}\right) \tag{81}$$

We can apply pseudo-inverse to the last equation in (80) if the following condition is satisfied [13] [24]:

$$\begin{gathered} span\left(\mathbf{U}_{13}^{H}\mathbf{A}_{1}\right)\subseteq span\left(\mathbf{S}_{13}\right) \\ span\left(\mathbf{A}_{1}\right)\subseteq span\left(\mathbf{U}_{13}\mathbf{S}_{13}\right) \\ span\left(\mathbf{A}_{1}\right)\subseteq span\left(\mathbf{U}_{13}\mathbf{S}_{13}\mathbf{W}_{13}^{H}\right) \\ span\left(\mathbf{A}_{1}\right)\subseteq span\left(\mathbf{H}_{13}\right) \end{gathered} \tag{82}$$

where we have used

$$span\left(\mathbf{U}_{13}\mathbf{S}_{13}\right)=span\left(\mathbf{U}_{13}\mathbf{S}_{13}\mathbf{W}_{13}^{H}\right) \tag{83}$$

in the third equation, as $\mathbf{W}_{13}$ is a full rank matrix and any full rank linear combination of $\mathbf{U}_{13}\mathbf{S}_{13}$ remains on the same subspace [24]. The last term in (82) is always true because $span\left(\mathbf{A}_{1}\right)=span\left(\mathbf{H}_{12}\right)\cap span\left(\mathbf{H}_{13}\right)$ from (75). Consequently, the pseudo-inverse can be applied to (80). We use the Moore-Penrose pseudo-inverse, on matrices $\mathbf{S}_{ij}$. Since they have the following structure:

$$\mathbf{S}=\begin{bmatrix}\tilde{\mathbf{S}}\\ \mathbf{0}\end{bmatrix}$$

the pseudo-inverse is reduced to:

$$\mathbf{S}^{\#}=\left(\mathbf{S}^{H}\mathbf{S}\right)^{-1}\mathbf{S}^{H}=\begin{bmatrix}\tilde{\mathbf{S}}^{-1} & \mathbf{0}\end{bmatrix} \tag{84}$$

Solving equations (80) and (81) by pseudo-inversion:

$$\begin{gathered} span\left(\bar{\mathbf{V}}_{3}\right)\subseteq span\left(\mathbf{S}_{13}^{\#}\mathbf{U}_{13}^{H}\mathbf{A}_{1}\right) \\ span\left(\bar{\mathbf{V}}_{3}\right)\subseteq span\left(\mathbf{S}_{23}^{\#}\mathbf{U}_{23}^{H}\mathbf{A}_{2}\right) \\ span\left(\bar{\mathbf{V}}_{3}\right)\subseteq span\left(\mathbf{S}_{13}^{\#}\mathbf{U}_{13}^{H}\mathbf{A}_{1}\right)\cap span\left(\mathbf{S}_{23}^{\#}\mathbf{U}_{23}^{H}\mathbf{A}_{2}\right)=span\left(\mathbf{T}_{3}\right) \end{gathered} \tag{85}$$

where matrix $\mathbf{T}_3$ spans the intersection space. Finally, precoder for user 3 can be expressed as follows:

$$\mathbf{V}_{3}=\mathbf{W}_{13}{}^{-H}\mathbf{U}_{T_3}\mathbf{Q}_{3} \tag{86}$$

where $\mathbf{U}_{T_3}$ are the left singular vectors of $\mathbf{T}_3$ and $\mathbf{Q}_3$ is any full-rank matrix. Matrix $\mathbf{Q}_3$ provides freedom for additional optimization.

3.4.3.2.2 Achievable DoF

The achievable DoF for the intersection space precoding are given by the next theorem:

Theorem 3.4.3-2*:* For the 3-user MIMO IC with constant channel coefficients and (M,N) antennas at each pair transmitter-receiver with $N>M$, the following DoF per user can be achieved:

$$d_j = \min\left(2(N-M),(3M-2N)^+\right) \tag{87}$$

Proof: The proof is presented in Appendix C.

□

3.4.4 Combined IA and ZF

In previous sections we have explored the intersection space precoding, which also solves the $M \neq N$ case. There, the precoding matrices are designed such that the interference space at each receiver lies on the intersection space of the interfering channel matrices. In this context, it is pointed that there are antenna configurations such that following this precoding scheme the desired signals cannot lie on the space of the intersection of the interfering channel matrices, for example $(M,N)=(5,6)$. In this section, we present a design allowing the desired signals to lie on this space. To that end, we transform the IA equation system into the following matrix system:

$$\begin{bmatrix} \mathbf{0} & \mathbf{H}_{12} & \mathbf{H}_{13} \\ \mathbf{H}_{21} & \mathbf{0} & \mathbf{H}_{23} \\ \mathbf{H}_{31} & \mathbf{H}_{32} & \mathbf{0} \end{bmatrix} \begin{bmatrix} \mathbf{V}_1^N \\ \mathbf{V}_2^N \\ \mathbf{V}_3^N \end{bmatrix} = \begin{bmatrix} \mathbf{0} \\ \mathbf{0} \\ \mathbf{0} \end{bmatrix} \qquad \mathbf{H}^N \mathbf{V}^N = 0$$
$$\mathbf{V}^N = null\left(\mathbf{H}^N\right) \tag{88}$$

The null space of the block matrix $\mathbf{H}^N \in \mathbb{C}^{3N \times 3M}$ has dimension $3M - 3N$ and hence, the only condition to be satisfied for the existence of the null-space is:

$$\begin{aligned} 3M - 3N &> 0 \\ M &> N \end{aligned} \tag{89}$$

3.4.4.1 Design of precoding matrices

Notice that (88) supports both ZF and IA conditions: writing (88) as a 3 equation system:

$$\begin{aligned} \mathbf{H}_{12}\mathbf{V}_2^N &= -\mathbf{H}_{13}\mathbf{V}_3^N \\ \mathbf{H}_{21}\mathbf{V}_1^N &= -\mathbf{H}_{23}\mathbf{V}_3^N \\ \mathbf{H}_{31}\mathbf{V}_1^N &= -\mathbf{H}_{32}\mathbf{V}_2^N \end{aligned} \tag{90}$$

Any solution for $\mathbf{V}_1^N, \mathbf{V}_2^N$ and $\mathbf{V}_3^N$ satisfying (90) satisfies also the IA conditions (66). Furthermore, there is a subset of solutions of (90) satisfying the ZF conditions (63):

$$\begin{bmatrix}\mathbf{H}_{21}\\ \mathbf{H}_{31}\end{bmatrix}\mathbf{V}_1^{ZF}=\mathbf{0}\quad\begin{bmatrix}\mathbf{H}_{12}\\ \mathbf{H}_{32}\end{bmatrix}\mathbf{V}_2^{ZF}=\mathbf{0}\quad\begin{bmatrix}\mathbf{H}_{13}\\ \mathbf{H}_{23}\end{bmatrix}\mathbf{V}_3^{ZF}=\mathbf{0}\qquad\mathbf{V}^{ZF}=\begin{bmatrix}\mathbf{V}_1^{ZF}\\ \mathbf{V}_2^{ZF}\\ \mathbf{V}_3^{ZF}\end{bmatrix} \tag{91}$$

This solutions can be extracted from $\mathbf{V}^N$. In order to do so, we multiply by the orthogonal projection of matrix $\mathbf{V}^{ZF}$, denoting the resulting product as $\mathbf{\Pi}$:

$$\begin{aligned}\mathbf{\Pi}&=\mathbf{P}^{\perp}_{\mathbf{V}^{ZF}}\mathbf{V}^N\\ \mathbf{P}^{\perp}_{\mathbf{V}^{ZF}}&=\mathbf{I}-\mathbf{V}^{ZF}\left(\left(\mathbf{V}^{ZF}\right)^H\mathbf{V}^{ZF}\right)^{-1}\left(\mathbf{V}^{ZF}\right)^H\end{aligned} \tag{92}$$

Notice that $\mathbf{\Pi}$ will be a deficient-rank matrix because we have projected $\mathbf{V}^N$ to a lower dimension subspace. Hence, we compute the SVD of $\mathbf{\Pi}$:

$$\mathbf{\Pi}=\begin{bmatrix}\mathbf{\Pi}_1 & \mathbf{\Pi}_2\end{bmatrix}\begin{bmatrix}\mathbf{\Lambda} & \mathbf{0}\\ \mathbf{0} & \mathbf{0}\end{bmatrix}\mathbf{S}^H \tag{93}$$

where $\mathbf{\Pi}_1$ is the matrix whose columns span the rank space of $\mathbf{\Pi}$, $\mathbf{\Pi}_2$ is the matrix whose columns span the null space of $\mathbf{\Pi}$, $\mathbf{\Lambda}$ is a diagonal matrix containing the singular values of $\mathbf{\Pi}$ and $\mathbf{S}$ is the matrix containing the right singular vectors of $\mathbf{\Pi}$. Since the rank space of $\mathbf{\Pi}$ is spanned by $\mathbf{\Pi}_1$, we denote this matrix $\mathbf{V}^{IA}$ because using it as a precoding matrix satisfies IA conditions but not ZF on transmission conditions.
Finally, we define the matrix $\mathbf{V}$, which is composed of two matrices:

$$\mathbf{V}=\begin{bmatrix}\mathbf{V}^{ZF} & \mathbf{V}^{IA}\end{bmatrix}=\begin{bmatrix}\mathbf{V}_1\\ \mathbf{V}_2\\ \mathbf{V}_3\end{bmatrix} \tag{94}$$

We cannot take all the columns of $\mathbf{V}$, only a number that does not exceed the maximum achievable DoF (whose value will be derived in Section 3.4.4.3) and therefore a selection of columns has to be done. To that end, the next section provides an algorithm achieving the optimum solution.

3.4.4.2 Selection of precoders in each transmission mode

The first thing to consider is that if a column of $\mathbf{V}$ is selected then the precoding matrix of each user will have a portion of this column. Let us illustrate it with an example: for a pair (M,N) let $\mathbf{V}$ be

$$\mathbf{V}=\left[\mathbf{V}^{ZF}(:,1)\quad \mathbf{V}^{ZF}(:,2)\quad \mathbf{V}^{ZF}(:,3)\quad \mathbf{V}^{IA}(:,1)\quad \mathbf{V}^{IA}(:,2)\right] \tag{95}$$

where $\mathbf{V}^{ZF}(:,i)$ is the $3M\times 1$ ith column of $\mathbf{V}^{ZF}$ and $\mathbf{V}^{IA}(:,i)$ is the $3M\times 1$ ith column of $\mathbf{V}^{IA}$. Suppose that we know that the DoF of the null-space precoding for this pair (M,N) is 4. Then, a selection of columns from $\mathbf{V}$ has to be done. For example, suppose 4 degrees of freedom can be achieved and the optimum selection is:

$$\mathbf{V}_{opt}=\left[\mathbf{V}^{ZF}(:,1)\quad \mathbf{V}^{ZF}(:,2)\quad \mathbf{V}^{ZF}(:,3)\quad \mathbf{V}^{IA}(:,1)\right] \tag{96}$$

Then the precoding matrix for each user is generated as follows:

$$\begin{aligned}\mathbf{V}_1&=\mathbf{V}_{opt}(1:M,:)\\ \mathbf{V}_2&=\mathbf{V}_{opt}(M+1:2M,:)\\ \mathbf{V}_3&=\mathbf{V}_{opt}(2M+1:3M,:)\end{aligned} \tag{97}$$

where $\mathbf{V}_{opt}(1:M,:)$ are the first M rows, and similarly for the rest of matrices. Hence, we will have to decide which transmission modes are used (ZF or IA) and the number of bitstreams transmitted by each.

The total number of columns of $\mathbf{V}^{N}$, $\mathbf{V}^{ZF}$ and $\mathbf{V}^{IA}$ is equal to the rank of these matrices:

$$\begin{aligned}rank\left(\mathbf{V}^{N}\right)&=3(M-N)\\ d^{ZF}=rank\left(\mathbf{V}^{ZF}\right)&=(M-2N)^{+}\\ d^{IA}=rank\left(\mathbf{V}^{IA}\right)&=3(M-N)-(M-2N)^{+}\end{aligned} \tag{98}$$

where d^{ZF} and d^{IA} represents the maximum DoF which could be achieved using this precoding scheme by ZF and IA, respectively. Now, we present an algorithm to select how many bitstreams are transmitted by ZF and how many by IA, i.e how the columns

of $\mathbf{V}$ are selected, considering that $d \le d^{ZF} + d^{IA} = 3(M-N)$ degrees of freedom can be achieved:

1. Select $d_1 = \min\left(d^{ZF}, d\right)$ of $\mathbf{V}^{ZF}$.
2. Add $d - d_1$ columns of $\mathbf{V}^{IA}$ to the selection.

Figure 17: Algorithm to select the best columns of $\mathbf{V}$ in order to maximize the DoF achieved

Precoding matrices $\mathbf{V}$ can incorporate matrices $\mathbf{Q}_1$ and $\mathbf{Q}_2$:

$$\begin{aligned} \bar{\mathbf{V}}^{ZF} &= \mathbf{V}^{ZF}\mathbf{Q}_1 \\ \bar{\mathbf{V}}^{IA} &= \mathbf{V}^{IA}\mathbf{Q}_2 \end{aligned} \tag{99}$$

which may select the precoders (or a combination of those) under some optimization criterion affecting the intended signal. As an example, if $d < d^{ZF}$ a selection of ZF precoders will be needed and still the condition:

$$\mathbf{H}^N \mathbf{V}^{ZF} \mathbf{Q}_1 = \mathbf{0}, \quad \forall \mathbf{Q}_1 \tag{100}$$

is satisfied. Let us define the matrix of direct channels:

$$\mathbf{H}^D = \begin{bmatrix} \mathbf{H}_{11} & \mathbf{0} & \mathbf{0} \\ \mathbf{0} & \mathbf{H}_{22} & \mathbf{0} \\ \mathbf{0} & \mathbf{0} & \mathbf{H}_{33} \end{bmatrix} \tag{101}$$

We want $\mathbf{H}^D \bar{\mathbf{V}}^{ZF}$ to have the maximum rank, in which case:

$$\begin{aligned} \mathbf{Q}_1 &= \arg\max_{\mathbf{Q}_1} \det\left(\left(\mathbf{H}^D \bar{\mathbf{V}}^{ZF}\right)^H \mathbf{H}^D \bar{\mathbf{V}}^{ZF}\right) \\ &\text{st} \quad \left(\bar{\mathbf{V}}^{ZF}\right)^H \bar{\mathbf{V}}^{ZF} = \mathbf{I} \end{aligned} \tag{102}$$

Another possibility is to maximize the sum of SNRs over all receiving modes as follows:

$$\begin{aligned} \mathbf{Q}_1 &= \arg\max_{\mathbf{Q}_1} \quad trace\left(\left(\mathbf{H}^D \bar{\mathbf{V}}^{ZF}\right)^H \mathbf{H}^D \bar{\mathbf{V}}^{ZF}\right) \\ &\text{st} \quad \left(\bar{\mathbf{V}}^{ZF}\right)^H \bar{\mathbf{V}}^{ZF} = \mathbf{I} \end{aligned} \tag{103}$$

Solution to this problem leads $\mathbf{Q}_1$ to be the d^{ZF} eigenvectors with higher eigenvalue of the matrix $\left(\mathbf{H}^D\mathbf{V}^{ZF}\right)^H \mathbf{H}^D\mathbf{V}^{ZF}$:

$$\mathbf{Q}_1 = eig\left(\left(\mathbf{H}^D\mathbf{V}^{ZF}\right)^H \mathbf{H}^D\mathbf{V}^{ZF}\right) \tag{104}$$

For the case of $\mathbf{V}^{IA}$ precoders, we cannot combine its columns because interference alignment would be broken. For the moment, we propose to exhaustively look for the selection of IA beamvectors so as to maximize any of the criteria in (102) or(103).

We simulate the former problem for different selections of the columns of $\mathbf{V}^{IA}$ and we observe that the mutual information varies depending on the selection of these columns (see Figure 18 and Figure 19). Notice that the column selection varies only the offset of the curve whereas increasing the number of antennas varies the offset and the slope of the curve.

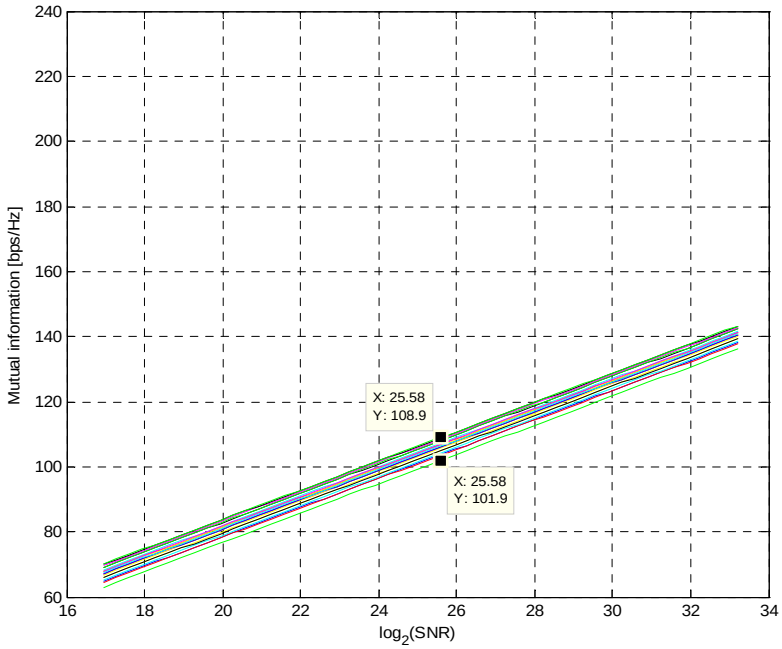

Figure 18: Mutual information as a function of the column selection for $(M,N)=(4,3)$. 1.5 DoF per user achieved.

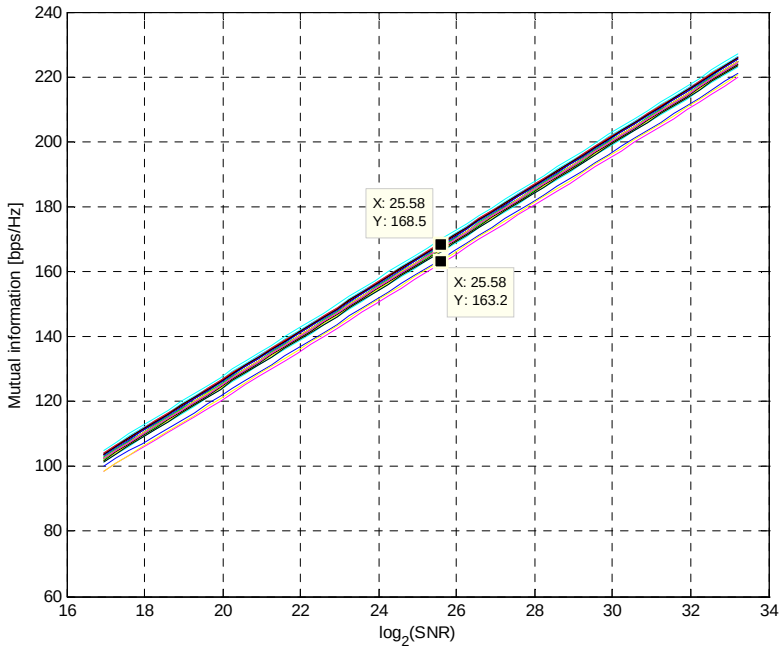

Figure 19: Mutual information as a function of the column selection for $(M,N)=(8,3)$. 2.5 DoF per user achieved.

3.4.4.3 Achievable DoF

The number of columns of $\mathbf{V}^{ZF}$ and $\mathbf{V}^{IA}$ provides the DoF but it needs to be upperbounded using the expression in section 3.4.2. The following theorem describes the number of degrees of freedom for each pair (M,N):

Theorem 3.4.4-1: For the 3-user MIMO IC with constant channel coefficients and (M,N) antennas at each pair transmitter-receiver with $M>N$ and $r=\frac{M}{N}$, the following DoF per user can be achieved using a combination of ZF precoding and IA:

$$d=\begin{cases} 3(M-N) & 1\le r\le \frac{7}{6} \\ \frac{N}{2} & \frac{7}{6}\le r\le 2 \\ \frac{M-N}{2} & 2\le r\le 3 \\ N & r\ge 3 \end{cases} \tag{105}$$

Proof: For ZF precoding, from section 3.4.2 is follows that the maximum DoF are:

$$d^{ZF} = \min\left((M-2N)^{+}, N\right)$$

IA approach to align interference at each receiver. Hence, if each user transmits d bitstreams we can divide each receiver space in two $d/2$ dimensional subspaces: one for the desired signals and one for the all interfering signals. Hence, if we use d^{ZF} dimensions with ZF mode, we only have $N - d^{ZF}$ dimensions at each receiver so as to make two partitions for IA mode. We also know that the columns of $\mathbf{V}^{IA}$ cannot be larger than $3(M-N) - d^{ZF}$ as shown in (98). Thus, the degrees of freedom achieved by IA are:

$$d^{IA} = \min\left(\left(\frac{N - d^{ZF}}{2}\right)^{+}, 3(M-N) - d^{ZF}\right) \tag{106}$$

Finally, the total number of DoF can be obtained as a piece-wise function of the ratio $r = \frac{M}{N}$ in (105).

□

3.4.5 GSVD precoding: a new strategy based on partial ZF

We describe in this section a type of precoding scheme that allows us to achieve most of the outerbounds defined in Theorem 3.3.2-1. Based on the transmission modes introduced at the last section, we identify:

- ZF mode: bitstreams transmitted with this mode do not create interference to the other 2 receivers. The number of bitstreams transmitted by this mode will be denoted as d_{ZF}. Precoding matrices using this mode are computed as $\bar{\mathbf{V}}^{ZF}$ in null-space precoding.
- Partial ZF mode: bitstreams transmitted with this mode do not create interference to one of the receivers and it is aligned on other. The number of bitstreams transmitted by this mode will be denoted as d_{pZF}.
- IA mode: bitstreams transmitted with this mode have to be aligned with other user's bitstreams in order to occupy the minimum number of dimensions when they are interference. The number of bitstreams transmitted by this mode will be denoted as d_{IA}.

The Partial ZF transmission mode gives us more liberty to achieve the outer degrees of freedom. The total DoF achieved by this technique could be decomposed as:

$$d = d_{IA} + d_{ZF} + d_{pZF} \tag{107}$$

3.4.5.1 Design of precoding matrices

For every user's precoding matrix $\mathbf{V}_i$, the DoF and transmission mode needs to be decided. It is also possible to use a combination of modes as the last section. The DoF d defines the number of columns of $\mathbf{V}_i$, while the design of each column depends on which mode is used on that column. In general, we can define $\mathbf{V}_i$ as:

$$\mathbf{V}_i = \left[\mathbf{V}_i^{ZF} \quad \mathbf{V}_i^{pZF} \quad \mathbf{V}_i^{IA} \right] \tag{108}$$

If a mode is not used, there is no representation of this mode at the precoding matrix. Next, we explain these 3 modes of transmission and we formulate the conditions when they can be used.

3.4.5.1.1 Mode 1: ZF

This mode is explained in section 3.4.2, where we stated that the achievable DoF are:

$$d_{ZF} = \min\left(\left(M - 2N\right)^{+}, N\right)$$

and the transmit conditions:

$$r = \frac{M}{N} > 2$$

3.4.5.1.2 Mode 2: partial ZF

We denote by $\mathbf{V}_i^{p,ZF}, i \in \{1,2,3\}$ the group of columns of the precoding matrix for user i $\mathbf{V}_i, i \in \{1,2,3\}$ using this mode. Bitstreams are divided in two groups:

$$\mathbf{V}_i^{p,ZF} = \left[\mathbf{V}_{ji}^{p,ZF} \quad \mathbf{V}_{ki}^{p,ZF}\right] \quad , \quad j,k \neq i \tag{109}$$

Each one of these two sub-matrices has to fit two conditions:

- It does not create interference to one user: $\mathbf{V}_{ji}^{p,ZF}$ is cancelled at receiver *j* and $\mathbf{V}_{ki}^{p,ZF}$ is cancelled at receiver *k*.
- It is aligned with other bitstreams transmitted by this mode at the user where they are not suppressed: $\mathbf{V}_{ji}^{p,ZF}$ is aligned at receiver k and $\mathbf{V}_{ki}^{p,ZF}$ is aligned at receiver j.

In order to ensure these two conditions, each precoding sub-matrix could be defined as the product of two matrices. The structure of the sub-matrices becomes

$$\mathbf{V}_{ji}^{p,ZF} = \mathbf{\Gamma}_{ji}\mathbf{Q}_{ki}, \qquad \mathbf{\Gamma}_{ji} = null\left(\mathbf{H}_{ji}\right) \tag{110}$$

where $\mathbf{Q}_{ki}$ is a matrix which ensures alignment of the ith user's bitstreams at receiver k. For example, precoding matrix for user 2 is:

$$\mathbf{V}_2^{p,ZF} = \left[\mathbf{V}_{12}^{p,ZF} \quad \mathbf{V}_{32}^{p,ZF}\right] = \left[\mathbf{\Gamma}_{12}\mathbf{Q}_{32} \quad \mathbf{\Gamma}_{32}\mathbf{Q}_{12}\right] \tag{111}$$

Matrices $\mathbf{Q}_{ji}$ have now to be designed in order to satisfy all the alignment problem:

$$span\left(\mathbf{H}_{12}\mathbf{\Gamma}_{32}\mathbf{Q}_{12}\right) = span\left(\mathbf{H}_{13}\mathbf{\Gamma}_{23}\mathbf{Q}_{13}\right) \tag{112}$$

which can be computed using GSVD as in [14]. Here we show as an example the solution for $\mathbf{Q}_{12}$ and $\mathbf{Q}_{13}$ for the alignment problem presented in (112). All the other alignment problems can be generalized straightforward using this example.

Let $\bar{\mathbf{H}}_{12} = \mathbf{H}_{12}\mathbf{\Gamma}_{32}$, $\bar{\mathbf{H}}_{13} = \mathbf{H}_{13}\mathbf{\Gamma}_{23}$ be the equivalent channels for users 2 and 3 at receiver 1. Using GSVD they can be written as:

$$\bar{\mathbf{H}}_{12} = \mathbf{W}\mathbf{D}_{12}\mathbf{U}_{12}^{H}, \qquad \bar{\mathbf{H}}_{13} = \mathbf{W}\mathbf{D}_{13}\mathbf{U}_{13}^{H} \tag{113}$$

where $\mathbf{W}$ is a $N \times N$ common left full rank matrix, $\mathbf{D}_{12}, \mathbf{D}_{13}$ are $N \times M$ diagonal matrices and $\mathbf{U}_{12}, \mathbf{U}_{13}$ are $M \times M$ matrices. One solution for (112) is to set:

$$\begin{aligned} \mathbf{Q}_{12} &= \mathbf{U}_{12}\tilde{\mathbf{D}}_{12}\mathbf{K}_{12} \\ \mathbf{Q}_{13} &= \mathbf{U}_{13}\tilde{\mathbf{D}}_{13}\mathbf{K}_{13} \end{aligned} \tag{114}$$

where $\mathbf{K}_{ji}$ are arbitrary random full rank matrices. In [14] is shown that these matrices are necessary in order to achieve all the DoF of the channel. The structure of matrices $\mathbf{D}_{ji}$ is also shown in detail. Here $\tilde{\mathbf{D}}_{ji}$ is the pseudoinverse of $\mathbf{D}_{ij}$:

$$\mathbf{D}_{ji} = \begin{bmatrix} \mathbf{D}_{ji} & \mathbf{0} \end{bmatrix} \Rightarrow \tilde{\mathbf{D}}_{ji} = \begin{bmatrix} \mathbf{D}_{ji}^{-1} \\ \mathbf{0} \end{bmatrix} \tag{115}$$

The next lemma shows the partial ZF transmit conditions.

Lemma 3.4.5-1: Partial ZF mode can only be used if $r > \frac{3}{2}$.

Proof: The alignment problem defined in (112) can be solved only if there is no null intersection between matrices $\bar{\mathbf{H}}_{12}$ and $\bar{\mathbf{H}}_{13}$. Using the Grassman formula:

$$\begin{aligned} &\dim\left(span\left(\bar{\mathbf{H}}_{ji}\right) \cap span\left(\bar{\mathbf{H}}_{jk}\right)\right) = \\ &= rank\left(\bar{\mathbf{H}}_{ji}\right) + rank\left(\bar{\mathbf{H}}_{jk}\right) - rank\left(\begin{bmatrix} \bar{\mathbf{H}}_{ji} & \bar{\mathbf{H}}_{jk} \end{bmatrix}\right) = \\ &= 2\left(M - N\right) - N = 2M - 3N \end{aligned} \tag{116}.$$

Thus, this mode can only be applied when:

$$\begin{aligned} \dim\left(span\left(\bar{\mathbf{H}}_{ji}\right) \cap span\left(\bar{\mathbf{H}}_{jk}\right)\right) > 0 \\ 2M - 3N > 0 \\ r > \frac{3}{2} \end{aligned} \tag{117}$$

Hence, the maximum number of columns for $\mathbf{V}_{ij}^{p,ZF} \quad i, j \in \{1,2,3\} \quad i \neq j$ would be the dimension of the intersection space, that is, *2M-3N*.

□

Assuming that all the users achieve the same DoF, the maximum number of columns for $\mathbf{V}_{i}^{p,ZF}, i \in \{1,2,3\}$ is twice the maximum number of columns for $\mathbf{V}_{ij}^{p,ZF} \quad i, j \in \{1,2,3\} \quad i \neq j$, that is:

$$d_{p,ZF} = 2\left(2M - 3N\right)^{+} \tag{118}$$

which are the DoF per user achieved by this mode.

3.4.5.1.3 Mode 3: IA

We present this mode as an extension of precoding methods presented at [14] for the MIMO X channel (see Chapter 1 and Section 3.1). For $r = 1$, there is an alternate form to achieve the outerbound as the CJ scheme presented in [16] but it also works for $M \neq N$. Equations of IA are shown below again. The problem is to design precoding matrices $\mathbf{V}_{i}^{IA}, i = 1,2,3$ so as to satisfy:

$$\begin{aligned} span(\mathbf{H}_{12}\mathbf{V}_2) = span(\mathbf{H}_{13}\mathbf{V}_3) \\ span(\mathbf{H}_{21}\mathbf{V}_1) = span(\mathbf{H}_{23}\mathbf{V}_3) \\ span(\mathbf{H}_{31}\mathbf{V}_1) = span(\mathbf{H}_{32}\mathbf{V}_2) \end{aligned}$$

Let us consider the GSVD (77) of the following channel matrices:

$$\begin{aligned} \mathbf{H}_{12} = \mathbf{W}_{12}\mathbf{D}_{12}\mathbf{U}_{12}^{H} \qquad \mathbf{H}_{21} = \mathbf{W}_{21}\mathbf{D}_{21}\mathbf{U}_{21}^{H} \\ \mathbf{H}_{13} = \mathbf{W}_{12}\mathbf{D}_{13}\mathbf{U}_{13}^{H} \qquad \bar{\mathbf{H}}_{23} = \mathbf{H}_{23}\mathbf{U}_{13} = \mathbf{W}_{21}\bar{\mathbf{D}}_{23}\bar{\mathbf{U}}_{23}^{H} \end{aligned} \tag{119}$$

and define

$$\begin{aligned}
&\mathbf{D}_{ij}^{\#} = \mathbf{D}_{ij}{}^{H}\left(\mathbf{D}_{ij}\mathbf{D}_{ij}^{H}\right)^{-1} \\
&\boldsymbol{\Omega}_1 = \bar{\mathbf{U}}_{23}\bar{\mathbf{D}}_{23}^{\#}, \\
&\boldsymbol{\Omega}_2 = eig\left(\mathbf{H}_{31}\mathbf{U}_{21}\mathbf{D}_{21}^{\#}\mathbf{K}_1, \mathbf{H}_{32}\mathbf{U}_{12}\mathbf{D}_{12}^{\#}\boldsymbol{\Omega}_1\mathbf{K}_1\right) \\
&\text{with } \mathbf{K}_1 \text{ and } \mathbf{K}_2 \text{ are free to design}
\end{aligned} \tag{120}$$

The precoders become

$$\begin{aligned}
\mathbf{V}_1^{IA} &= \mathbf{U}_{21}\mathbf{D}_{21}^{\#}\mathbf{K}_1\boldsymbol{\Omega}_2\mathbf{K}_2 \\
\mathbf{V}_1^{IA} &= \mathbf{U}_{21}\mathbf{D}_{21}^{\#}\mathbf{K}_1\boldsymbol{\Omega}_2\mathbf{K}_2 \\
\mathbf{V}_3^{IA} &= \mathbf{U}_{13}\mathbf{D}_{13}^{\#}\boldsymbol{\Omega}_1\mathbf{K}_1\boldsymbol{\Omega}_2\mathbf{K}_2
\end{aligned} \tag{121}$$

where matrices $\mathbf{K}_1$ and $\mathbf{K}_2$ are arbitrary full-rank matrices. Based on $span(\mathbf{A}) = span(\mathbf{AK})$ for any full-rank matrix $\mathbf{K}$, it is straightforward to see that precoding matrices in (121) satisfy the IA equations. The design procedure is explained in appendix D.

The approach of IA is to divide the dimensional receiver space into two subspaces, one for interference and another for desired signals. However, this partition has to be done in respect to the dimensions which are not being used for other modes. Hence and similarly to section 3.4.4, the maximum number of DoF which could be achieved by this mode are:

$$d_{IA} = \frac{N - d_{others}}{2} \tag{122}$$

where $d_{others} = d_{ZF} + d_{p,ZF}$ represent DoF achieved by other modes.

3.4.5.2 Time extension

We know that in the MIMO IC the outerbounds DoF can be non-integer values. In such a case, the achievable methods require using time extension applied directly to matrices $\mathbf{H}_{ji}$.

This method works directly for mode 1 and mode 2. However, for mode 3 we have to take into account some considerations. Notice that when using mode 3 with *M=N* odd, the matrix $\boldsymbol{\Omega}_2$ in (120) is equivalent to the matrix $\bar{\mathbf{E}}$ at [16] (see Appendix B.III). There, it is shown that the extended matrix $\bar{\mathbf{E}}$ contains the same eigenvectors as the non-

extended matrix $\mathbf{E}$ with a particular structure. Furthermore, in [16] the eigenvectors of $\bar{\mathbf{E}}$ which are used for the precoding matrix $\bar{\mathbf{V}}_1$ are those with different eigenvalue.

In our case, eigenvectors of $\mathbf{\Omega}_2$ will not have the same structure as eigenvectors of $\bar{\mathbf{E}}$ because of using GSVD. In this regard, the eigenvectors of $\mathbf{\Omega}_2$ with different eigenvalue will be selected.

3.4.5.3 Achievable DoF

Innerbound using this method is presented in the next theorem:

Theorem 3.4.5-1: For the 3-user MIMO IC with constant channel coefficients with (M,N) antennas at each pair transmitter-receiver, our scheme based on ZF, partial ZF and IA can achieve d DoF. A closed-form expression of d is shown below.

$$d = d_{ZF} + d_{pZF} + d_{IA} = \begin{cases} \dfrac{\min(M,N)}{2} & 1 \le r \le \dfrac{3}{2} \\ \max(M,N) - \min(M,N) & \dfrac{3}{2} < r < \dfrac{5}{3} \\ \dfrac{(R+1)\min(M,N)}{R+2} & \dfrac{5}{3} \le r < 2 \\ \dfrac{\max(M,N)}{R+1} & 2 \le r < 3 \\ \min(M,N) & r \ge 3 \end{cases} \tag{123}$$

with $R = \left\lfloor \dfrac{\max(M,N)}{\min(M,N)} \right\rfloor$, $r = \dfrac{\max(M,N)}{\min(M,N)}$ and:

$$d_{ZF} = \min\left(\left(\max\left(M,N\right)-2\min\left(M,N\right)\right)^{+},\min\left(M,N\right)\right)$$

$$d_{pZF} = \begin{cases} 2\left(2\max\left(M,N\right)-3\min\left(M,N\right)\right)^{+} & r<\frac{5}{3} \\ \frac{\left(R+1\right)\min\left(M,N\right)}{R+2} & \frac{5}{3}\le r\le 2 \\ 2\min\left(M,N\right)-\frac{2\max\left(M,N\right)}{3} & 2<r<3 \\ 0 & r\ge 3 \end{cases}$$

$$d_{IA} = \begin{cases} \frac{\min\left(M,N\right)}{2} & 1\le r\le\frac{3}{2} \\ 5\min\left(M,N\right)-3\max\left(M,N\right) & \frac{3}{2}<r<\frac{5}{3} \\ 0 & r\ge\frac{5}{3} \end{cases} \tag{124}$$

Proof: We assume $M > N$ without loss of generality due to reciprocity. In such a case, d, d_{ZF}, d_{pZF} and d_{IA} can be rewritten as follows:

$$d = d_{ZF} + d_{pZF} + d_{IA} = \begin{cases} \frac{N}{2} & 1\le r\le\frac{3}{2} \\ M-N & \frac{3}{2}<r<\frac{5}{3} \\ \frac{\left(R+1\right)N}{R+2} & \frac{5}{3}\le r<2 \\ \frac{M}{R+1} & 2\le r<3 \\ N & r\ge 3 \end{cases}, \quad r=\frac{M}{N},\ R=\left\lfloor\frac{M}{N}\right\rfloor$$

$$d_{ZF} = \min\left(\left(M-2N\right)^{+},N\right)$$

$$d_{pZF} = \begin{cases} 2\left(2M-3N\right)^{+} & r<\frac{5}{3} \\ \frac{\left(R+1\right)N}{R+2} & \frac{5}{3}\le r\le 2 \\ 2N-\frac{2M}{3} & 2<r<3 \\ 0 & r\ge 3 \end{cases} \qquad d_{IA} = \begin{cases} \frac{N}{2} & 1\le r\le\frac{3}{2} \\ 5N-3M & \frac{3}{2}<r<\frac{5}{3} \\ 0 & r\ge\frac{5}{3} \end{cases} \tag{125}$$

We prove innerbound of d for each range of values for r:

- $r \geq 3$: N bitstreams are transmitted by ZF. Since they do not create interference to unintended users, desired signals can be decoded correctly and each user can achieve N degrees of freedom.

- $2 \leq r < 3$: Since $2 \leq r < 3$, we have $R = 2$ and so $d = \frac{M}{3}$. $2N - \frac{2M}{3}$ bitstreams are transmitted by partial ZF and $M - 2N$ by ZF. Notice time extension is needed of level 3 in order to achieve these degrees of freedom. Hence, we have to prove that $6N - 2M$ and $3M - 6N$ bitstreams transmitted by mode 2 and 1 respectively can be achieved in a 3-user constant $3N \times 3M$ MIMO IC. Thus, $d = M$ in the extended channel.

  Bitstreams transmitted by ZF do not create interference to unintended users and half of the bitstreams transmitted by partial ZF create interference only at one unintended user. Moreover, these bitstreams are aligned with bitstreams of the other user transmitted by this mode. So each receiver has $3N - (6N - 2M)/2 = M$ free dimensions to allocate the desired signals. Now, the only condition to satisfy is:

$$\begin{aligned} d_{p,ZF} = 3(2M - 3N)^+ &\geq (6N - 2M)/2 \\ 6M - 9N &\geq (3N - M) \\ r &\geq \frac{12}{7} \end{aligned} \tag{126}$$

  which is ensured because $2 \leq r < 3$.

- $\frac{5}{3} \leq r < 2$: Since range of r, we have $R = 1$ and then $d = \frac{2N}{3}$. All $\frac{2N}{3}$ bitstreams are transmitted by partial ZF. We consider a time extension of level 3 as the later case. Thus, each user transmits $2N$ bitstreams and each receiver has $3N$ dimensions to allocate desired and interference signals. Since partial ZF mode suppress half of the interference of each user and then align the remaining unintended signals, interference will occupy only N dimensions and desired signals can be decoded correctly. Another conditions to be satisfied is:

$$\begin{aligned} 3(2M-3N)^{+} &\geq \frac{1}{2}(2N) \\ 6M-9N &\geq N \\ r &\geq \frac{10}{6}=\frac{5}{3} \end{aligned} \tag{127}$$

which is ensured because $\frac{5}{3} \leq r < 2$.

- $\frac{3}{2} < r < \frac{5}{3}$: $2(2M-3N)$ bitstreams are transmitted by partial ZF and $5N-3M$ bitstreams are transmitted by IA. Since desired signals occupy $M-N$ dimensions at each receiver, we only have $2N-M$ dimensions to allocate interference.

  Partial ZF conditions impose that only $2M-3N$ bitstreams of each user create interference and they are aligned. Thus, we have to allocate $5N-3M$ bitstreams on a $N-(2M-3N)$ signal space:

$$\begin{aligned} N-(2M-3N) &\geq 5N-3M \\ 4N-2M &\geq 5N-3M \\ r &\geq 1 \end{aligned} \tag{128}$$

  which is ensured because $\frac{3}{2} < r < \frac{5}{3}$.

- $1 \leq r \leq \frac{3}{2}$: Since $d_{p,ZF} = 2(2M-3N)^{+} = 0$, all $\frac{N}{2}$ bitstreams are transmitted by mode 3. Each receiver send $\frac{N}{2}$ bitstreams and each receiver signal space is divided in two equal parts. Since $r < 2$, IA is feasible.

□

Corollary 3.4.5-1 is formulated based on Theorem 3.4.5-1:

Corollary 3.4.5-1: For the 3-user MIMO constant IC with (M,N) antennas at each pair transmitter-receiver with $M > \frac{5}{3}N$, the total number of degrees of freedom is d , which is described as follows:

$$d=\begin{cases}\dfrac{(R+1)N}{R+2} & \dfrac{5}{3}\le r<2\\ \dfrac{M}{R+1} & 2\le r<3\\ N & r\ge 3\end{cases} \tag{129}$$

with $r=\dfrac{M}{N}$.

Proof: The proof is obtained by verifying that the achievable presented at Theorem 3.4.5-1 match with the outerbound shown in Theorem 3.3.2-1 for $M>\dfrac{5}{3}N$.

□

3.4.6 Rank deficient channels and asymmetric channels

In this section, we show some examples of how GSVD precoding can be used and provide some inner DoF which can be achieved when rank deficient channel matrices or different number of transmit or receive antennas are considered. Unfortunately there is no outerbound on the DoF for any channel rank in the literature. As a consequence, we cannot compare our resulting inner DoF with. Furthermore, until here we consider that the outerbound specify the maximum DoF sum that can be achieved assuming equal rate per user. In this section, we consider that each user can be served in a different rate.

The results of this section could be useful when Line of Sight (LOS) conditions are assumed, because the channel matrices modeling the MIMO IC may become rank deficient matrices. In the first place, we present one example where decreasing antennas of the system does not hurt the DoF sum. To illustrate this idea, consider two different antenna deployments:

User	1	2	3
Transmitter	M	M	M
Receiver	N	N	N

Table 3: Symmetric antenna deployment.

Number of antennas at each terminal

User	1	2	3
Transmitter	M	M	M
Receiver	N	N	$N-1$

Table 4: Asymmetric antenna deployment.

Number of antennas at each terminal

From now on, the antenna deployment in Table 3 will be referred to as the (M,N) symmetric case. We will show an example where the sum DoF obtained with these two antenna deployments is the same.

3.4.6.1 The (4,2) asymmetric case

We begin with a 3-user MIMO interference channel where the first two users have 4 antennas at the transmitter and 2 antennas at the receiver, whereas the third user has 4 antennas at the transmitter and 1 antenna at the receiver. We refer to this system as the (4,2) asymmetric case, that is, asymmetric system of Table 4 with $M=4, N=2$. From the last section, we know that the (4,2) symmetric case could achieve 1.33 DoF per user based on partial ZF precoding whereas the (4,1) symmetric case could achieve 1 DoF per user based on ZF precoding. Notice that from the first case to the second one, 3 antennas of the system have been decreased whereas the (4,2) asymmetric case assumes only one antenna is decreased. How many DoF can be achieved in this channel?

In the first hand, the tuple:

$$(d_1, d_2, d_3) = (1.33, 1.33, 1) \tag{130}$$

can be achieved based on partial ZF and ZF precoding and considering a time extension T=3. Hence, in the extended channel the DoF achieved are $(d_1, d_2, d_3) = (4, 4, 3)$. In this scheme, the number of bitstreams by each mode for each user is different:

- User 1 and user 2 send 2 bitstreams by ZF and two bitstreams by partial ZF, which are cancelled at the third user.

- User 3 sends 1 bitstream by IA and 2 bitstreams by ZF, which are cancelled at the first and the second receiver respectively.

Notice that since $\mathbf{H}_{3j} \in \mathbb{C}^{1\times 4}$, user 1 and user 2 become able to use ZF precoding, but not user 3 because of ZF precoding transmit conditions. This result shows that there are some cases where each user can achieve the same DoF independently of the number of antennas lost by the other users.

Furthermore, it can be shown that the tuple:

$$(d_1, d_2, d_3) = (1.66, 1.33, 1) \tag{131}$$

can be achieved for this channel. For *T=3*, the DoF achieved in the extended channel are $(d_1, d_2, d_3) = (5, 4, 3)$. Bitstreams per mode for each user are:

- User 1 sends 3 bitstreams by ZF and 2 bitstreams by partial ZF, which are cancelled at the third user.
- User 2 sends 3 bitstreams by ZF and 1 bitstream by partial ZF, which is cancelled at the third user.
- User 3 sends 3 bitstreams by partial ZF. 2 bitstreams are cancelled at the first receiver and 1 bitstream is cancelled at the second receiver.

As a consequence, the DoF sum of the (4,2) assymetric case is equal to the DoF sum of the (4,2) symmetric case and losing one antenna does not becomes any penalty.

3.4.6.2 The (4,2) symmetric case with deficient channel matrices

Now we consider the (4,2) symmetric case where the channel matrix between transmitter and receiver 3, $\mathbf{H}_{33}$, is assumed rank deficient, that is:

$$rank(\mathbf{H}_{33}) = 1 \tag{132}$$

As a consequence, the DoF achieved by user 3 can be upper bounded by:

$$d_3 \leq 1 \tag{133}$$

It is easy to prove that the following mode distribution achieves (131):

- User 1 sends 5 bitstreams by partial ZF. 3 bitstreams are cancelled at the second receiver and 2 bitstreams are cancelled at the third receiver.
- User 2 sends 4 bitstreams by partial ZF. 3 bitstreams are cancelled at the first receiver and 1 bitstreams is cancelled at the third receiver.
- User 3 sends 3 bitstreams by partial ZF. 2 bitstreams are cancelled at the first receiver and 1 bitstream at the second receiver.

Furthermore, when matrices $\mathbf{H}_{31}$ $\mathbf{H}_{32}$ and $\mathbf{H}_{33}$ are rank deficient, it can be shown that (131) can be yet achieved and thus, the DoF sum is maintained although rank deficient channel matrices are assumed. The mode distribution is given by,

- User 1 sends 3 bitstreams by ZF and 2 bitstreams by partial ZF, which are cancelled at the third receiver.
- User 2 sends 3 bitstreams by ZF and 1 bitstream by partial ZF, which is cancelled at the third receiver.
- User 3 sends 3 bitstreams by partial ZF. 1 bitstream is cancelled at the second receiver and 2 bitstreams at the first receiver.

Notice that, similarly to the (4,2) assymetric case, when $\mathbf{H}_{31}$ $\mathbf{H}_{32}$ are defficient rank matrices user 1 and user 2 become able to use ZF precoding.

3.5 NEW INNERBOUNDS FOR R<5/3

At the time of writting, a new scheme was presented by Mohamed Amir et al in [35]. This work analyzes the IC as well, achieving the same results for $r \geq 5/3$. There are some differences between our scheme and theirs. For the range $2 \leq r \leq 3$, [35] performs a scheme using random receiver matrices U_i and designing the precoding matrices as

$$\mathbf{V}_i = null\left(\mathbf{U}_j\mathbf{H}_{ji}\right) \cap null\left(\mathbf{U}_k\mathbf{H}_{ki}\right) = null\left(\begin{bmatrix}\mathbf{U}_j\mathbf{H}_{ji} \\ \mathbf{U}_k\mathbf{H}_{ki}\end{bmatrix}\right)$$

This scheme achieves the outerbound on the DoF as GSVD precoding but the matrices $\mathbf{U}_j$ need to be known by all the transmitters and the corresponding *j*th receiver whereas in our scheme the receive filter $\mathbf{P}_j^{\perp}$ is needed only by the *j*th receiver. This is an important issue when considering backhaul rate limitations in a RACN scheme such as in chapter 4.

For the range $5/3 \leq r \leq 2$, their scheme divides each precoding matrix in $L+1$ blocks:

$$\mathbf{V}_i = \begin{bmatrix}\mathbf{V}_i^1 & \mathbf{V}_i^2 & \ldots & \mathbf{V}_i^{L+1}\end{bmatrix}$$

where L is any integer value greater than zero and $\mathbf{V}_i^j \in \mathbb{C}^{M\times\tilde{d}}$. It turns out that when $L=1$, our scheme for partial ZF in section 3.4.5 coincides with their scheme. This parameter L allows them to design the granularity of the precoding matrix by $\tilde{d}$. Using their scheme, they obtain not only the best known innerbound for the DoF for the 3-user MIMO IC with constant channel coefficients, but also to achieve the outerbound for some cases not achieved by GSVD precoding. Moreover, the scheme used in [35] employs a procedure to satisfy the IA equations different from apply the GSVD to the channel matrices as us. Although the slope of the curve cannot be improved because the outerbound on the DoF is achieved, we think that our procedure could improve the offset of the curve maximizing the SNR at each receiver.

Table 5 shows some of these outerbounds achieved by their scheme.

M/N	5/3	7/5	9/7	11/9
d_j	2	3	4	5

Table 5: Outerbounds achieved by the work in [35]

3.6 RESULTS

In this section, we present the results for the IC achieved by this work. Table 6 summarizes the main results of the techniques presented in this section:

Technique	Conditions	Inner DoF per user
ZF precoding	$M > 2N$	$d_j = \min\left((M-2N)^+, N\right)$
CJ precoders	$M = N$	$d_j = \frac{M}{2}$
Intersection space precoding	$M < N < \frac{3M}{2}$	$d_j = \min\left(2(N-M)^+, (3M-2N)^+\right)$
Combined IA and ZF	$M > N$	$d_j = d_{ZF} + d_{IA}$ $d^{ZF} = \min\left((M-2N)^+, N\right)$ $d^{IA} = \min\left(\left(\frac{N-d^{ZF}}{2}\right)^+, 3(M-N)-d^{ZF}\right)$
GSVD precoding	The innerbound depends on the value of the ratio $r = \frac{M}{N}$	$d_j = \begin{cases} \frac{N}{2} & 1 \le r \le \frac{3}{2} \\ M-N & \frac{3}{2} < r < \frac{5}{3} \\ \frac{2N}{3} & \frac{5}{3} \le r < 2 \\ \frac{M}{3} & 2 \le r < 3 \\ N & r \ge 3 \end{cases}$

Table 6: Results of the innerbounds presented in this work

Figure 20 and Figure 21 shows a comparison among the outerbound defined in Theorem 3.3.2-1 and the best innerbound achieved by this work for $N = 4$ based on GSVD precoding in section 3.4.5. Recall on the fact that for $M < \frac{5}{3}N$ there could be one scheme achieving the outerbound or not, but for $M \ge \frac{5}{3}N$ the total DoF of the channel are achieved.

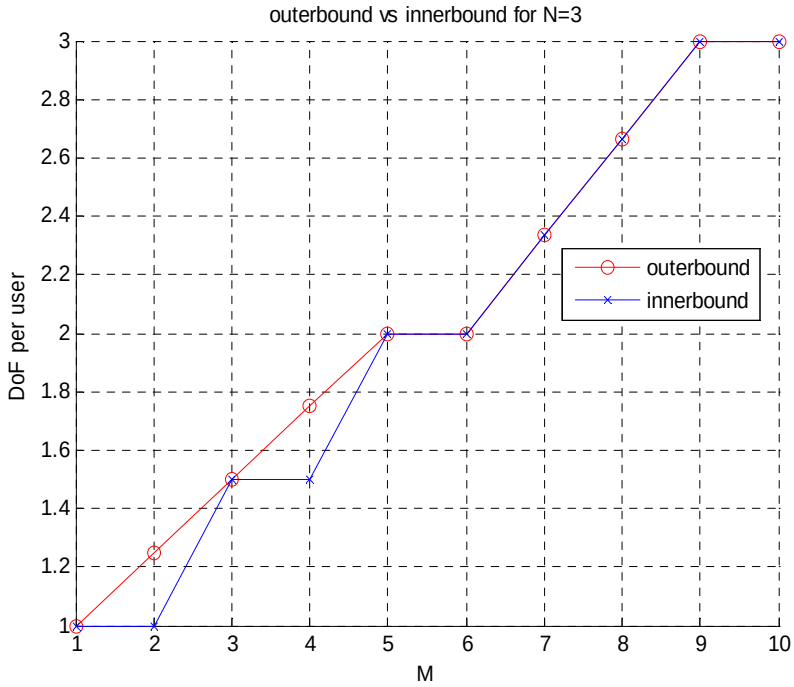

Figure 20: Outerbound vs innerbound for *N=3*. Dof per user as a function of the number of antennas at the transmitters *M*.

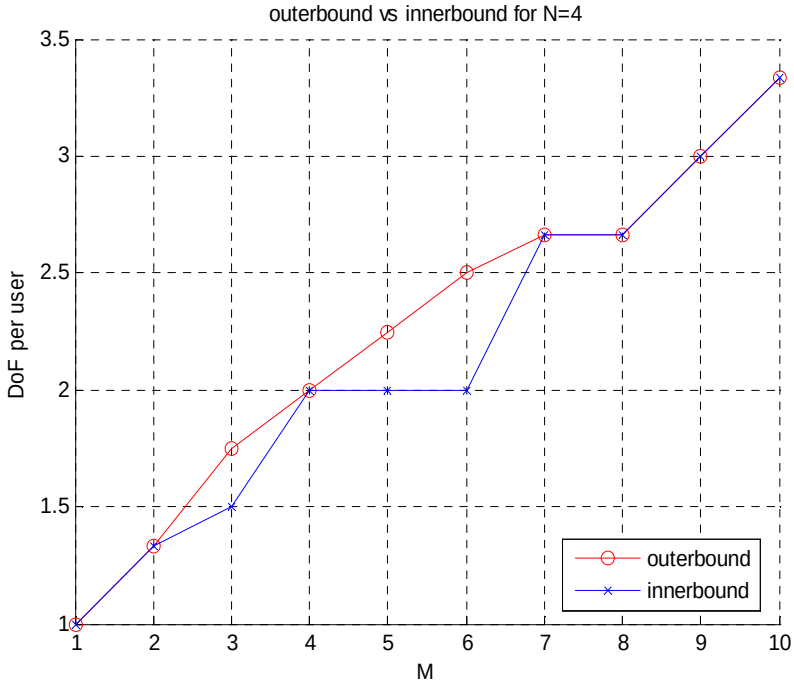

Figure 21: Outerbound vs Innerbound for *N=4*. Dof per user as a function of the number of antennas at the transmitters *M*.

Table 7, Table 8, Table 9 and Table 10 show the outerbound on the DoF per user for the 3-user MIMO IC formulated in Theorem 3.3.2-1 and the inner DoF of the

schemes proposed throughout section 3.4 for all the possible combinations of the pair (M, N) for $M, N = 1...12$. Table 7 shows the outerbound on the DoF per user. Since the outerbound is always greater than or equal to the innerbounds, the rest of tables show the difference between outerbound and that innerbound. Hence, given one scheme a value equal to 0 for a pair (M, N) means that this scheme achieves the outerbound.

Notice that there are some cells with a cross, which means that this precoding scheme cannot be used due to transmit conditions. Moreover, remember the principle of reciprocity, section 2.5, which ensures that any scheme that can be used given any values of (M, N) can be used if these two values are exchanged due to reciprocity. As a consequence, all the tables are symmetric.

M\N	1	2	3	4	5	6	7	8	9	10	11	12
1	0.5	0,66	1	1	1	1	1	1	1	1	1	1
2	0.66	1	1,25	1,33	1,66	2	2	2	2	2	2	2
3	1	1.25	1.5	1.75	2	2	2,33	2,66	3	3	3	3
4	1	1.33	1.75	2	2.25	2,5	2,66	2,66	3	3,33	3,66	4
5	1	1.66	2	2.25	2.5	2.75	3	3,25	3,33	3,33	3,66	4
6	1	2	2	2.5	2.75	3	3.25	3.5	3,75	4	4	4
7	1	2	2.33	2.66	3	3.25	3.5	3.75	4	4.25	4,5	4,66
8	1	2	2.66	2.66	3,25	3.5	3.75	4	4.25	4.5	4.75	5
9	1	2	3	3	3,33	3.75	4	4.25	4.5	4.75	5	5.25
10	1	2	3	3.33	3,33	4	4.25	4.5	4.75	5	5.25	5.5
11	1	2	3	3.66	3.66	4	4.5	4.75	5	5.25	5.5	5.75
12	1	2	3	4	4	4	4.66	5	5.25	5.5	5.75	6

Table 7: Outerbound on the Degrees of freedom of the 3-user MIMO IC

M\N	1	2	3	4	5	6	7	8	9	10	11	12
1	0	0	0	0	0	0	0	0	0	0	0	0
2	0	0	0,25	0	0	0	0	0	0	0	0	0
3	0	0.25	0	0.25	0	0	0	0	0	0	0	0
4	0	0	0.25	0	0,25	0,5	0	0	0	0	0	0
5	0	0	0	0.25	0	0,25	0,5	0,25	0,5	0,75	0	0
6	0	0	0	0.5	0.25	0	0,25	0,5	0,75	0	0	0
7	0	0	0	0	0,5	0.25	0	0,25	0,5	0,75	0,5	0
8	0	0	0	0	0,25	0.5	0.25	0	0,25	0,5	0,75	1
9	0	0	0	0	0	0.75	0.5	0.25	0	0,25	0,5	0,75
10	0	0	0	0	0	0	0.75	0.5	0,25	0	0,25	0,5
11	0	0	0	0	0	0	0.5	0.75	0,5	0.25	0	0,25
12	0	0	0	0	0	0	0	1	0.75	0.5	0.25	0

Table 8: Relative DoF achieved by GSVD precoding. Each cell contains the difference between the outerbound and the GSVD precoding innerbound

M\N	1	2	3	4	5	6	7	8	9	10	11	12
1	x	x	x	x	x	x	x	x	x	x	x	x
2	x	x	x	x	x	x	x	x	x	x	x	x
3	x	x	x	0.75	x	x	x	x	x	x	x	x
4	x	x	0,75	x	0.25	x	x	x	x	x	x	x
5	x	x	x	0,25	x	0.75	2	x	x	x	x	x
6	x	x	x	x	0,75	x	1.25	1.5	x	x	x	x
7	x	x	x	x	2	1,25	x	1.75	1	3.25	x	x
8	x	x	x	x	x	1,5	1,75	x	2.25	0.5	2,75	x
9	x	x	x	x	x	x	1	2,25	x	2.75	1	2.25
10	x	x	x	x	x	x	3,25	0,5	2,75	x	3.25	1.5
11	x	x	x	x	x	x	x	2,75	1	3,25	x	3.75
12	x	x	x	x	x	x	x	x	2,25	1,5	3,75	x

Table 9: Relative DoF achieved by intersection space precoding.

M\N	1	2	3	4	5	6	7	8	9	10	11	12
1	x	0,16	0	0	0	0	0	0	0	0	0	0
2	0.16	x	0,25	0,33	0,16	0	0	0	0	0	0	0
3	0	0.25	x	0,25	0,5	0,5	0,33	0,16	0	0	0	0
4	0	0.33	0.25	x	0,25	0,5	0,66	0,66	0,5	0,33	0,16	0
5	0	0.16	0.5	0.25	x	0,25	0,5	0,75	0,83	0,83	0,66	0
6	0	0	0.5	0.5	0.25	x	0,25	0,5	0,75	0	0	0
7	0	0	0.33	0.66	0,5	0.25	x	0,75	0,5	0,75	1	1,16
8	0	0	0.16	0.66	0,75	0.5	0.75	x	1,25	0,5	0,75	1
9	0	0	0	0.5	0.83	0.75	0.5	1.25	x	1,75	0,5	0,75
10	0	0	0	0.33	0.83	0	0.75	0.5	1,75	x	2,25	0,5
11	0	0	0	0.16	0.66	0	1	0.75	0,5	2.25	x	2,75
12	0	0	0	0	0	0	1.16	1	0.75	0.5	2.75	x

Table 10: Relative DoF achieved by Combined IA and ZF precoding.

4 RACN WITH BS COORDINATION

In this section, we present the application of the schemes derived in the previous chapter in a relay-assisted cellular network (RACN). Likewise, we design the resource allocation, taking into account different user access modes. Finally, the performance of the new cellular network is evaluated at system level. First, section 4.1 introduces the system and some state of the art strategies. Section 0 explain the advantages of relay-assisted transmissions in respect to direct transmissions. Section 4.3 presents the system model considered to design the precoders at the BSs. The next two sections (4.4 and 4.5) describe the user access modes envisioned in the two hops. The resource allocation is designed in section 4.6, where we present different optimization problems depending on the user access modes considered. Finally, section 4.7 presents the system level results in terms of spectral efficiency and outage rate.

4.1 INTRODUCTION

Next generation wireless networks face two objectives:

a) Enhance the homogeneous coverage for uniformly distributed users.

b) Design high spectral efficiency techniques able to combat the wireless channel impairments.

In this regard, MIMO relay-assisted transmissions or networked MIMO (N-MIMO) [27] [28], are able to address them. In the first hand, using relays allows increasing the rate of the downlink transmission if the RS are positioned in a high place (in Line of Sight, LOS) for a better quality of the BS-RS links (high SNR) and better coverage in the RS-MS transmissions, due to the path-loss improvement in the RS-MS over the BS-MS pathloss. However, there are three drawbacks: RSs could have LOS with the other BSs, and hence the inter-cell interference could be increased; and the spatial channel could become rank deficient, which could diminish the MIMO channel gains. Finally, we are transmitting the same information twice and hence, similarly to when we use time extension (section 2.4), the actual rate is decreased. The factor which affects the effective rate of each hop will depend on the duration of each hop. For equal duration, the effective rate of each hop is half the rate of each hop.

Likewise, N-MIMO is based on the cooperation of base stations (BSs), and can be understood as having a single "super" BS with a high number of antennas distributed among the BSs. The work in [27] considers the network cooperation as a means to provide spectrally efficient communications in single-hop cellular downlink systems. Furthermore, the antenna gains are chosen in such a way to minimize the out-of-cell interference, and hence to increase the downlink system capacity. On the other hand, in [28] a clustered BS cooperation strategy is proposed for a large single-hop cellular MIMO network, which includes full intra-cluster cooperation to enhance the sum rate and limited inter-cluster cooperation to reduce interference for the cluster edge users.

However, there are some technological issues impairing cooperation between BSs, such as the backhaul link quality in terms of rate limitation or packet delays. In this work, we exploit the coordination of BSs for the transmissions in the first hop rather than the cooperation, assuming we are able to exchange some parameters through the backhaul link like channel matrices of the first hop. We assume that a central unit collets channel state information, compute those parameters and distribute them to other BSs. Other works deal with the problem of *decentralized computation*. For example, in [29] the authors provide some examples of iterative algorithms that utilize the reciprocity of wireless networks to achieve interference alignment with only local channel knowledge at each node.

However, in our scheme each BS distributes the necessary control data to its associated RS. Some works take into account the coordination case [30][31]. The work in [30] presents the design of coordinated dynamic resource sharing algorithms and reuse techniques among BS/RS cells and evaluate its performance. Our work is based on a similar framework. In [31] some interference coordination algorithms are discussed and compared, which can be based either on global system knowledge or purely on local system knowledge. Furthermore, they apply their results using orthogonal frequency division multiplexing accessing (OFDMA) and review the IEEE 802.16e.

The network deployment studied here is depicted in Figure 22. There are 3 cells, each one containing 1 BS and 2 half-duplex RSs. Each RS serves to 1 MS. Transmission is carried out in two orthogonal phases due to half-duplex RS. The following forwarding protocol is assumed: the BSs transmit in a first phase to one (or two) relays of its cell and afterwards, one or all RSs transmit to their associated MSs.

When relay stations are used in a network, one might consider different decoding roles, which can be grouped in two categories,

- Amplify and forward relaying. The relay amplifies and forwards the received signal. It can be used when the relay does not have the ability of decoding. The optimal duration of each phase is half the total duration of the transmission [3][4].
- Decode and forwarding relaying. The relay decodes and transmits the signal. The duration of each phase has an impact on the final performance of the protocol, which has to be optimized.[7]

We consider that relays have the ability of decoding the signal (Decide and Forward Relaying), which allows us to improve the performance of the system by designing the duration of each phase.

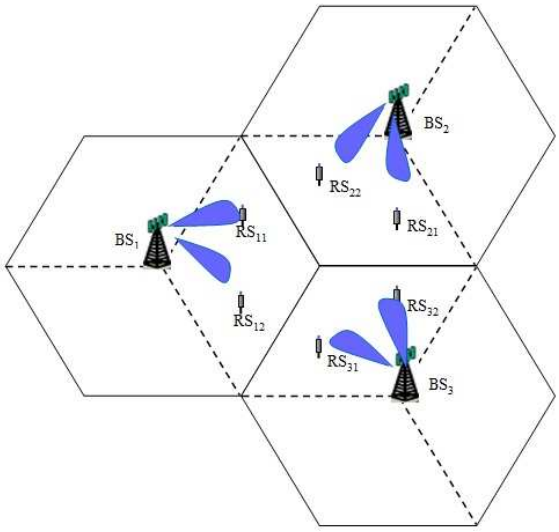

Figure 22: Example of a first hop transmission for the RACN.
There are 3 base stations serving 2 relay stations.

Moreover, we consider different channel state information at the transmitters (CSIT) for each hop:

- In the first hop, we assume there is CSIT available at each BS. This is because the RSs are positioned in a high place and there is line of sight (LOS) for a better quality of the BS-RS links and a better coverage of the

RS-MS links. We assume that the channel coherence time of the BS-RS link is large, so the transmission of the channel matrices is not overloading the backhaul significantly.

- In the second hop, the conditions mentioned above do not hold because the RSs and the MSs use to be in non-line of sight (NLOS) and the MSs could be moving. As a consequence, the channel cannot be assumed static and the control data to be sent for channel estimation would be excessive.

For the first hop (BS-RS transmission) we propose IA or ZF-BD precoding to combat the interference generated by other BSs, while orthogonal in time and simultaneous transmissions are proposed for the second hop (RS-MS transmission).

The resources to be optimized are the duration of the two phases of the relay-assisted transmission, the MIMO transmission precoders at the BSs in order to maximize capacity[1] and the transmit power of each BS. The next section shows a toy example that illustrates how the phase duration influences on the performance of the relay-assisted transmission and justifies the use of coordinated precoding in the BS-RS link.

[1] From now on, we refer to capacity as the bitrate achieved with our precoders, i.e the mutual information of chapters 2 and 3.

4.2 HALF-DUPLEX RELAY TRANSMISSION

Consider a system with a BS, a RS and a MS as shown in the next figure:

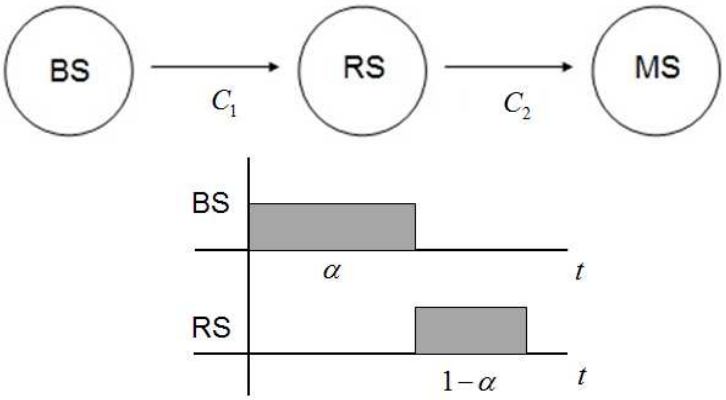

Figure 23: Example of optimization in a simple system. BS transmits during a fraction α of the transmission time and RS transmits during a fraction $1-\alpha$.

Let us consider optimization of the transmission time. In the first hop of duration α, the BS transmits to the RS. In the second hop of duration $1-\alpha$, the RS transmits to the MS. We assume the capacity of the BS-RS link is C_1 and the capacity of the RS-MS link is C_2. The rate achieved by each link would be

$$\begin{aligned} r_1 &= \alpha C_1 \\ r_2 &= (1-\alpha) C_2 \end{aligned} \tag{134}$$

Information flow in the relay implies that if αC_1 bps/Hz are transmitted in the first hop, then the same throughput is needed on the second hop. Hence, the actual rate would be,

$$r = \min(r_1, r_2) = \min\left(\alpha C_1, (1-\alpha) C_2\right) \tag{135}$$

Now consider the optimum duration α such that maximizes the rate:

$$\alpha_{opt} = \arg\max_{\alpha} \min\left(\alpha C_1, (1-\alpha) C_2\right) \tag{136}$$

This problem can be solved by plotting αC_1 and $(1-\alpha) C_2$ as a function of α:

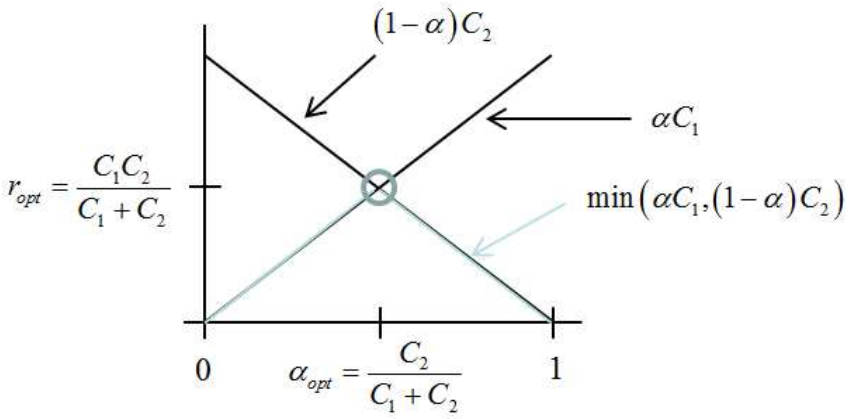

Figure 24: Rate of each hop, rate of the system
and optimum values for α and r

When the problem is extended to K users, assuming that the access of each user is orthogonal, it can be formulated as follows:

$$\begin{aligned} &\max_{\alpha_{1i},\alpha_{2i},i=1\ldots K} \sum_{i=1}^{K} \alpha_{1i} C_{1i} \\ &\text{s.t} \sum_{i=1}^{K} (\alpha_{1i} + \alpha_{2i}) = 1 \\ &\alpha_{1i} C_{1i} = \alpha_{2i} C_{2i}, i = 1\ldots K \end{aligned} \tag{137}$$

where α_{1i} and α_{2i} are the duration of the first and the second hop of the ith user.

As a consequence, the rate achieved optimizing the duration of each hop is always better than merely half the total transmission time, i.e $\alpha = \frac{1}{2}$:

$$r_{opt} = \frac{C_1 C_2}{C_1 + C_2} \geq \frac{1}{2} \min(C_1, C_2) \tag{138}$$

Maximizing the lower bound implies to maximize the capacity of each hop so as to improve the total rate in respect to the case non-relayed case, that is,

$$r_{opt} = \frac{C_1 C_2}{C_1 + C_2} \geq r_D \tag{139}$$

where r_D achieved transmitting directly from the BS to the MS. The use of relays impacts directly on C_2 because the RS is closer to the MS than the BS. Hence, C_2 is much greater than r_D for far users in the cell.

In order not to be limited by the first hop, RS must be placed in high positions and LOS propagation is sought. This is at the expenses of having also LOS propagation to the other BSlinks and hence high levels of interference. In this regard, the use of coordinated transmissions in the first hop deals with the interference generated and are able to enhance the values of C_1.

4.3 SYSTEM MODEL

We define the tuple (M,N,S), where M is the number of antennas at each BS, N is the number of antennas at each RS and S is the number of antennas at each MS.
For all access modes, consider $\mathbf{H}_{1ij}, i=1,2,3$, $j=1,2,...,6$ the $N\times M$ channel matrix between the ith BS and the jth RS and $\mathbf{H}_{2ij}, i=1,2,...,6$, $j=1,2,...,6$ the $S\times N$ channel matrix between the ith RS and the jth MS. Consider these two matrices with equivalent properties to the channel matrices described in the channel model of the chapter 2. The precoding matrices will be denoted by $\mathbf{V}_{1ij}, i=1,2,3$, $j=1,2$ for the first hop, which is the precoding matrix for the jth RS of the ith cell and $\mathbf{V}_{2ij}, i=1,2,3$, $j=1,2$ for the second hop, which is the precoding matrix for the jth MS of the ith cell.
Each cell is denoted by a number $i=1,2,3$, and it contains the ith BS, denoted by BS_i. The two relays of the ith cell are denoted by RS_{i1} and RS_{i2}. Finally, the MS served by each RS is denoted by the same subscript, that is, the MS served by RS_{ij} is denoted by MS_{ij}.

In this chapter we talk about capacity or mutual information without further distinction. In information theory the difference among these two terms is important because we are characterizing the capacity as the tightest value of the mutual information. Here we compute the capacity in the first hop C_{1ij} and the second hop C_{2ij} using the expression of the mutual information shown in section 2.2 and a water-filling solution will be applied in order to improve the rate of link.

4.4 ACCESS MODES IN THE FIRST HOP

4.4.1 Uncoordinated Transmission: Zero-Forcing Block diagonalization

We propose 4 access modes with no coordination between BS based on Zero-Forcing Block Diagonalization (ZF-BD) precoding explained in [8]. The key idea is similar to the ZF precoding scheme in chapter 3. Figure 25 shows these access modes:

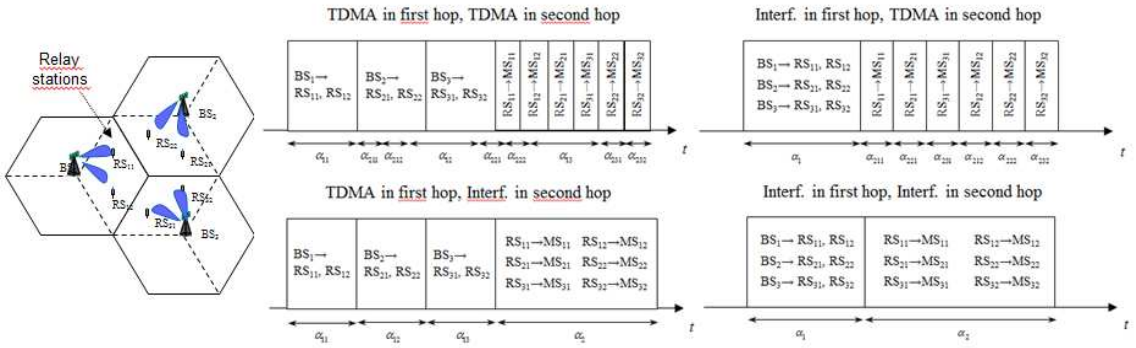

Figure 25: Scheduling plans for uncoordinated transmission in the first hop

These four options assume that a BS transmits simultaneously to its entire RSs. They can be divided into two groups: TDMA in the first hop and simultaneous transmission in the first hop. The first one considers each BS transmits to its entire associated RSs orthogonally in time with the others BSs. The second option considers all the BSs transmit simultaneously to its RSs. Hence, the second option allows inter-cell interference.

As an example, consider the ZF-BD TDMA-Interf access mode (bottom-left of Figure 25), which means ZF-BD TDMA in the first hop and simultaneous transmission in the second hop. The transmissions carried out in the first hop are done over 3 orthogonal phases. In the *i*th phase, BS_i transmits to RS_{i1} and RS_{i2} simultaneously, that is, each BS transmits to all the RSs of its cell without inter-cell interference. Each BS distributes its total transmitted power over the messages intended to its associated RS, referenced by $P_{BS,i1}$ and $P_{BS,i2}$ for the *i*th BS. Moreover, the duration $\alpha_{1i}, i = 1,2,3$ of each phase has to be designed.

The second hop consists in a single phase where each jth RS of the ith cell, RS_{ij}, transmits to its associated MS, MS_{ij}. Notice that this access mode allows interference in the second hop. For this hop, the duration α_2 will be designed. The transmitter power of each RS will be equal to $P_{RS,ij} = P_{RS,\max}, i = 1,2,3$, $j = 1,2$ because there is not CSIT available at the RSs.

The precoding matrices for the first hop are computed considering a 2-user MIMO BC. For this channel, we will design the precoding matrices employing a ZF-BD strategy [8], which results in the following six conditions:

$$\begin{array}{lll} \mathbf{H}_{111}\mathbf{V}_{112} = \mathbf{0} & \mathbf{H}_{121}\mathbf{V}_{122} = \mathbf{0} & \mathbf{H}_{131}\mathbf{V}_{132} = \mathbf{0} \\ \mathbf{H}_{112}\mathbf{V}_{111} = \mathbf{0} & \mathbf{H}_{122}\mathbf{V}_{121} = \mathbf{0} & \mathbf{H}_{132}\mathbf{V}_{131} = \mathbf{0} \end{array} \quad (140)$$

Thus, the precoding matrices can be computed merely as the null space of the cross-channel matrix of each cell,

$$\begin{array}{lll} \mathbf{V}_{112} = null\left(\mathbf{H}_{111}\right) & \mathbf{V}_{122} = null\left(\mathbf{H}_{121}\right) & \mathbf{V}_{132} = null\left(\mathbf{H}_{131}\right) \\ \mathbf{V}_{111} = null\left(\mathbf{H}_{112}\right) & \mathbf{V}_{121} = null\left(\mathbf{H}_{122}\right) & \mathbf{V}_{131} = null\left(\mathbf{H}_{132}\right) \end{array} \quad (141)$$

Notice that a bound for the number of transmitted messages has to be set, as done in section 3.4.2 to not exceed the number of antennas N at each RS. Hence, the number of columns of $\mathbf{V}_{1ij}$ is upper bounded by

$$DoF_{ZF,RACS} = \min\left(\left(M - N\right)^{+}, N\right) \quad (142)$$

These precoding matrices will be also optimized as explained for the ZF mode in section 3.4.4.2 in order to maximize the mutual information at each receiver and the transmit correlation matrix will optimized using the water-filling algorithm, section 2.3.

4.4.2 Coordinated Transmission: Interference Alignment

For the coordinated transmission, we propose 2 access modes using IA in the first hop, which are shown in Figure 26:

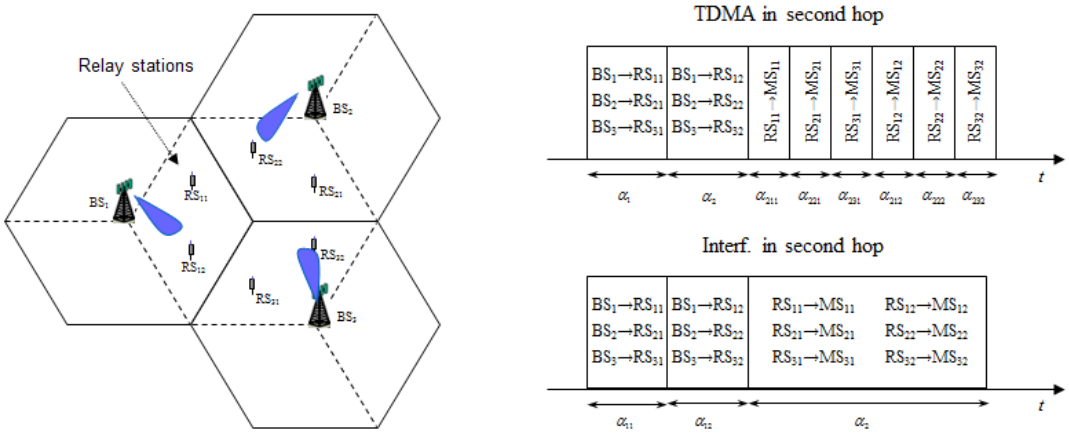

Figure 26: Scheduling plans for coordinated transmission in the first hop

As an example, consider the IA-TDMA access mode, i.e Interference Alignment in the first hop and TDMA in the second hop. There, the transmissions carried out in the first hop are done over 2 orthogonal phases. In each one of these phases, one RS of each cell is served. We consider that all $RS_{i1}, i=1,2,3$ are served in the first phase and all $RS_{i2}, i=1,2,3$ are served in the second phase. Thus, in each phase we can consider a 3-user MIMO IC with constant channel coefficients as in chapter 3. Since GSVD precoding (section 3.4.5) is the best scheme in terms of DoF, the precoding matrices for the first hop will be designed using this scheme. The duration of each one of the phases $\alpha_{1j}, j=1,2$ will be designed whereas each BS will use all the transmitted power to serve its RS and hence, it has not to be optimized, i.e $P_{BS,i}=P_{BS,\max}, i=1,2,3$.

Since TDMA is used in the second hop, each MS is served orthogonally in time with the others and thus, the durations $\alpha_{2ij}, i=1,2,3$, $j=1,2$ will be designed. Notice also that in the second hop each RS transmits with all the available power because no interference is created to other users. Hence, $P_{RS,ij}=P_{RS,\max}, i=1,2,3$, $j=1,2$.

4.5 ACCESS MODES IN THE SECOND HOP

For the second hop, the precoding matrices are computed as diagonal matrices allocating equal power to each antenna. It is because we consider CSIT is not available at the RSs and hence, power allocation is not possible. Hence, the precoding matrix at each RS is given by:

$$\mathbf{V}_{2ij} = \frac{P_{RS,\max}}{N}\mathbf{I} \tag{143}$$

where P_{RS} is the total transmitted power for each RS.

Each MS considers the received interference as additive noise. The capacity of the second hop when TDMA is used can be computed as:

$$C_{2ij} = \log_2 \left| \mathbf{I} + \frac{P_{RS,\max}}{N\sigma_n^2}\mathbf{H}_{2ij}\mathbf{H}_{2ij}^H \right| \tag{144}$$

On the other hand, when simultaneous transmission is employed in the second hop, the capacity is given by:

$$C_{2ij} = \log_2 \left| \mathbf{I} + \frac{P_{RS,\max}}{N}\mathbf{H}_{2ij}\mathbf{H}_{2ij}^H\mathbf{R}_n^{-1} \right| \tag{145}$$

where $\mathbf{R}_n$ is the interference plus noise correlation matrix which results that treating interference as noise and is given by:

$$\mathbf{R}_{n,ij} = \sigma_n^2\mathbf{I} + \sum_{\substack{p=1,k=1 \\ (p,k)\neq(i,j)}}^{3,2} \left(\mathbf{H}_{2\,pk}\mathbf{V}_{2\,pk}\right)\left(\mathbf{H}_{2\,pk}\mathbf{V}_{2\,pk}\right)^H \tag{146}$$

4.6 RESOURCE ALLOCATION

In this section, we review some optimization concepts relatively to convex problems which will be necessary to approach the resource allocation. Next, we show in detail two cases of optimization for IA-TDMA and ZF-BD TDMA-Interf access modes. The other cases can be easily solved based on these examples and are summarized in Table 11 and Table 12.

4.6.1 Convex problems

In this section, we review some concepts of optimization and convex problems. From [32], it follows that a problem defined as:

$$\begin{aligned} &\min_{\mathbf{x}} f_0(\mathbf{x}) \\ &\text{subject to} \\ &\quad f_i(\mathbf{x}) \le 0 \quad i = 1...m \\ &\quad h_i(\mathbf{x}) \le 0 \quad i = 1...p \end{aligned} \tag{147}$$

is convex if:

- The objective function $f_0(\mathbf{x})$ is convex.
- The inequality constraint functions $f_i(\mathbf{x})$ are convex.
- The equality constraint functions $h_i(\mathbf{x})$ are affine.

If an optimization problem can be written as (147) and satisfies the convexity conditions we can guarantee there is only a unique solution, which can be found by gradient methods [32].

The objective function is the function we are minimizing. In our scheme, it will be a function of the finals rates. Some examples for $f(\mathbf{r})$ are presented here:

$$\begin{aligned} (\text{SR}): &\quad f(\mathbf{r}) = -\mathbf{1}^T \mathbf{r} \\ (\text{WSR}): &\quad f(\mathbf{r}) = -\mathbf{w}^T \mathbf{r} \\ (\text{MinR}): &\quad f(\mathbf{r}) = -\min(r_{11}, r_{12}, ..., r_{32}) \\ (\text{GM}): &\quad f(\mathbf{r}) = -\sqrt[6]{r_{11} r_{12} ... r_{32}} \end{aligned} \tag{148}$$

where $\mathbf{r}$ is a vector containing the rates. We denote them as sum-rate (SR), weighted sum-rate (WSR), min-rate (MinR) and geometric mean (GM) respectively. The objective functions which will be used in the sequel are SR and GM. While the first one maximizes the spectral efficiency of the system, the second one allows us to deal with the bitrate of those users in bad channel conditions at the cost of decreasing the performance of those users in better channel conditions. We will see in the simulation results of section 4.7 the impact of objective function choice on the performance of the system. It can be easily proved that both functions are convex.

Moreover, there are two properties in this area which are summarized next. In the first hand, all the linear functions are affine and convex. This property ensures that

$$\sum_{i=1}^{K}\alpha_{i1}+\sum_{i=1}^{K}\alpha_{i2}=1 \tag{149}$$

is convex. On the other hand, the function $x\log_2(y)$ is not convex, but it becomes convex if the following change of variables is done [32]:

$$y=\frac{t}{x} \tag{150}$$

This property will be used when ZF-BD is used in the first hop.

4.6.2 IA in the first hop

For the IA-TDMA access mode, the resources are allocated by solving the following problem:

$$\begin{aligned}&\max_{\mathbf{r},\boldsymbol{\alpha}} f(\mathbf{r})\\ &\text{subject to}\\ &\sum_{i=1}^{2}\alpha_{1i}+\sum_{i=1}^{2}\sum_{j=1}^{3}\alpha_{2ij}=1\\ &r_{ij}-\alpha_{1i}C_{1ij}\le 0 \qquad i=1,2,3\ ;j=1,2\\ &r_{ij}-\alpha_{2ij}C_{2ij}\le 0 \qquad i=1,2,3\ ;\ j=1,2\end{aligned} \tag{151}$$

where r_{ij} is the final transmission rate of the ijth user and the second and third constraints impose $r_{ij}=\min\left(\alpha_{1j}C_{1ij},\alpha_{2ij}C_{2ij}\right)$. The convexity of this problem can be proved by using the concepts reviewed in the last section.

4.6.3 ZF-BD in the first hop

For the ZF-BD TDMA-Interf access mode, the resources are allocated by solving the following problem:

$$\max_{\mathbf{r},\boldsymbol{\alpha},P_{BS,ij}} f(\mathbf{r})$$

subject to

$$\begin{aligned}
&\sum_{i=1}^{3}\alpha_{1i}+\alpha_2=1 \\
&\sum_{j=1}^{2}P_{BS,ij}=P_{BS,\max} \qquad i=1,2,3 \\
&r_{ij}-\alpha_{1i}C_{1ij}\left(P_{BS,ij}\right)\le 0 \qquad i=1,2,3\ ;j=1,2 \\
&r_{ij}-\alpha_2 C_{2ij}\le 0 \qquad i=1,2,3\ ;\ j=1,2
\end{aligned} \tag{152}$$

This problem is similar to the one shown in (151) but here we also must allocate the transmitted power of each BS distributed along its two RS messages. Hence, we have to find the optimum value for $P_{BS,ij}$ and the power transmitted by each mode ϕ_{ijk}, which will be optimized by water-filling (section 2.3) . This variable appears in the expression of the mutual information, which is given by:

$$C_{1ij}\left(P_{BS,ij}\right)=\sum_{k=1}^{n_{ij}}\log_2\left(1+\frac{\lambda_{ijt}^2}{\sigma_n^2}\phi_{ijk}\left(P_{BS,ij}\right)\right) \tag{153}$$

where σ_n^2 is the noise power, n_{ij} are the number of modes used and λ_{ijk}^2 are the singular values of the equivalent channel matrix $\mathbf{H}_{eq}=\mathbf{H}_{1ij}\mathbf{V}_{1ij}$. Hence, the capacity in the first hop is given by:

$$C_{1ij}\left(P_{BS,ij}\right)=\sum_{k=1}^{n_{ij}}\log_2\left(1+\frac{\lambda_{ijt}^2}{\sigma_n^2}\left(\frac{P_{BS,ij}}{Mn_{ij}}+\frac{\sigma_n^2}{n_{ij}}\sum_{l=1}^{n_{ij}}\frac{1}{\lambda_{ijl}^2}-\frac{\sigma_n^2}{\lambda_{ijk}^2}\right)^+\right) \tag{154}$$

where M is the number of antennas at the BS. The problem in (152) has unique solution if we can guarantee its convexity

$$r_{ij}-\alpha_{1i}\sum_{k=1}^{n_{ij}}\log_2\left(1+\frac{\lambda_{ijt}^2}{\sigma_n^2}\left(\frac{P_{BS,ij}}{Mn_{ij}}+\frac{\sigma_n^2}{n_{ij}}\sum_{l=1}^{n_{ij}}\frac{1}{\lambda_{ijl}^2}-\frac{\sigma_n^2}{\lambda_{ijk}^2}\right)^+\right)\le 0 \tag{155}$$

This expression can be rewritten grouping all the constants in dummy variables:

$$\begin{aligned}
&A_{ij}=Mn_{ij} \quad , \quad B_{ijk}=\frac{\sigma_n^2}{n_{ij}}\sum_{l=1}^{n_{ij}}\frac{1}{\lambda_{ijl}^2}-\frac{\sigma_n^2}{\lambda_{ijk}^2} \\
&r_{ij}-\alpha_{1i}\sum_{k=1}^{n_{ij}}\log_2\left(1+\frac{\lambda_{ijt}^2}{\sigma_n^2}\left(\frac{P_{BS,ij}}{A_{ij}}+B_{ijk}\right)^+\right)\le 0
\end{aligned} \tag{156}$$

Assuming that the *k*th mode is used and hence another constraint $\phi_{ijk} > 0$ is introduced, (156) is reduced to:

$$K_{ijk} = \frac{\lambda_{ijk}^2}{\sigma_n^2 A_{ij}} \quad , \quad D_{ijk} = \frac{\lambda_{ijk}^2}{N_{ij}} \sum_{l=1}^{N_{ij}} \frac{1}{\lambda_{ijl}^2}$$
$$r_{ij} - \alpha_{1i} \sum_{k=1}^{N_{ij}} l\log_2 \left(P_{BS,ij} K_{ijk} + D_{ijk} \right) \le 0 \qquad (157)$$

This inequality is not convex, but it may become convex applying a change of variables as explained in section 4.6.1. Finally, the optimization problem is given by:

$$\max_{\mathbf{r},\mathbf{t},\boldsymbol{\alpha}} f(\mathbf{r})$$
subject to
$$\sum_{i=1}^{3} \alpha_{1i} + \alpha_2 = 1$$
$$\sum_{j=1}^{2} t_{ij} = \alpha_{1i} P_{BS,i\max} \qquad i = 1...3 \ ; \ j = 1...2 \qquad (158)$$
$$r_{ij} - \alpha_{1i} C_{1ij} \left(\frac{t_{ij}}{\alpha_{1i}} \right) \le 0 \ , \ i = 1...3 \ ; \ j = 1...2$$
$$r_{ij} - \alpha_2 C_{2ij} \le 0 \ , \ i = 1,2,3 \ ; \ j = 1...2$$
$$\phi_{ijk} \ge 0 \ \Rightarrow \ -t_{ij} - \alpha_{1i} M n_{ij} \cdot \left(\frac{\sigma_n^2}{n_{ij}} \sum_{l=1}^{n_{ij}} \frac{1}{\lambda_{ijl}^2} - \frac{\sigma_n^2}{\lambda_{ijk}^2} \right) \le 0 \ ; i = 1...3 \ ; j = 1...2 \ ; \ k = 1...n_{ij}$$

Notice that the second equality constraint has been rewritten with the new variable t_{ij} and we add the non-negative power implicit constraint in the last inequality.

4.6.4 Summary of the optimization problems

In this section, we present all the resource allocation problems depending on each access mode of each hop. Table 11 shows the resource allocation problems when IA is used in the first hop (Figure 25)

TDMA	$\max_{\mathbf{r},\boldsymbol{\alpha}} f(\mathbf{r})$ subject to $\sum_{i=1}^{2}\alpha_{1i}+\sum_{i=1}^{3}\sum_{j=1}^{2}\alpha_{2ij}=1$ $r_{ij}-\alpha_{1j}C_{1ij}\le 0 \qquad i=1,...,3\ ;\ j=1,...,2$ $r_{ij}-\alpha_{2ij}C_{2ij}\le 0 \qquad i=1,...,3\ ;\ j=1,...,2$
Interf	$\max_{\mathbf{r},\boldsymbol{\alpha}} f(\mathbf{r})$ subject to $\sum_{j=1}^{2}\alpha_{1j}+\alpha_{2}=1$ $r_{ij}-\alpha_{1j}C_{1ij}\le 0 \qquad i=1,...,3\ ;\ j=1,...,2$ $r_{ij}-\alpha_{2}C_{2ij}\le 0 \qquad i=1,...,3\ ;\ j=1,...,2$

Table 11: Resource allocation optimization problems for IA in the first hop

Next, Table 12 shows all the combinations for the first and the second hop when ZF precoding is used in the first hop (Figure 26):

TDMA-TDMA	$\max_{\mathbf{r},\mathbf{t},\boldsymbol{\alpha}} f(\mathbf{r})$ subject to $\sum_{i=1}^{3}\alpha_{1i}+\sum_{i=1}^{3}\sum_{j=1}^{2}\alpha_{2ij}=1$ $\sum_{\mathrm{j}=1}^{2}t_{ij}=\alpha_{1i}P_{BS,i} \qquad i=1,2,3\ ;\ j=1,2$ $r_{ij}-\alpha_{1i}C_{1ij}\left(\frac{t_{ij}}{\alpha_{1i}}\right)\le 0\ ,\ i=1,2,3\ ;\ j=1,2$ $r_{ij}-\alpha_{2ij}C_{2ij}\le 0\ ,\ i=1,2,3\ ;\ j=1,2$ $\phi_{ijk}\ge 0 \ \Rightarrow\ -t_{ij}-\alpha_{1i}Mn_{ij}\cdot\left(\frac{\sigma_n^2}{n_{ij}}\sum_{l=1}^{n_{ij}}\frac{1}{\lambda_{ijl}^2}-\frac{\sigma_n^2}{\lambda_{ijk}^2}\right)\le 0\ ;i=1,2,3\ ;j=1,2\ ;k=1...n_{ij}$ with $C_{1ij}\left(\frac{t_{ij}}{\alpha_{1i}}\right)=\sum_{k=1}^{n_{ij}}\log_2\left(1+\frac{\lambda_{ijt}^2}{\sigma_n^2}\phi_{ijk}\right)$ and $\phi_{ijk}=\left(\frac{t_{ij}}{\alpha_{1i}Mn_{ij}}+\frac{\sigma_n^2}{n_{ij}}\sum_{l=1}^{n_{ij}}\frac{1}{\lambda_{ijl}^2}-\frac{\sigma_n^2}{\lambda_{ijk}^2}\right)^{+}$

TDMA-Interf

$$\max_{\mathbf{r},\mathbf{t},\boldsymbol{\alpha}} f(\mathbf{r})$$

subject to

$$\sum_{i=1}^{3} \alpha_{1i} + \alpha_2 = 1$$

$$\sum_{j=1}^{2} t_{ij} = \alpha_{1i} P_{BS,i} \qquad i = 1,2,3 \;;\; j = 1,2$$

$$r_{ij} - \alpha_{1i} C_{1ij}\left(\frac{t_{ij}}{\alpha_{1i}}\right) \le 0 \;,\; i = 1,2,3 \;;\; j = 1,2$$

$$r_{ij} - \alpha_2 C_{2ij} \le 0 \;,\; i = 1,2,3 \;;\; j = 1,2$$

$$\phi_{ijk} \ge 0 \;\Rightarrow\; -t_{ij} - \alpha_{1i} M n_{ij} \cdot \left(\frac{\sigma_n^2}{n_{ij}} \sum_{l=1}^{n_{ij}} \frac{1}{\lambda_{ijl}^2} - \frac{\sigma_n^2}{\lambda_{ijk}^2}\right) \le 0 \;;\; i = 1,2,3 \;;\; j = 1,2 \;;\; k = 1 \ldots n_{ij}$$

$$\text{with } C_{1ij}\left(\frac{t_{ij}}{\alpha_{1i}}\right) = \sum_{k=1}^{n_{ij}} \log_2\left(1 + \frac{\lambda_{ijt}^2}{\sigma_n^2}\phi_{ijk}\right) \text{ and } \phi_{ijk} = \left(\frac{t_{ij}}{\alpha_{1i} M n_{ij}} + \frac{\sigma_n^2}{n_{ij}} \sum_{l=1}^{n_{ij}} \frac{1}{\lambda_{ijl}^2} - \frac{\sigma_n^2}{\lambda_{ijk}^2}\right)^+$$

Interf-TDMA

$$\max_{\mathbf{r},\mathbf{t},\boldsymbol{\alpha}} f(\mathbf{r})$$

subject to

$$\alpha_1 + \alpha_2 = 1$$

$$\sum_{j=1}^{2} t_{ij} = \alpha_1 P_{BS,i} \qquad i = 1,2,3 \;;\; j = 1,2$$

$$r_{ij} - \alpha_1 C_{1ij}\left(\frac{t_{ij}}{\alpha_1}\right) \le 0 \;,\; i = 1,2,3 \;;\; j = 1,2$$

$$r_{ij} - \alpha_2 C_{2ij} \le 0 \;,\; i = 1,2,3 \;;\; j = 1,2$$

$$\phi_{ijk} \ge 0 \;\Rightarrow\; -t_{ij} - \alpha_1 M n_{ij} \cdot \left(\frac{\sigma_n^2}{n_{ij}} \sum_{l=1}^{n_{ij}} \frac{1}{\lambda_{ijl}^2} - \frac{\sigma_n^2}{\lambda_{ijk}^2}\right) \le 0 \;;\; i = 1,2,3 \;;\; j = 1,2 \;;\; k = 1 \ldots n_{ij}$$

$$\text{with } C_{1ij}\left(\frac{t_{ij}}{\alpha_1}\right) = \sum_{k=1}^{n_{ij}} \log_2\left(1 + \frac{\lambda_{ijt}^2}{\sigma_n^2}\phi_{ijk}\right) \text{ and } \phi_{ijk} = \left(\frac{t_{ij}}{\alpha_1 M n_{ij}} + \frac{\sigma_n^2}{n_{ij}} \sum_{l=1}^{n_{ij}} \frac{1}{\lambda_{ijl}^2} - \frac{\sigma_n^2}{\lambda_{ijk}^2}\right)^+$$

Interf-Interf

$$\max_{\mathbf{r},\mathbf{t},\boldsymbol{\alpha}} f(\mathbf{r})$$

subject to

$$\alpha_1 + \sum_{i=1}^{3}\sum_{j=1}^{2} \alpha_{2ij} = 1$$

$$\sum_{j=1}^{2} t_{ij} = \alpha_1 P_{BS,i} \qquad i = 1,2,3 \;;\; j = 1,2$$

$$r_{ij} - \alpha_1 C_{1ij}\left(\frac{t_{ij}}{\alpha_1}\right) \le 0 \;,\; i = 1,2,3 \;;\; j = 1,2$$

$$r_{ij} - \alpha_{2ij} C_{2ij} \le 0 \;,\; i = 1,2,3 \;;\; j = 1,2$$

$$\phi_{ijk} \ge 0 \;\Rightarrow\; -t_{ij} - \alpha_1 M N_{ij} \cdot \left(\frac{\sigma_n^2}{N_{ij}} \sum_{l=1}^{n_{ij}} \frac{1}{\lambda_{ijl}^2} - \frac{\sigma_n^2}{\lambda_{ijk}^2}\right) \le 0 \;;\; i = 1,2,3 \;;\; j = 1,2 \;;\; k = 1 \ldots n_{ij}$$

	with $C_{1ij}\left(\frac{t_{ij}}{\alpha_1}\right)=\sum_{k=1}^{n_{ij}}\log_2\left(1+\frac{\lambda_{ijt}^2}{\sigma_n^2}\phi_{ijk}\right)$ and $\phi_{ijk}=\left(\frac{t_{ij}}{\alpha_1 M n_{ij}}+\frac{\sigma_n^2}{n_{ij}}\sum_{l=1}^{n_{ij}}\frac{1}{\lambda_{ijl}^2}-\frac{\sigma_n^2}{\lambda_{ijk}^2}\right)^+$

Table 12: Resource allocation optimization problems for ZF in the first hop

4.7 SIMULATION RESULTS

4.7.1 Simulation conditions and assumptions

In this section, we present the simulation results for the RACN. The evaluation of the proposed approach is done on a radio access network based on 802.16m specifications [33]. Table 13 summarizes the main simulation parameters:

Number of cells	3
Inter-BS distance	500m to 1500m
Mid frequency	2.6 Ghz
Channel Bandwidth	20 Mhz
BS transmit power	40 dBm
RS transmit power	30 dBm
BS antenna gain	10,6 dBi
RS antenna gain	5 dBi
Noise spectral density	-174 dBm/Hz
Random user deployments and channel realizations	800
Users per scenario	6
Antennas elements at each BS	M=4
Antennas elements at each RS	N=2
Antennas elements at each MS	S=1
LOS conditions BS-RS	LOS
LOS conditions RS-MS	NLOS

Table 13: RACN Simulation parameters

Channel models adopted are outdoor-to-outdoor obtained from [34].

Two fundamental measures are adopted: *cellular spectral efficiency* S_e, as the average sum-rate over the cell area, and ε% *outage rate* $O_r(\varepsilon)$, as the peak achievable rate of the 100-ε worst users in the cell. Both capture most of the benefits offered by coordination of BS and relay-based transmission. These two measures have been evaluated for distinct access modes, objective functions and inter-BS distances and are defined by

$$S_e = \frac{1}{6}\sum_{i=1}^{3}\sum_{j=1}^{2} r_{ij} \qquad \varepsilon = \Pr\left(r_{ij} > O_r(\varepsilon) \mid i \in \{1,2,3\}, j \in \{1,2\}\right) \tag{159}$$

4.7.2 Influence of the second hop access mode

The results are shown in Figure 27 to Figure 30. As explained throughout chapter 4, the different options for each hop are:

- Access modes in the first hop: IA, ZF-BD TDMA and ZF-BD with simultaneous transmission, which will be named *ZF-BD Interf*.
- Access modes in the second hop: TDMA and simultaneous transmission, named as *Interf*

The objective functions considered are sum-rate (SR) and geometric mean (GM), whose analytical form is shown in (148). The inter-BS distances could take the values 500m, 750m, 1000m, 1250m and 1500m, which are depicted in black, blue, red, magenta and green respectively.

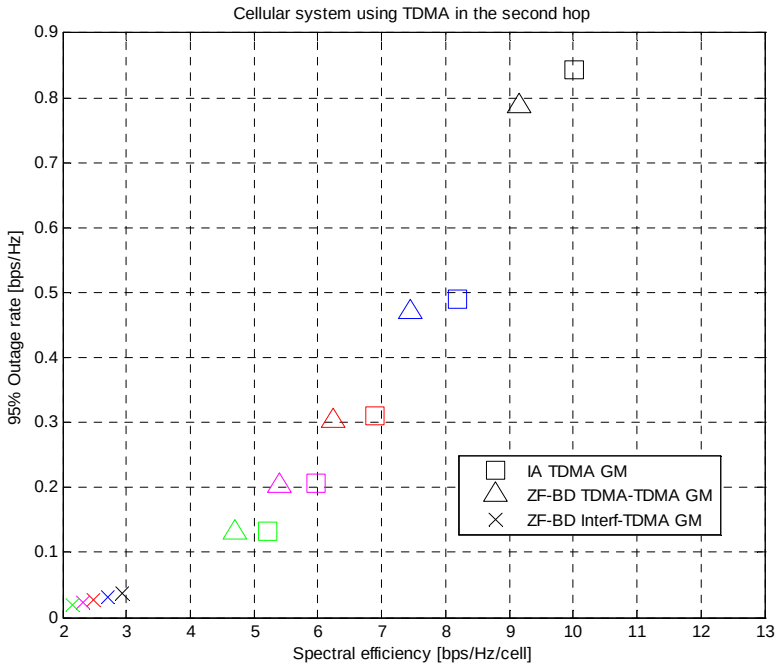

Figure 27: Evaluation of the system using TDMA in the second hop and GM as objective function. Black, blue, red, magenta and green represent inter-BS distance equal to 500, 750, 1000, 1250 and 1500m respectively

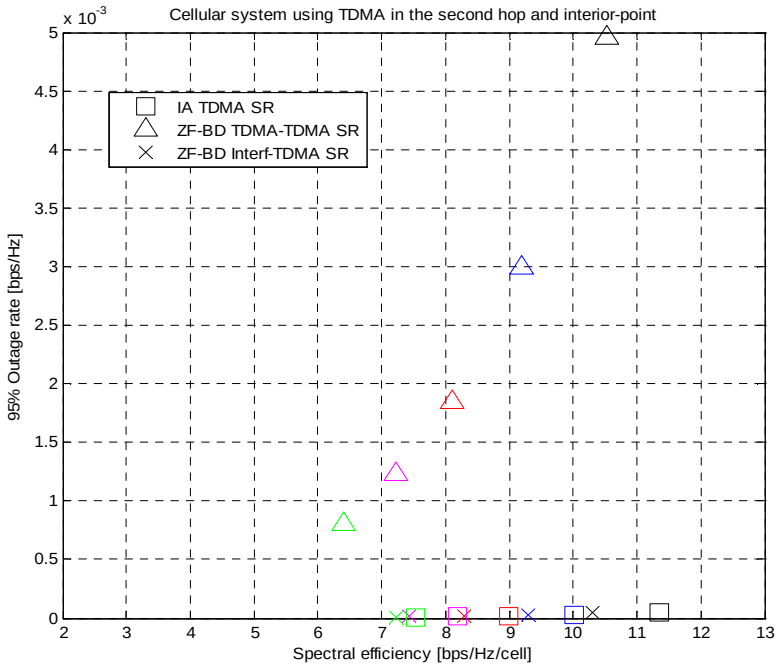

Figure 28: Evaluation of the system using TDMA in the second hop and SR as objective function. Black, blue, red, magenta and green represent inter-BS distance equal to 500, 750, 1000, 1250 and 1500m respectively

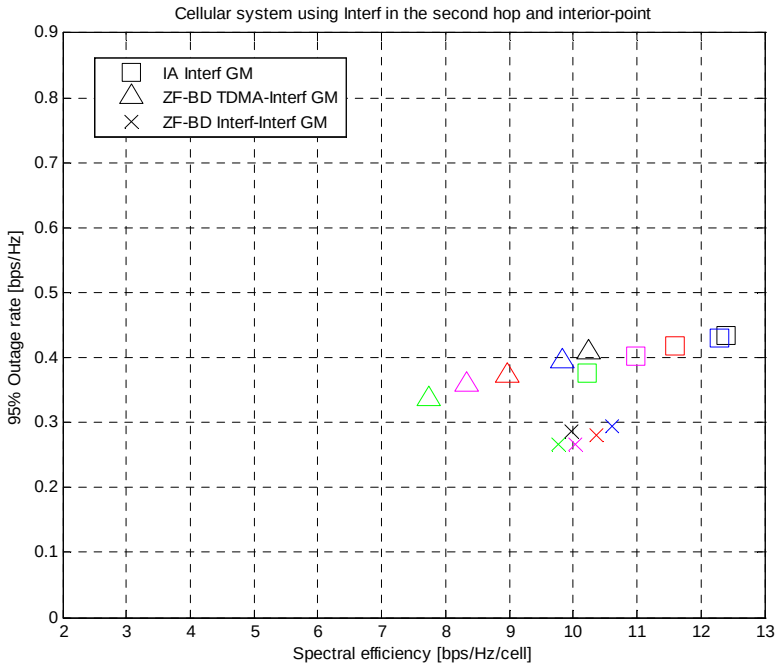

Figure 29: Evaluation of the system using simultaneous transmission in the second hop and GM as objective function. Black, blue, red, magenta and green represent inter-BS distance equal to 500, 750, 1000, 1250 and 1500m respectively

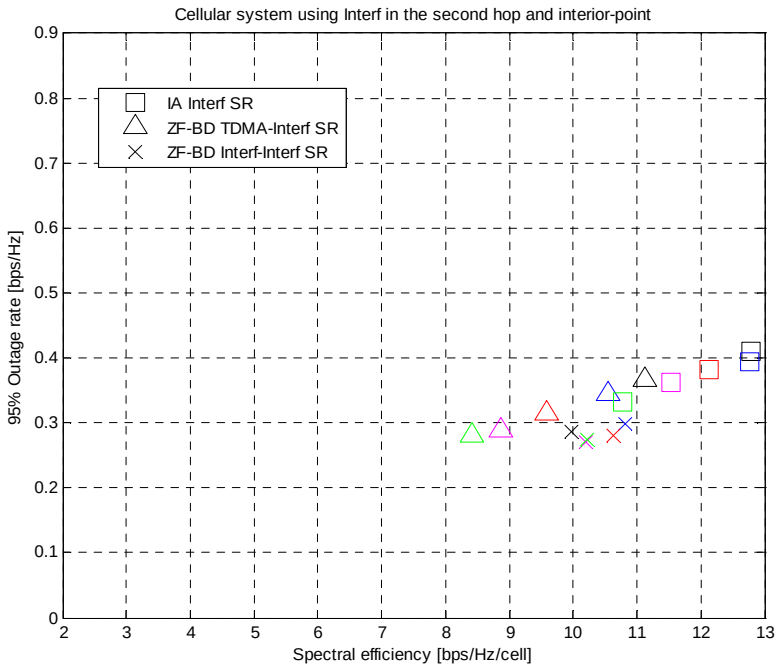

Figure 30: Evaluation of the system using simultaneous transmission in the second hop and SR as objective function. Black, blue, red, magenta and green represent inter-BS distance equal to 500, 750, 1000, 1250 and 1500m respectively

4.7.3 Inter-BS distance influence

In Figure 27 and Figure 28, we observe that the performance of the system decreases as the inter-BS distance increases. However, in Figure 29 and Figure 30, ZF-BD Interf-Interf and IA Interf do not follow exactly this behavior. Notice that these cases take place when simultaneous transmission is employed in the second hop. Let us analyze first Figure 30. The conclusions extracted from this figure are also valid for Figure 29. In the first hand, it can be observed that the black cross, which denotes the ZF-BD-Interf-Interf access mode using the smallest inter-BS distance, shows the worst performance among the ZF-BD Interf-Interf symbols. We think that when simultaneous transmissions are employed in both hops, intermediate values for the inter-BS distance are suitable because of the trade-off between intra-cell interference and inter-cell interference. While using small values for the inter-BS distance reduces the pathloss and hence, increases the cell coverage, the inter-cell interference is also increased because other BSs are closer. Conversely, using large values for the inter-BS distance attenuate the inter-cell interference, but also the desired signals because users may stay in far positions.

On the other hand, we observe that the blue square and the black square in Figure 30 are very closer. This would mean that decreasing the inter-BS distance does not provide great improvements on the spectral efficiency (the same could be seen in Figure 29 in terms of outage rate), causing an effect of *saturation.* In particular, in those cases where

$$C_{BS-MS} > \frac{C_{BS-RS} C_{RS-MS}}{C_{BS-RS} + C_{RS-MS}} \tag{160}$$

there are no gains associated to the use of relays, and the MS should prefer to receive directly from the BS.

4.7.4 Using different objective functions

The differences provided by using different objective functions are significant in all the figures. When the SR is used as the objective function, we observe greater values in the spectral efficiency than using the GM whereas using the GM improves the outage of the system at the cost of losing spectral efficiency. A similar tendency occurs with TDMA and Interf access modes. While the first allows the system to distribute the duration of the phases among the users, the last forces the users to transmit simultaneously. As a consequence, the TDMA access mode favours the outage rate whereas the Interf access mode tends to improve the spectral efficiency improving the performance of the users with good conditions. However, when the access mode and the objective function follow opposed tendencies, the results show that the objective function has a greater impact. Figure 28 shows an example of this behavior, where it can be observed that using TDMA in the second hop leads to poor outage rate results due to the objective function is SR.

4.7.5 NLOS in the BS-RS links

From Figure 27, we observe that ZF-BD Interf-TDMA achieves very poor results. In this regard, we simulate the same system and channel realizations considering NLOS in the BS-RS links, obtaining simulation results on Figure 31. The results show an improvement of this access mode whereas the other modes get slightly worst results than considering LOS. However, the performance order remains the same. This can be explained by two reasons, which actually are the same. In the first hand, when LOS is considered, the pathloss in the BS-RS links is lower than considering NLOS. Therefore, inter-cell interference is greater in the LOS case and this explains the improvement of ZF-BD Interf-TDMA access mode. On the other hand, the pathloss increment in the BS-RS links affects also to the direct channels, obtaining worst results for IA-TDMA and ZF-BD TDMA TDMA. This is because these access modes do not depend on the interference power in the first hop, and the changes observed from Figure 27 to Figure 31 are caused by an attenuation of the direct channel.

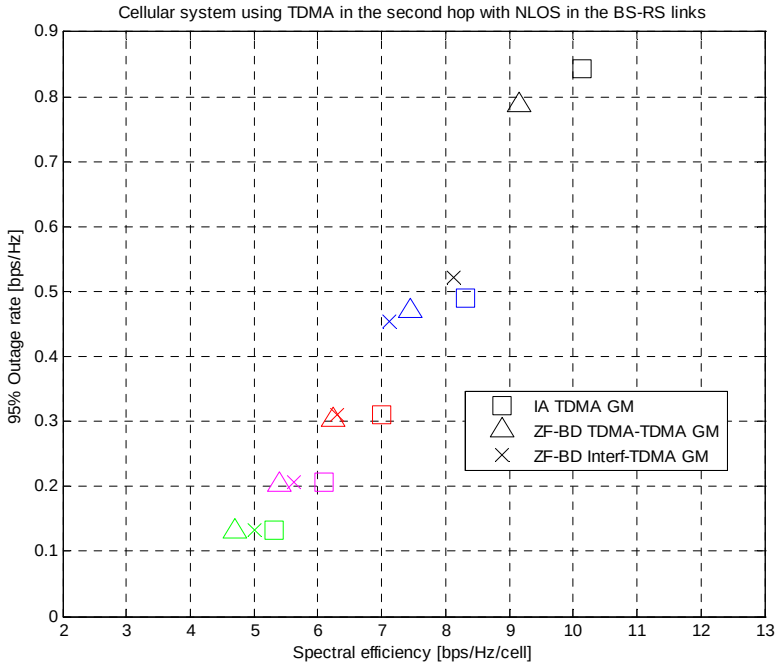

Figure 31: Evaluation of the system using TDMA in the second hop, GM as objective function and considering NLOS in the BS-RS links. Black, blue, red, magenta and green represent inter-BS distance equal to 500, 750, 1000, 1250 and 1500m respectively

4.7.6 Conclusions

In conclusion, depending on each feature we will use one access mode or other but always using IA in the first hop. If we want to maximize the spectral efficiency, then the best access mode would be IA-Interf SR. Furthermore, few improvements of the Outage rate can be achieved by using GM instead of SR on this access mode. On the other hand, if we want to maximize the outage rate the best scheme would be IA –TDMA GM. We also conclude that using ZF-BD in the first hop is not a good choice. Moreover, when only in-cell CSIT is available the best access mode is ZF-BD TDMA in the first hop, with similar behavior than IA-TDMA in respect to the second hop access mode and the objective function choice.

5 CONCLUSIONS AND FUTURE WORK

The 3-user MIMO interference channel with constant channel coefficients, M antennas at the transmitters and N at the receivers has been analyzed. For this channel, a new outerbound for the degrees of freedom based on [19] and [20] has been presented. Likewise, some schemes have been proposed in order to achieve this outerbound. The results show that GSVD precoding is the best of the proposed schemes, achieving the outerbound for the ratio $M/N \geq 5/3$. This scheme divides the precoding matrices in 3 blocks, which represents the transmission modes to be used: IA, ZF and partial ZF. Depending on the range of $r = M/N$, the outerbound is achieved by

$$\begin{array}{cc} \text{ZF} & \text{for } r > 3 \\ \text{partial ZF and ZF} & \text{for } 2 < r < 3 \\ \text{IA and partial ZF} & \text{for } 5/3 < r < 2 \end{array}$$

whereas if $r < 5/3$, IA can be used to approach to the outerbound. Moreover, some examples of asymmetric cases have been presented.

The innerbounds presented for the 3-user MIMO IC have been implemented to be used in the first hop of a relay-assisted cellular network. Resource allocation and system performance has been evaluated in terms of spectral efficiency and outage rate for different access modes. The results show that using IA in the first hop is the best access mode and there are different options for the second hop and the objective function so as to improve the performance in terms of spectral efficiency or outage rate. When only in-cell CSIT is available, the best access mode for the first hop is ZF-BD TDMA.

Extension to the multicarrier case has been presented but not implemented because of time scarcity, which could be done in the future. We think that transmission through multiple carriers could help the system to manage interference. Since the MIMO channel coefficients are random, each user might have different channel gains for each

subcarrier and hence, the allocated power at each subcarrier might be distributed accordingly, increasing spectral efficiency and outage rate.

There are several lines for future research having as a basis the work developed here:

- Extend the novel ideas (partial ZF transmission mode and GSVD procedure) of this work to the *K*-user interference channel. Some works deals with the IA equations for *K* users. [19].

- The Broadcast Interference Channel, whereby each transmitter serves many receivers.

- Analyze the 3-user asymmetric MIMO interference channel with possibly different number of antennas at each transmitter and each receiver or rank deficient channels. Although we provide some examples in this work, it leaves as line of research to generalize the DoF achieved for the $\left(M_j, N_j\right)$ case

- Analyze the impact of quantized channels when precoders are designed so as to align the interference

- Based on [35], extend the GSVD precoding to a similar framework with a parameter L, which will be useful for $r < 5/3$.

- Implement minimum mean square error (MMSE) precoders and receivers instead of ZF. This type of receivers used to work better in the signal to noise ratio regime.
- Extend these schemes to interference networks. In these networks there are various transmitters and receivers sharing information between them. The point is that each transmitter might send messages to more than receiver.

6 REFERENCES

[1] D. Tse and P. Viswanath. “Fundamentals of Wireless Communication”. Cambridge University Press, 2005.

[2] E. Telatar, “Capacity of multi-antenna Gaussian channels,” Eur. Trans.Telecomm. ETT, vol. 10, no. 6, pp. 585–596, Nov. 1999.

[3] T.M.Cover, J.A. Thomas. Elements of Information Theory. John Wiley & Sons, 1991.

[4] T.M.Cover, A.A. El Gamal, “Capacity theorems for the relay channel”, *IEEE Trans. on Information Theory*, vol. 25, no. 5, pp. 474-584, Sept. 1979.

[5] IEEE 802.16j-06/013r1, “Multi-hop relay system evaluation methodology (Channel Model and Performance Metric)”, October 2006, http://www.ieee802.org/16/relay/.

[6] A.Host-Madsen, J.Zhang, “Capacity bounds and power allocation for wireless relay channels”, *IEEE Trans. on Information Theory*, vol. 51, no. 6, pp. 2020-2040, June 2005.

[7] Olga Muñoz, Josep Vidal, Adrian Agustin, “Linear Transceiver Design in Non-Regenerative Relays with Channel State Information”, *IEEE Trans. Signal Processing*, vol 55, no 6, Junio 2007, pp 2593-2604

[8] Q. H. Spencer, A. L. Swindlehurst and M. Haardt, “Zero Forcing methods for Downlink Spatial Multiplexing in Multiuser MIMO channels,” IEEE Trans. Sig. Proc., vol. 52, no. 2, pp. 461-471, Feb 2004.

[9] M. Maddah-Ali, A. Motahari, and A. Khandani, “Communication Over X Channel: Signaling and Performance Analysis” Unive.Waterloo,Waterloo, ON, Canada, Tech. Rep. UW-ECE-2006-27, Dec. 2006.

[10] S. Jafar and S. Shamai, “Degrees of freedom region for the MIMO X channel,” arXiv:cs.IT/0607099v3, May 2007.

[11] M.A. Maddah-Ali, A.S. Motahari, A.K. Khandani, “Communication over MIMO X channels: Interference Alignment, Decomposition and performance analysis”, IEEE Trans. on Information Theory, vol.54, no. 8, Aug. 2008.

[12] D. P. Palomar, J. M. Cioffi and M.A. Lagunas, “Uniform power allocation in MIMO channels: A game-theoretic approach”, IEEE Trans. on Information Theory, vol. 49, no. 7, pp. 1707-1727, July 2003.

[13] G.H. Golub, C.F.V. Loan, “Matrix Computations”, 3rd ed. Baltimore:Johns Hopkins Univ. Press, 1996.

[14] A.Agustin, J.Vidal, “Improved Interference Alignment Precoding for the MIMO X channel” , IEEE Itl. Conf. on Communications (ICC) June 2011, Kyoto, Japan

[15] A. Host-Madsen and A. Nosratinia, “The multiplexing gain of wireless networks,” in Proc. ISIT, 2005.

[16] V. R. Cadambe and S. A. Jafar, "Interference Alignment and Degrees of Freedom of the K-User Interference Channel" IEEE Trans.on Inform. Theory, vol. 54, No.8, August 2008.

[17] Cadambe, V.R. Jafar, S.A. Chenwei Wang. "Interference Alignment With Asymmetric Complex Signaling—Settling the Høst-Madsen–Nosratinia Conjecture", Information Theory, IEEE Transactions on . August 2010

[18] A. S. Motahari, S. O. Gharan, and A. K. Khandani, "Forming pseudo-MIMO by embedding infinite rational dimensions along a single real line: Removing barriers in achieving the DOFs of single antenna systems," http://arxiv.org/abs/0908.2282, Aug. 2009.

[19] Tiangao Gou, Syed A. Jafar, "Degrees of Freedom of the K User MxN MIMO Interference Channel", IEEE Transactions on Information Theory, Dec. 2010, Vol. 56, Issue: 12, Page(s): 6040-6057

[20] M. Razaviyayn, L. Gennady, and Z. Luo, "On the degrees of freedom achievable through interference alignment in a MIMO interference channel" Private communication, submitted to SPAWC 2011.

[21] Ghasemi, A. S. Motahari, and A. K. Khandani., "Interference alignment for the k-user mimo interference channel.," In Proceedings of IEEE International Symposium on Information Theory (ISIT), pp. 360 –364, June 2010.

[22] Yetis, C.M.; Tiangao Gou; Jafar, S.A.; Kayran, A.H.; , "On Feasibility of Interference Alignment in MIMO Interference Networks" Signal Processing, IEEE Transactions on , vol.58, no.9, pp.4771-4782, Sept. 2010

[23] K. S. Gomadam, V. R. Cadambe, and S. A. Jafar, "Approaching the capacity of wireless networks through distributed interference alignment MIMO fading channels," Arxiv pre-print cs.IT/0803.3816 [Online]. Available: http://arxiv.org/abs/0803.3816

[24] S. Lipschutz, "Schaum's outline of Theory and problems of Linear Algebra", 2n ed, McGraw-Hill 1991. Schaums Outline Series, ISBN 0-07-038007-4

[25] K. Gomadam, V. Cadambe, and S. Jafar, "Approaching the Capacity of Wireless Networks through Distributed Interference Alignment". Available: http://arxiv.org/abs/0803.3816 Mar. 2008

[26] K. S. Gomadam, V. R. Cadambe, and S. A. Jafar, "Approaching the capacity of wireless networks through distributed interference alignment MIMO fading channels," Arxiv pre-print cs.IT/0803.3816 [Online]. Available: http://arxiv.org/abs/0803.3816

[27] G. J. Foschini, K. Karakayali, R. A. Valenzuela, "Network Coordination for Spectrally Efficient Communications in Cellular Systems", IEE Proc.-Commun., Vol. 153, No. 4, August 2006.

[28] J. Zhang, et al, "Networked MIMO with Clustered Linear Precoding", IEEE Trans on Wireless Communications, vol. 8, no. 4, April 2009.

[29] Krishna Gomadam, Viveck R. Cadambe, Syed A. Jafar. Approaching the Capacity of Wireless Networksthrough Distributed Interference Alignment. Available at http://arxiv.org/abs/0803.3816v1

[30] C. Antonopoulos, C. Abgrall, Z. Becvar, E. Calvanese, R. Hoshyar, M. Imran, P. Mach, O. Muñoz, J. Vidal, A. Agustin, B. Wolz, Z. Xie, "Multi-cell Coordination Techniques for OFDMA Multi-hop Cellular Networks", ROCKET project deliverable 4D2, Dec 2009, available at www.ict-rocket.eu.

[31] M. C. Necker "Interference coordination in cellular OFDMA networks", IEEE Network, 22, November/December 2008.

[32] S. Boyd, L. Vandenberghe, "Convex Optimization", Cambridge University Press, USA, 2004.

[33] IEEE 802.16 Broadband Wireless Access Group, "IEEE 802.16m system requirements", IEEE 802.16m-07/002r4, October 2007.

[34] WINNER II consortium, "Channel Models Part II: Radio Channel Measurements and Analysis Results", Deliverable 1.1.2, IST-4-027756 WINNER II, September 2007.

[35] Mohamed Amir, Amr El-Keyi, and Mohammed Nafie "A New achievable DoF Region for the 3-user MxN Symmetric Interference Channel" arXiv:1105.4026v1 [cs.IT] 20 May 2011 [Online]. Available at: http://arxiv.org/abs/1105.4026

[36] A. Goldsmith, "Wireless Communications". Cambridge: Cambridge University Press, 2005.

APPENDIX

A. Proof of Theorem 3.3.2-1

The proof is based on the outerbounds defined in [19] by Gou and Jafar and in [20] by Razaviyayn, Lyubeznik and Luo. We denote these two outerbounds by $DoF_{GJ}(M,N)$ and $DoF_{RLL}(M,N)$. Let us assume $M \geq N$ without loss of generality due to reciprocity. Hence, (58) is rewritten as:

$$DoF = \begin{cases} \frac{M+N}{4} & 1 \leq r < \frac{5}{3} \\ \frac{2N}{3} & \frac{5}{3} \leq r < 2 \\ \frac{M}{3} & 2 \leq r < 3 \\ N & r \geq 3 \end{cases}, \; r = \frac{M}{N} \tag{161}$$

In the first place, the outerbound defined in [19] is:

$$DoF_{GJ}(M,N) = \begin{cases} N & R \geq 3 \\ \frac{M}{R+1} & R < 3 \end{cases}, \quad R = \left\lfloor \frac{M}{N} \right\rfloor \tag{162}$$

where $\lfloor a \rfloor$ is the floor operator, that is, the largest integer not greater than a. The authors of [19] conjecture that this upperbound is not tight when $r \neq R$. In this regard, we will show that the previous outerbound can be easily enhanced when $\frac{5}{3} \leq r < 2$:

$$DoF_{GJ}(M,N) = \begin{cases} \frac{2N}{3} & \frac{5}{3} \leq r \leq 2 \\ \frac{M}{3} & 2 \leq r \leq 3 \\ N & r \geq 3 \end{cases}, \; R = \left\lfloor \frac{M}{N} \right\rfloor, \; r = \frac{M}{N} \tag{163}$$

where it has been particularized $R = 2$ in the range $2 \leq r \leq 3$.

In order to prove this improvement, consider a pair (M,N) such that $R \neq r$ and $R<3$. The outerbound defined in [19] is given by $\frac{M}{R+1}$. From Lemma 3.3.2-1, it follows that increasing the number of antennas at the transmitter side cannot hurt the degrees of freedom. According to that, we bound with the next tight case, i.e $(\tilde{M},N)=(M+m,N)$ with the minimum m such that:

$$\tilde{R}=\left\lfloor \frac{\tilde{M}}{N} \right\rfloor=\left\lfloor \frac{M+m}{N} \right\rfloor=\frac{M+m}{N}=\tilde{r}=R+1 \tag{164}$$

For example, let $(M,N)=(4,3)$ with:

$$R=\left\lfloor \frac{4}{3} \right\rfloor=1 \quad r=\frac{4}{3} \tag{165}$$

For that case, the minimum m such that:

$$\tilde{R}=\tilde{r} \tag{166}$$

is 2. Hence:

$$\begin{gathered}\tilde{R}=\left\lfloor \frac{4+2}{3} \right\rfloor=\left\lfloor \frac{6}{3} \right\rfloor=\frac{6}{3}=\tilde{r} \\ \tilde{R}=\tilde{r}=R+1=2\end{gathered} \tag{167}$$

Back to the general case for (M,N), the outerbound for the pair $(\tilde{M},N)=(M+m,N)$ is given by:

$$DoF_{GJ}(\tilde{M},N)=\frac{\tilde{M}}{\tilde{R}+1}=\frac{(M+m)}{\tilde{R}+1}=\frac{\tilde{R}N}{\tilde{R}+1}=\frac{(R+1)N}{R+2} \tag{168}$$

For $\frac{5}{3} \le r < 2$, it results (163) because $R = 1$. Notice that this idea cannot be applied for $r \ge 2$ because the next tight case would be $\tilde{r} = 3$. Throughout this section, we will prove that (163) is a better outerbound than (162) when $\frac{5}{3} \le r < 2$.

Secondly, work presented in [20] provides another outerbound:

$$DoF_{RLL}(M,N) = \frac{M+N}{4} \tag{169}$$

We prove outerbound defined in (58) for each range of r by combining (163) and (169) :

- $r \ge 3$:

$$\begin{gathered} DoF_{GJ} < DoF_{RLL} \\ N < \frac{M+N}{4} \\ 1 < \frac{r+1}{4} \\ r > 3 \end{gathered} \tag{170}$$

  For $r = 3$, we have $DoF_{CJ} = DoF_{RLL}$ and these two outerbounds are valid.

- $2 \le r < 3$:

$$\begin{gathered} DoF_{GJ} < DoF_{RLL} \\ \frac{M}{R+1} < \frac{M+N}{4} \\ \frac{r}{2+1} < \frac{r+1}{4} \\ r < 3 \end{gathered} \tag{171}$$

  In (171) we apply $R = 2$ because $2 \le r < 3$. Thus, we have the following implicit condition:

$$R = \lfloor r \rfloor = 2 \quad \Rightarrow \quad 2 \le r < 3 \tag{172}$$

  Remember that for $r = 2$, DoF_{GJ} is tight.

- $\frac{5}{3} \le r < 2$:

$$\begin{gathered} DoF_{GJ} < DoF_{Luo} \\ \frac{(R+1)N}{R+2} < \frac{M+N}{4} \\ \frac{(1+1)}{1+2} < \frac{r+1}{4} \\ r > \frac{5}{3} \end{gathered} \tag{173}$$

Again, in (173) we apply $R=1$ because $\frac{5}{3} \le r < 2$. Thus, we have the following implicit condition:

$$R = \lfloor r \rfloor = 1 \quad \Rightarrow \quad 1 \le r < 2 \tag{174}$$

Moreover, we prove that (163) is an outerbound better than the one defined in [19].

$$\begin{gathered} \frac{(R+1)N}{R+2} < \frac{M}{R+1} \\ \frac{(1+1)}{1+2} < \frac{r}{1+1} \\ r > \frac{4}{3} \end{gathered} \tag{175}$$

Finally, for $r = \frac{5}{3}$ we have $DoF_{GJ} = DoF_{RLL}$ and any of these two outerbounds is valid.

- $1 \le r < \frac{5}{3}$:

$$\begin{gathered} DoF_{RLL} < DoF_{GJ} \\ \frac{M+N}{4} < \frac{M}{R+1} \\ \frac{r+1}{4} < \frac{r}{1+1} \\ r > 1 \end{gathered} \tag{176}$$

For $r = 1$, $DoF_{GJ} = DoF_{RLL}$ and any of these two outerbounds is valid.

Finally, notice that as mentioned in section 2.5, without loss of generality we can assume that the number of transmit antennas is greater than or equal to that of receive antennas, i.e., these outerbound are valid for the $N < M$ case.

B. Proof of Theorem 3.4.3-1

B.I. Design of precoding matrices for M even

Problem defined in (73) can be simplified as follows:

$$\begin{aligned} span(\mathbf{H}_{12}\mathbf{V}_2) &= span(\mathbf{H}_{13}\mathbf{V}_3) \\ \mathbf{V}_3 &= (\mathbf{H}_{23})^{-1}\mathbf{H}_{21}\mathbf{V}_1 \\ \mathbf{V}_2 &= (\mathbf{H}_{32})^{-1}\mathbf{H}_{31}\mathbf{V}_1 \end{aligned} \tag{177}$$

Now let us define the following matrices:

$$\begin{aligned} \mathbf{E} &= (\mathbf{H}_{31})^{-1}\mathbf{H}_{32}(\mathbf{H}_{12})^{-1}\mathbf{H}_{13}(\mathbf{H}_{23})^{-1}\mathbf{H}_{21} \\ \mathbf{F} &= (\mathbf{H}_{32})^{-1}\mathbf{H}_{31} \\ \mathbf{G} &= (\mathbf{H}_{23})^{-1}\mathbf{H}_{21} \end{aligned} \tag{178}$$

Notice that (177) and (178) require that channel matrices are invertible. Next, we show the solution presented in [16] for the precoding matrices of each user:

$$\begin{aligned} span(\mathbf{V}_1) = span(\mathbf{E}\mathbf{V}_1) \quad &\Rightarrow \quad \mathbf{V}_1 = \begin{bmatrix} \mathbf{e}_1 & \mathbf{e}_2 & \dots & \mathbf{e}_{M/2} \end{bmatrix} \\ \mathbf{V}_2 &= \mathbf{F}\mathbf{V}_1 \\ \mathbf{V}_3 &= \mathbf{G}\mathbf{V}_1 \end{aligned} \tag{179}$$

where $\mathbf{e}_i, i = 1...M/2$ is an arbitrary set of $M/2$ eigenvectors of $\mathbf{E}$. Notice that this scheme is only valid when M is even.

B.II. Achievability for M even

For any M even number, we prove $M/2$ degrees of freedom can be achieved. In order to do that, we have to prove that the interference is linearly independent of the desired signals at each receiver. For example, at receiver 1, the receiver linear independence condition boils down to:

$$\begin{aligned} span(\mathbf{H}_{11}\mathbf{V}_1) \cap span([\mathbf{H}_{12}\mathbf{V}_2 \quad \mathbf{H}_{13}\mathbf{V}_3]) = \varnothing \\ span(\mathbf{H}_{11}\mathbf{V}_1) \cap span(\mathbf{H}_{12}\mathbf{V}_2) = \varnothing \\ span(\mathbf{V}_1) \cap span(\mathbf{K}\mathbf{V}_1) = \varnothing \end{aligned} \tag{180}$$

where $\mathbf{K} = (\mathbf{H}_{11})^{-1}\mathbf{H}_{12}$. Here we simplify:

$$span([\mathbf{H}_{12}\mathbf{V}_2 \quad \mathbf{H}_{13}\mathbf{V}_3]) = span(\mathbf{H}_{12}\mathbf{V}_2) \tag{181}$$

because of IA conditions in (73). Equation (180) is equivalent to saying that all the columns of the following $M \times M$ matrix are linearly independent.

$$\mathbf{C}_1 = [\mathbf{V}_1 \quad \mathbf{K}\mathbf{V}_1] = [\mathbf{e}_1 \quad \mathbf{e}_2 \quad \ldots \quad \mathbf{e}_{M/2} \quad \mathbf{K}\mathbf{e}_1 \quad \mathbf{K}\mathbf{e}_2 \quad \ldots \quad \mathbf{K}\mathbf{e}_{M/2}] \tag{182}$$

It is easily seen to be true because $\mathbf{K}$ is a random full rank rotation matrix. For example, consider the case $M = 2$ where:

$$\mathbf{C}_1 = [\mathbf{e}_1 \quad \mathbf{K}\mathbf{e}_1] \tag{183}$$

Then, the probability of $\mathbf{e}_1$ being eigenvector of a random matrix $\mathbf{K}$ is zero and interference can be suppressed by ZF. As a consequence, $M/2$ degrees of freedom can be achieved by each user.

B.III. Design of precoding matrices for M odd

If M is odd, we need to consider a two time-slot symbol extension of the channel. As explained in section 2.4, extended channel matrices for a time extension of level 2 can be expressed as follows:

$$\bar{\mathbf{H}}_{ij} = \mathbf{I}_2 \otimes \mathbf{H}_{ij} = \begin{bmatrix} \mathbf{H}_{ij} & \mathbf{0} \\ \mathbf{0} & \mathbf{H}_{ij} \end{bmatrix} \tag{184}$$

All the terms in (179) should be extended:

$$\begin{aligned} span\left(\bar{\mathbf{V}}_1\right) &= span\left(\bar{\mathbf{E}}\bar{\mathbf{V}}_1\right) \\ \bar{\mathbf{V}}_2 &= \bar{\mathbf{F}}\bar{\mathbf{V}}_1 \\ \bar{\mathbf{V}}_3 &= \bar{\mathbf{G}}\bar{\mathbf{V}}_1 \end{aligned} \tag{185}$$

Now, if we analyze eigenvectors of $\bar{\mathbf{E}}$, it could be seen that they have an especial structure because they are eigenvectors of an extended matrix. In fact it could be proved that:

$$span\left(\mathbf{e}_i\right) \in eig\left(\mathbf{E}\right) \Rightarrow span\left(\begin{bmatrix}\mathbf{e}_i \\ \mathbf{0}\end{bmatrix}, \begin{bmatrix}\mathbf{0} \\ \mathbf{e}_i\end{bmatrix}\right) \in eig\left(\bar{\mathbf{E}}\right) \tag{186}$$

This expression can be understood as follows. If $\mathbf{e}_i$ is an eigenvector of $\mathbf{E}$, then it could be extended in order to become an eigenvector of $\bar{\mathbf{E}}$. However, it appears twice in the eigenvectors of $\bar{\mathbf{E}}$. Notice that a linear combination of the two extended eigenvectors is also an eigenvector of $\bar{\mathbf{E}}$.

For the odd case, the solution presented in [16] for $\bar{\mathbf{V}}_1$ is:

$$\bar{\mathbf{V}}_1 = \begin{bmatrix} \mathbf{e}_1 & \mathbf{0} & \mathbf{e}_3 & \dots & \mathbf{0} & \mathbf{e}_M \\ \mathbf{0} & \mathbf{e}_2 & \mathbf{0} & \dots & \mathbf{e}_{M-1} & \mathbf{e}_M \end{bmatrix} \tag{187}$$

Note that only eigenvectors with different eigenvalues are chosen and the last column is chosen so as to ensure the linear independence condition, as we will show in the next section.

B.IV. Achievability for M odd

In this section, we will show that columns of $\bar{\mathbf{V}}_1$ have been chosen in order to satisfy the linear independence condition for each receiver. Similarly to the even case, we have to prove that:

$$\begin{aligned} span\left(\bar{\mathbf{H}}_{11}\bar{\mathbf{V}}_1\right) \cap span\left(\left[\bar{\mathbf{H}}_{12}\bar{\mathbf{V}}_2 \quad \bar{\mathbf{H}}_{13}\bar{\mathbf{V}}_3\right]\right) = \varnothing \\ span\left(\bar{\mathbf{H}}_{11}\bar{\mathbf{V}}_1\right) \cap span\left(\bar{\mathbf{H}}_{12}\bar{\mathbf{V}}_2\right) = \varnothing \\ span\left(\bar{\mathbf{V}}_1\right) \cap span\left(\bar{\mathbf{K}}\bar{\mathbf{V}}_1\right) = \varnothing \end{aligned} \tag{188}$$

where $\bar{\mathbf{K}} = \left(\bar{\mathbf{H}}_{11}\right)^{-1}\bar{\mathbf{H}}_{12}$. Equation (188) is equivalent to saying that all the columns of the following $2M \times 2M$ matrix are linearly independent.

$$\mathbf{C}_1 = \begin{bmatrix} \mathbf{e}_1 & \mathbf{0} & \mathbf{e}_3 & ... & \mathbf{0} & \mathbf{e}_M & \mathbf{K}\mathbf{e}_1 & \mathbf{0} & \mathbf{K}\mathbf{e}_3 & ... & \mathbf{0} & \mathbf{K}\mathbf{e}_M \\ \mathbf{0} & \mathbf{e}_2 & \mathbf{0} & ... & \mathbf{e}_{M-1} & \mathbf{e}_M & \mathbf{0} & \mathbf{K}\mathbf{e}_2 & \mathbf{0} & ... & \mathbf{K}\mathbf{e}_{M-1} & \mathbf{K}\mathbf{e}_M \end{bmatrix} \tag{189}$$

Let us define:

$$\begin{aligned} \mathbf{P} &= \left[\mathbf{e}_1, \mathbf{e}_3, ..., \mathbf{e}_{M-2}, \mathbf{K}\mathbf{e}_1, \mathbf{K}\mathbf{e}_3, ..., \mathbf{K}\mathbf{e}_{M-2}\right] \\ \mathbf{Q} &= \left[\mathbf{e}_2, \mathbf{e}_4, ..., \mathbf{e}_{M-1}, \mathbf{K}\mathbf{e}_2, \mathbf{K}\mathbf{e}_4, ..., \mathbf{K}\mathbf{e}_{M-1}\right] \end{aligned} \tag{190}$$

$\mathbf{P}$ and $\mathbf{Q}$ are full rank almost surely with $rank\left(\mathbf{P}\right) = rank\left(\mathbf{Q}\right) = M-1$. Moreover, because of the construction of $\mathbf{V}_1$, we can guarantee all columns of $\mathbf{C}_1$ are linearly independent except for column M and column $2M$. Now suppose $\mathbf{C}_1$ is a rank-deficient matrix. Then the following condition has to be satisfied:

$$\alpha_M \mathbf{e}_M + \alpha_{2M}\mathbf{K}\mathbf{e}_M \in span\left(\mathbf{P}\right) \cap span\left(\mathbf{Q}\right) \tag{191}$$

where α_M and α_{2M} are scalars. In other words, if $\mathbf{C}_1$ is a rank-deficient matrix, a linear combination of $\mathbf{e}_M$ and $\mathbf{K}\mathbf{e}_M$ has to lie on the span of the intersection of $\mathbf{P}$ and $\mathbf{Q}$. (191) is equivalent to:

$$span\left(\left[\mathbf{e}_M, \mathbf{K}\mathbf{e}_M\right]\right) \cap span(\mathbf{P}) \cap span(\mathbf{Q}) \neq \varnothing \tag{192}$$

Is it possible? What is the rank of the intersection between $span(\mathbf{P})$ and $span(\mathbf{Q})$? Using the Grasmman formula (see section 5.9 of [24]):

$$\begin{aligned} \dim\left(span(\mathbf{P}) \cap span(\mathbf{Q})\right) &= \dim(\mathbf{P}) + \dim(\mathbf{Q}) - rank\left[\mathbf{P} \quad \mathbf{Q}\right] = \\ &= 2(M-1) - M = M - 2 \end{aligned} \tag{193}$$

Hence, since $\dim\left(span(\mathbf{P}) \cap span(\mathbf{Q})\right) = M - 2$, we can say that $span(\mathbf{P}) \cap span(\mathbf{Q})$ is the set containing all the vectors of the M dimensional space, except those which belongs to a subspace of dimension 2. Since the set $\{\mathbf{e}_M, \mathbf{K}\mathbf{e}_M\}$ is drawn from an eigenvector $\mathbf{e}_M$ that does not lies on either $span(\mathbf{P})$ or $span(\mathbf{Q})$, it can be ensured with probability one that this space of dimension 2 is spanned by $[\mathbf{e}_M, \mathbf{K}\mathbf{e}_M]$. In other words:

$$span\left(\left[\mathbf{e}_M, \mathbf{K}\mathbf{e}_M\right]\right) \cap span(\mathbf{P}) \cap span(\mathbf{Q}) = \varnothing \tag{194}$$

Hence, the linear independence condition is satisfied at receiver 1. Similar arguments can be applied to receiver 2 and 3. Therefore, all the desired signals are linearly independent of the interference at each receiver and they can be decoded by ZF.

C. Proof of Theorem 3.4.3-2

The proof is mainly based on the rank of the precoding matrix $\mathbf{V}_3$ (i.e. the number of transmitted bitstreams), which is related to the rank of matrix $\mathbf{U}_{T_3}$ in (86). First of all, using the Grassman formula, the rank of the intersection space matrix defined above is $rank(\mathbf{A}_i) = 2M - N$. Now, we analyze some terms appearing in the expressions of the last section:

- $span(\hat{\mathbf{S}}_{13})$: The span of the pseudo-inverse of matrix $\mathbf{S}_{13}$. If $\frac{N}{2} < M < N$, $\mathbf{S}_{13}$ is a $N \times M$ diagonal matrix of the form $\begin{bmatrix} \tilde{\mathbf{S}}_{13} \\ \mathbf{0} \end{bmatrix}$ and then $\hat{\mathbf{S}}_{13}$ is a $M \times N$ matrix which could be expressed as follows: $\begin{bmatrix} \tilde{\mathbf{S}}_{13}^{-1} & \mathbf{0} \end{bmatrix}$.

- $span(\hat{\mathbf{S}}_{13}\mathbf{S}_{13})$: It always will be a $M \times M$ identity matrix $\mathbf{I}_M$.

- $span(\hat{\mathbf{S}}_{13}\mathbf{U}_{13}^H\mathbf{A}_1)$: $M \times rank(\mathbf{A}_{31}) = M \times (2M - N)$ matrix. Here we use that $\hat{\mathbf{S}}_1$ is a $M \times N$ matrix and $\mathbf{U}_1^H$ is a $N \times N$ full rank matrix. Thus, $rank(\hat{\mathbf{S}}_1\mathbf{U}_1^H\mathbf{A}_{31}) = rank(\mathbf{A}_{31})$ because it is the minimum rank of all the ranks in this product and the rank of a matrix product is at most the smallest among the rank of its factors.

- $span(\hat{\mathbf{S}}_{23}\mathbf{U}_{23}^H\mathbf{A}_2)$: Similarly to $span(\hat{\mathbf{S}}_{13}\mathbf{U}_{13}^H\mathbf{A}_1)$, it is a $M \times (2M - N)$ matrix.

- $span(\hat{\mathbf{S}}_{13}\mathbf{U}_{13}^H\mathbf{A}_1) \cap span(\hat{\mathbf{S}}_{23}\mathbf{U}_{23}^H\mathbf{A}_2)$: Applying again the Grassman formula:

$$rank(\mathbf{U}_{T_3}) = rank(\mathbf{T}_3) = 2 \cdot (2M - N) - M = 3M - 2N \qquad (195)$$

By construction, matrix $\mathbf{U}_{T_3}$ will have M rows and the number of columns will be equal to the rank of $span(\hat{\mathbf{S}}_{13}\mathbf{U}_{13}^{H}\mathbf{A}_1) \cap span(\hat{\mathbf{S}}_{23}\mathbf{U}_{23}^{H}\mathbf{A}_2)$. The rank of $\mathbf{U}_{T3}$ may be expressed as follows:

$$rank\left(\mathbf{U}_{T_3}\right) = \left(3M - 2N\right)^{+} \tag{196}$$

Hence, this method could only be applied when $r = \frac{N}{M} > 1.5$.

However, this innerbound has to be upper bounded. Remember that only the components of the desired signal which lie on the orthogonal space of $span(\mathbf{A}_i)$ are decoded. We refer to this space as $span\left(\mathbf{A}_i^{\perp}\right)$ and its dimension is given by:

$$\dim\left(span\left(\mathbf{A}_i^{\perp}\right)\right) = N - \dim\left(span\left(\mathbf{A}_i\right)\right) = N - \left(2M - N\right) = 2\left(N - M\right) \tag{197}$$

As a consequence, there are some cases, where

$$\dim\left(span\left(\mathbf{A}_i^{\perp}\right)\right) < \dim\left(span\left(\mathbf{A}_i\right)\right) \tag{198}$$

and the innerbound will be equal to $2\left(N - M\right)$. Finally, the total degrees of freedom per user that could be achieved by this method could be expressed as shown below:

$$DoF = \min\left(2\left(N - M\right), \left(3M - 2N\right)^{+}\right) \tag{199}$$

D. IA procedure using GSVD precoding

In this appendix we prove that the IA conditions

$$span(\mathbf{H}_{12}\mathbf{V}_2) = span(\mathbf{H}_{13}\mathbf{V}_3)$$
$$span(\mathbf{H}_{21}\mathbf{V}_1) = span(\mathbf{H}_{23}\mathbf{V}_3)$$
$$span(\mathbf{H}_{31}\mathbf{V}_1) = span(\mathbf{H}_{32}\mathbf{V}_2)$$

for $M = N$ are satisfied using the following precoding matrices:

$$\mathbf{V}_1^{IA} = \mathbf{U}_{21}\mathbf{D}_{21}^{\#}\mathbf{K}_1\mathbf{\Omega}_2\mathbf{K}_2$$
$$\mathbf{V}_1^{IA} = \mathbf{U}_{21}\mathbf{D}_{21}^{\#}\mathbf{K}_1\mathbf{\Omega}_2\mathbf{K}_2$$
$$\mathbf{V}_3^{IA} = \mathbf{U}_{13}\mathbf{D}_{13}^{\#}\mathbf{\Omega}_1\mathbf{K}_1\mathbf{\Omega}_2\mathbf{K}_2$$

where $\mathbf{U}_{ij}$ and $\mathbf{D}_{ij}$ are defined applying the GSVD (77) to the following channel matrices,

$$\begin{aligned} \mathbf{H}_{12} &= \mathbf{W}_{12}\mathbf{D}_{12}\mathbf{U}_{12}^H \qquad & \mathbf{H}_{21} &= \mathbf{W}_{21}\mathbf{D}_{21}\mathbf{U}_{21}^H \\ \mathbf{H}_{13} &= \mathbf{W}_{12}\mathbf{D}_{13}\mathbf{U}_{13}^H \qquad & \bar{\mathbf{H}}_{23} &= \mathbf{H}_{23}\mathbf{U}_{13} = \mathbf{W}_{21}\bar{\mathbf{D}}_{23}\bar{\mathbf{U}}_{23}^H \end{aligned} \tag{200}$$

$\mathbf{D}_{ij}^{\#}$, $\mathbf{\Omega}_1$ and $\mathbf{\Omega}_2$ are given by,

$$\begin{aligned} \mathbf{D}_{ij}^{\#} &= \mathbf{D}_{ij}{}^H\left(\mathbf{D}_{ij}\mathbf{D}_{ij}^H\right)^{-1} \\ \mathbf{\Omega}_1 &= \bar{\mathbf{U}}_{23}\bar{\mathbf{D}}_{23}^{\#}, \\ \mathbf{\Omega}_2 &= eig\left(\mathbf{H}_{31}\mathbf{U}_{21}\mathbf{D}_{21}^{\#}\mathbf{K}_1, \mathbf{H}_{32}\mathbf{U}_{12}\mathbf{D}_{12}^{\#}\mathbf{\Omega}_1\mathbf{K}_1\right) \end{aligned} \tag{201}$$

and $\mathbf{K}_1$ and $\mathbf{K}_2$ are free to design.

We begin by solving the IA equation for the 1st receiver. Let us apply the GSVD to matrices $\mathbf{H}_{12}$ and $\mathbf{H}_{13}$ in the first alignment equation:

$$\mathbf{H}_{12} = \mathbf{W}_{12}\mathbf{D}_{12}\mathbf{U}_{12}^H, \quad \mathbf{H}_{13} = \mathbf{W}_{12}\mathbf{D}_{13}\mathbf{U}_{13}^H \tag{202}$$

Then, if we set

$$\begin{aligned} \mathbf{V}_2 &= \mathbf{U}_{12}\mathbf{D}_{12}^{\#} \\ \mathbf{V}_3 &= \mathbf{U}_{13}\mathbf{D}_{13}^{\#} \end{aligned} \tag{203}$$

where $\mathbf{D}_{ij}^{\#} = \mathbf{D}_{ij}{}^{H}\left(\mathbf{D}_{ij}\mathbf{D}_{ij}^{H}\right)^{-1}$ is the pseudo-inverse of $\mathbf{D}_{ij}$; the alignment equation at receiver 1 is satisfied:

$$\begin{aligned} \text{span}\left(\mathbf{H}_{12}\mathbf{V}_2\right) &= \text{span}\left(\mathbf{H}_{13}\mathbf{V}_3\right) \\ \text{span}\left(\mathbf{H}_{12}\mathbf{U}_{12}\mathbf{D}_{12}^{\#}\right) &= \text{span}\left(\mathbf{H}_{13}\mathbf{U}_{13}\mathbf{D}_{13}^{\#}\right) \\ \text{span}\left(\mathbf{W}_{12}\mathbf{D}_{12}\mathbf{U}_{12}^{H}\mathbf{U}_{12}\mathbf{D}_{12}^{\#}\right) &= \text{span}\left(\mathbf{W}_{12}\mathbf{D}_{13}\mathbf{U}_{13}^{H}\mathbf{U}_{13}\mathbf{D}_{13}^{\#}\right) \\ \text{span}\left(\mathbf{W}_{12}\right) &= \text{span}\left(\mathbf{W}_{12}\right) \end{aligned} \tag{204}$$

Moreover, for any full-rank matrix multiplied by the right-hand side, the alignment condition is also satisfied:

$$\begin{aligned} \text{span}\left(\mathbf{W}_{12}\right) &= \text{span}\left(\mathbf{W}_{12}\right) \\ \text{span}\left(\mathbf{W}_{12}\boldsymbol{\Omega}_1\right) &= \text{span}\left(\mathbf{W}_{12}\boldsymbol{\Omega}_1\right) \end{aligned} \tag{205}$$

and hence, precoding matrices for user 2 and 3 can be designed as:

$$\begin{aligned} \mathbf{V}_2 &= \mathbf{U}_{12}\mathbf{D}_{12}^{\#}\boldsymbol{\Omega}_1 \\ \mathbf{V}_3 &= \mathbf{U}_{13}\mathbf{D}_{13}^{\#}\boldsymbol{\Omega}_1 \end{aligned} \tag{206}$$

Next, we need to resolve the alignment condition for the second user:

$$span\left(\mathbf{H}_{21}\mathbf{V}_1\right) = span\left(\mathbf{H}_{23}\mathbf{V}_3\right) \tag{207}$$

Substituting (206) in (207):

$$\begin{aligned} span\left(\mathbf{H}_{21}\mathbf{V}_1\right) &= span\left(\mathbf{H}_{23}\mathbf{V}_3\right) \\ span\left(\mathbf{H}_{21}\mathbf{V}_1\right) &= span\left(\mathbf{H}_{23}\mathbf{U}_{13}\boldsymbol{\Omega}_1\right) \\ span\left(\mathbf{H}_{21}\mathbf{V}_1\right) &= span\left(\bar{\mathbf{H}}_{23}\boldsymbol{\Omega}_1\right) \end{aligned} \tag{208}$$

Using again the GSVD to $\mathbf{H}_{21}$ and $\bar{\mathbf{H}}_{23}$

$$\mathbf{H}_{21} = \mathbf{W}_{21}\mathbf{D}_{21}\mathbf{U}_{21}^{H}, \quad \bar{\mathbf{H}}_{23} = \mathbf{W}_{21}\bar{\mathbf{D}}_{23}\bar{\mathbf{U}}_{23}^{H} \tag{209}$$

In order to satisfy this equation, we can set:

$$\begin{aligned}\mathbf{V}_1 &= \mathbf{U}_{21}\mathbf{D}_{21}^{\#}\mathbf{K}_1\mathbf{\Omega}_2 \\ \mathbf{V}_3 &= \mathbf{U}_{13}\mathbf{D}_{13}^{\#}\mathbf{\Omega}_1\mathbf{K}_1\mathbf{\Omega}_2 \\ \mathbf{V}_2 &= \mathbf{U}_{12}\mathbf{D}_{12}^{\#}\mathbf{\Omega}_1\mathbf{K}_1\mathbf{\Omega}_2 \\ \mathbf{\Omega}_1 &= \bar{\mathbf{U}}_{23}\bar{\mathbf{D}}_{23}^{\#}\end{aligned} \tag{210}$$

where $\mathbf{K}_1$ and $\mathbf{\Omega}_2$ are arbitrary matrices. Notice that redefining $\mathbf{V}_3$ implies to redefine $\mathbf{V}_2$ so as to satisfy (204).

Finally, the third alignment equation

$$\begin{aligned}span\left(\mathbf{H}_{31}\mathbf{V}_1\right) &= span\left(\mathbf{H}_{32}\mathbf{V}_2\right) \\ span\left(\mathbf{H}_{31}\mathbf{U}_{21}\mathbf{K}_1\mathbf{\Omega}_2\right) &= span\left(\mathbf{H}_{32}\mathbf{U}_{12}\mathbf{\Omega}_1\mathbf{K}_1\mathbf{\Omega}_2\right)\end{aligned} \tag{211}$$

can be satisfied by setting

$$\mathbf{\Omega}_2 = eig\left(\mathbf{H}_{31}\mathbf{U}_{21}\mathbf{D}_{21}^{\#}\mathbf{K}_1, \mathbf{H}_{32}\mathbf{U}_{12}\mathbf{D}_{12}^{\#}\mathbf{\Gamma}_1\mathbf{K}_1\right) \tag{212}$$

where $eig\left(\mathbf{A},\mathbf{B}\right)$ are the generalized eigenvalues of $\mathbf{A}$ and $\mathbf{B}$. Notice that we can multiply by the right-hand all the precoding matrices by any full-rank matrix $\mathbf{K}_2$ and the IA equations are also accomplished. Finally, $\mathbf{K}_1$ and $\mathbf{K}_2$ are free to design for instance, as those matrices maximizing SNR at each receiver.